Mathematical modeling for contrasting dynamics of a plant herbivore interaction

by

Sultanah Hadi Masmali

M.S., Cleveland State University, 2015

AN ABSTRACT OF A DISSERTATION

submitted in partial fulfillment of the
requirements for the degree

DOCTOR OF PHILOSOPHY

Department of Mathematics
College of Arts and Sciences

KANSAS STATE UNIVERSITY
Manhattan, Kansas

2022

Abstract

The Nicholas-Bailey model was designed to study population dynamics of host-parasite systems. The model was first developed by Nicholson and Bailey (1935) and applied to parasites (Encarsia Formosa) and hosts (Trialeurodes vaporariorum). These types of models are presented by discrete-time equations for biological systems that involve two species, e.g. a parasite population and its hosts. In this dissertation, we develop and then investigate a revised version of Nicholson-Bailey's discrete host-parasite model. Additionally, we incorporate and analyze the Allee effect dynamics in this newly constructed model.

In Chapter one of this dissertation, we outline some background and literature. Second, we provide basic definitions of ordinary differential equations. We define several core concepts of dynamical systems including stability and instability analysis, manifold analysis, stable and unstable manifold, invariant manifold, center manifold, bifurcation, and the Lambert W function. Then we provide some known results and theorems that are useful in this research investigation.

Third, we study the dynamics behavior of the newly developed system of a host-parasite model with four positive parameters in the first closed quadrant. A re-scaling procedure will be then applied to reduce the model to a two-parameter model that reproduces the entire dynamics of the original model. The model always possesses two boundary steady states and a third interior steady state may exist for particular conditions imposed on the parameters. Moreover, by applying the linearized stability function, we find thresholds for which the system is stable or unstable. We then study locally the long-term stability of steady states and center manifold theory based on the separating boundary curves for non-hyperbolic steady states, that is analyzing steady states when crossing from stable to unstable regions. We then analyze the stability for one or two parameter bifurcation (co-dimension one or two) depending on a different range of parameters, by considering

the linearization of the model about each of the steady states. We show a period-doubling bifurcation occurs once the eigenvalue crosses these thresholds, leading to chaos. Numerical simulations support the results and conclusions.

Fourth, we introduce the density dependence of the Allee effect and population dynamics into the model by adding a parameter to the modified system of the Nicholson-Bailey model. We then study the local stability of its steady states. Multiple bifurcation analyses of the system, including the period-doubling behavior and Neimark-Sacker bifurcation, will be analyzed. We then identify regions where the Allee effect system ultimately leads to chaos. Finally, the modified systems of the Nicholson-Bailey model and the Allee effect model are compared by analyzing different short-term and long-term dynamical behaviors and results acquired from the two systems.

Mathematical modeling for contrasting dynamics of a plant herbivore interaction

by

Sultanah Hadi Masmali

M.S., Cleveland State University, USA, 2015

A DISSERTATION

submitted in partial fulfillment of the
requirements for the degree

DOCTOR OF PHILOSOPHY

Department of Mathematics
College of Art and Sciences

KANSAS STATE UNIVERSITY
Manhattan, Kansas

2022

Approved by:

Major Professor
Majid Jaberi-Douraki

Copyright

Abstract

The Nicholas-Bailey model was designed to study population dynamics of host-parasite systems. The model was first developed by Nicholson and Bailey (1935) and applied to parasites (Encarsia Formosa) and hosts (Trialeurodes vaporariorum). These types of models are presented by discrete-time equations for biological systems that involve two species, e.g. a parasite population and its hosts. In this dissertation, we develop and then investigate a revised version of Nicholson-Bailey's discrete host-parasite model. Additionally, we incorporate and analyze the Allee effect dynamics in this newly constructed model.

In Chapter one of this dissertation, we outline some background and literature. Second, we provide basic definitions of ordinary differential equations. We define several core concepts of dynamical systems including stability and instability analysis, manifold analysis, stable and unstable manifold, invariant manifold, center manifold, bifurcation, and the Lambert W function. Then we provide some known results and theorems that are useful in this research investigation.

Third, we study the dynamics behavior of the newly developed system of a host-parasite model with four positive parameters in the first closed quadrant. A re-scaling procedure will be then applied to reduce the model to a two-parameter model that reproduces the entire dynamics of the original model. The model always possesses two boundary steady states and a third interior steady state may exist for particular conditions imposed on the parameters. Moreover, by applying the linearized stability function, we find thresholds for which the system is stable or unstable. We then study locally the long-term stability of steady states and center manifold theory based on the separating boundary curves for non-hyperbolic steady states, that is analyzing steady states when crossing from stable to unstable regions. We then analyze the stability for one or two parameter bifurcation (co-dimension one or two) depending on a different range of parameters, by considering

the linearization of the model about each of the steady states. We show a period-doubling bifurcation occurs once the eigenvalue crosses these thresholds, leading to chaos. Numerical simulations support the results and conclusions.

Fourth, we introduce the density dependence of the Allee effect and population dynamics into the model by adding a parameter to the modified system of the Nicholson-Bailey model. We then study the local stability of its steady states. Multiple bifurcation analyses of the system, including the period-doubling behavior and Neimark-Sacker bifurcation, will be analyzed. We then identify regions where the Allee effect system ultimately leads to chaos. Finally, the modified systems of the Nicholson-Bailey model and the Allee effect model are compared by analyzing different short-term and long-term dynamical behaviors and results acquired from the two systems.

Table of Contents

List of Figures x

List of Tables xiii

Acknowledgements xiv

Dedication xv

1 Introduction 1

2 Preliminaries 15

2.1 Stability of a Steady State 15

2.2 Hyperbolic and Non-Hyperbolic Steady States 16

2.3 Invariant Manifolds 19

2.3.1 Stable and Unstable Manifolds 20

2.3.2 Center Manifolds 21

2.4 Bifurcation 24

2.4.1 Properties of Bifurcation 24

2.4.2 Period-Doubling Bifurcation 26

2.4.3 Saddle-Node Bifurcation 27

2.4.4 Neimark-Sacker Bifurcation 27

2.5 Persistence of Dynamical Systems 32

2.6 Lambert W Function 33

2.6.1 Properties of Lambert W Function 33

2.6.2 Real Branches 33

3 Stability Analysis and Bifurcations of a Modified Nicholson-Bailey Type Model 35
3.1 Introduction 36
3.2 Steady States of the MNB Model 38
3.3 Analysis of Local Stability 40
3.4 Global Stability of the Boundary Steady State S_1 47
3.4.1 Persistence of the Model 48
3.5 Stability of the Interior Steady State S_2 53
3.6 Bifurcation Analysis 56
3.6.1 Period-Doubling Bifurcations (Flip Bifurcation) 56
3.7 Concluding Remarks and Simulations 62

4 Dynamics of a Modified Nicholson-Bailey Model with Allee effect 64
4.1 Introduction 65
4.2 The Model 65
4.3 Stability of the Boundary Steady States 74
4.4 Stability Regions of the Interior Steady-States 86
4.4.1 One Parameter Bifurcation (Co-Dimension 1) 87
4.4.2 Two Parameter Bifurcation (Co-Dimension 2) 95
4.5 Bifurcation Analysis 109
4.5.1 Neimark–Sacker Bifurcation 110
4.5.2 Period-Doubling Bifurcations 117

Bibliography 124

List of Figures

2.1 Different stability regions (stable, repelling, and saddle) in the trace-determinant (tr-det) plane. 18

2.2 The local stable and unstable manifolds pass through 0. 20

2.3 The cobweb diagram can show if the center manifold is stable or unstable. 24

2.4 The incidence of the three main types of bifurcation in the trace-determinant (tr-det) plane. Neimark-Sacker bifurcation when det =1, Period-doubling bifurcation when $\det = -\operatorname{tr} -1$, and Saddle-Node bifurcation when $\det = \operatorname{tr} -1$. 25

2.5 From left to right: a positive eigenvalue approaches the unit circle ($\lambda = 1$), a negative eigenvalue approaches the unit circle ($\lambda = -1$), or a pair of simple complex eigenvalues reach the unit circle ($\lambda_{1,2} = e^{\pm i\theta_0}$, $0 < \theta_0 < \pi$). 26

2.6 Real branches of the Lambert W and inverse functions for $W_0(\mathrm{x})$ (dark purple curve) and $W_{-1}(\mathrm{x})$ (purple curve). 34

3.1 Three dark purple curves show the graph of function f_1 for different parameter values $k = 0.5, 1$ and 2, respectively. The function f_2, the light purple, is independent of k. The functions f_1 and f_2 have a positive intersection when $k > 1$. 40

3.2 The center manifold is half-stable when $k = 1$ for $u = h(v)$. 44

3.3 The center manifold is asymptotically stable when $r = 2$ for $v = h(u)$. 45

3.4 The center manifold is half-stable when $k = 1$ and $r = 2$ for $u = h(v)$. 47

3.5 Stability regions of system (3.7) for different parameter values of r. The stable region is highlighted in orange, the green indicates the saddle region, and the red refers to the repeller region. The intersection point of the yellow with saddle curve occurs at $x = e$. 55

3.6 Stability regions of system (3.7) for $(x, k)-$plane. The curve $k = f_5(x) = x$ gives the existence regions, and under this curve, they are not acceptable regions. 56

3.7 Stability of the period doubling bifurcation of system (3.7). 60

4.1 The two boundary steady states and the two interior steady states S_1, S_2, S_3 and S_4 with colors (green, dark green, purple, and dark purple) respectively. In the (r, x)-plane where the parameter $\alpha = 1.8621$ and $k = 0.5$. 69

4.2 From left to right: The curves $k = \frac{r}{\alpha}e^{r(1-\frac{r}{\alpha})}$, $k = 1$, $k = \frac{r}{\alpha}$, $k = \frac{r}{\alpha+2}e^{1-\frac{2-r}{\alpha}}$ are green, green, pink, and orange respectively. The curves $k = \frac{r}{\alpha-1}e^{r(1-\frac{r}{\alpha-1})}$, $k = 1$, $k = \frac{r}{\alpha-1}$, $x = 1$ are green, green, pink, and white respectively. Contribution of number of boundary and interior steady states of system (4.6) in (α, k)-plane. . . . 75

4.3 Stability regions of the boundary steady-states $(x_1^*, 0)$ and $(x_2^*, 0)$ where $r = 1.5$. The two green curves are $k = 1$ and $k = \frac{re^{\frac{\alpha-r}{\alpha}}}{\alpha}$. The pink curve is $k = \frac{r}{\alpha}$ and the orange curve is $k = \frac{re^{\frac{2+\alpha-r}{\alpha}}}{2+\alpha}$. 78

4.4 Center manifold is half-stable or semi-stable for $r = 3.8621$ and $u = h(v)$. 83

4.5 The center manifold is half-stable or semi-stable. Here $\alpha = 0.43$ for $u = h(v)$. . . . 85

4.6 Center manifold is stable when $k = 2.3448$ and $r = 2$ for $v = h(u)$. 86

4.7 Stability regions of $(x, r)-$ plane for different values of α where $\alpha = 0.20513$, $\alpha = 1$, and $\alpha = 2.3590$. 89

4.8 The stability regions of the $(x, \alpha)-$plane interior steady-states points $(z_1^*, z_1^* - 1)$ and $(z_2^*, z_2^* - 1)$ where $r = 0.82051$, $r = 1$, and $r = 1.3097$. 91

4.9 Stability regions of $(x, k)-$plane for the interior steady-states points where $r = .8$, $r = 1$, and $r = 1.0345$. 96

4.10 Top Left: No interior steady states exist when $\alpha < 1$. Top right: when $\alpha > 1$, the steady state W_0 is saddle (purple curve below the green curve), however, W_{-1} changes its stability for different values of parameter r (dark purple curve is: repeller between the green and yellow curves, stable between the yellow and red curves, and saddle above red). In the top row, we have $k = 0.5$. Bottom Left: Only W_0 exists in different regions (repeller, stable, and saddle, similar to the top left case) when $\alpha < 1$. However, we will only have W_{-1} for different (in)stability regions (repeller, stable, and saddle) when $\alpha > 1$. For the bottom panels, we assume $k = 1.5$. 98

4.11 Stability regions of co-dimension two for the $(\alpha, k)-$plane where the parameter $r = 0.42625$ (top left), $r = 1$ (top right) and $r = 1.2588$ (bottom). 105

4.12 Stability regions of the two co-dimension (α, r) plane where the parameter $k = 1$ (left) and $k = 1.6668$ (right). 109

4.13 Neimark-Sacker bifurcation for different k values. It is unstable when $a(0) > 0$ and stable when $a(0) < 0$. 117

4.14 Results for period doubling bifurcation when $\alpha = 1.4$ which is stable. 122

4.15 Stability regions of the boundary steady-state points $(x_1^*, 0)$ and $(x_2^*, 0)$ where $r = 1.3$ with the regions of the interior steady states $(z_1^*, z_1^* - 1)$ and $(z_2^*, z_2^* - 1)$. . . . 123

List of Tables

3.1 Stability of the period doubling bifurcation for the given numerical values of $(r^*, \lambda_2, \mathcal{K})$. 61

4.1 The numerical values for the positive steady state and for the coefficient $a(0)$ corresponding to parameters (α, k). 116

4.2 The numerical exact values for $(r^*, \lambda_2, \mathcal{H})$ for the given values of the parameter r^*. 121

Acknowledgments

Praise, gratitude, and all thanks are to Almighty Allah for giving me the strength and the courage to complete this dissertation. Thanks to Allah through his grace, guidance, and help, none of this would have been possible without Allah's blessings.

I would like to acknowledge my committee members, and a special thanks goes to my major professor, Dr. Majid Jaberi-Douraki for his extraordinary effort and generous help. I would like to express my deepest thanks to my committee members Dr. Nathan Albin, and Dr. Tanya Firsova for their support and assistance during my doctoral program journey. Their guidance, experience, and encouragement were invaluable. Also, I am deeply grateful to the other members of my academic advisory committee Dr. Behrooz Mirafzal, and Dr. Vincent Amanor-Boadu, their insights and valuable advice were greatly appreciated. It was an honor to work with each of them. As well, I would like to thank the faculty and staff of the K-State Mathematics Department. Special thanks to Dr. Pietro Poggi-Corradini, Dr. Andrew Bennett, Dr. Sarah Reznikoff, Dr. David Yetter, Dr. David Auckly, and Dr. Victor Turchin for their guidance and assistance. I would like to also thank Dr. Reza GhamarShoushtari for his guidance.

In addition, I would like to extend my sincere gratitude to Jazan University and my country, Saudi Arabia. I am grateful for the scholarship you provided to fund my education.

I am extremely grateful to all my family members for making success possible for me. I can never thank my parents enough for their love and support, and patience. To my father, Hadi, I am grateful for his endless love, support, and prayers for me. I would like to thank my wonderful mother, Maryam, for her prayers, support, and love throughout my academic journey. Also, I want to thank my mother-in-law, Salihah, for her patience, love, and prayers.

Furthermore, I want to express my gratitude to the person who has supported me more than anyone else. I would like to express my gratitude to my dear husband, Dr. Abdullah, for his encouragement and for motivating me when I needed it. I cannot thank him enough for the support and sacrifice he has made, as well as the care, encouragement, and patience he has shown me

throughout this doctoral journey.

I am grateful to my caring brothers and sisters and my nieces and nephews for giving me strength and encouragement. Thank you to my brothers, Eissa, Ali, Mohammed, and Abdulrahman, and my sisters, Eman, Layla, Mona, Aminah, and Rawan. I appreciate their support, encouragement, prayers, and belief in me.

Finally, I would like to express my gratitude to my amazing children, Nooran, Ameer, Loreen, Asser, and Nawaf, who has been my inspiration, drive, and motivation, for their unwavering love and support. I appreciate all their understanding and devotion while I was occupied with getting my degree.

Dedication

To my parents,

To my brothers and sisters,

To my children,

With love

I dedicate this dissertation to you.

Chapter 1

Introduction

Mathematical modeling can be defined as developing a system of equations (differential, integral, functional, etc.) called models to represent a phenomenon such as a biological event or a physiological event that is either observable or not[1]. It examines how models can be used to investigate real-world problems. In ecology, variables affecting herbivory, such as plant defense, natural herbivore enemies, adaptive herbivory and the consequences on plant community dynamics are studied. Conventional models of plant-herbivore interactions are based on the predator–prey system[2;3]. The interaction between herbivores and plants is one of most fundamental processes in ecology, and it has been the subject of scientific observation and thought since Aristotle[4], although mathematical modeling of plant-herbivore interactions has only been used for the past few decades[4]. The well-known predator-prey models of Lotka and Volterra were among the first mathematical models in ecology[5;6]. There are a wide range of characteristics of plant-herbivore interactions that are included in the theory and modeling of plant-herbivore systems and extend beyond the Lotka-Volterra model and continuous-time models joined by discrete-time difference equation models[7]. In these studies, interactive herbivory refers to conditions in which the herbivore biomass is affected by plant biomass, and proportionately, the plant biomass is disturbed by herbivore biomass; in other words, there is a feedback loop. Because the plant has a positive effect on herbivore growth rate and the herbivore has a negative effect on plant growth rate, this feedback unlike cooperative systems is negative.

It is worth mentioning that plant-herbivore dynamics were first divided into two categories by Caughley: noninteractive and interactive[8]. For noninteractive models, consumers have no effect on plant or vegetation growth. That is, herbivore-vegetation interactions are unique in which they do not deplete the plants' critical biomass[7], because it has no effect on the vegetation's growth rate or size.

Biologists and agricultural ecologists are particularly interested in discrete models with difference equations for interacting populations, since their time units are discrete. Models in discrete time are actually more plausible when populations do not overlap in their generations than models based on continuous time, although they might require more sophisticated theories to analyze. A population with a one-year life cycle, such as insects, certainly experiences this phenomenon.

Below are some of the recent studies in the field of dynamical systems. Several forms of mathematical models are used in these studies, from continuous to partial to discrete, but they all relate to interactive systems.

Gutierrez et al. provided a model that was a system of partial differential equations. They considered the affect of herbivores on various plant sections which was based on the McKendrick von Foerster equation[9].

Leah Edelstein-Keshet described her model for a plant-herbivore system with plant quality and herbivore density as variables[10]. The mathematical model for her study was presented by the following system

$$\frac{dq}{dt} = f(q,h),$$
$$\frac{dh}{dt} = g(q,h)$$

where the functional responses f and g represent the rates of change in plant quality and herbivore population, respectively. Depending on the forms of q and h, both functions were determined or conjectured based on biological information corresponding to a particular plant and herbivore system.

An interesting difference equation model was formulated and analyzed by Allen et al. for the plant-herbivore system[12]. According to their model, two control strategies, cane removal and pes-

ticide application, were developed in their work. They found that there were two equilibria in the system, one where the pest was present (disease state) and one where the pest was absent (disease-free state). Different regions were found in parameter space for global stability of the equilibria. In the absence of global stability, it was shown that there existed periodic or quasiperiodic solutions. The analyzed system is given below:

$$V_{n+1} = \frac{V_n h\left(A_n\right)}{\alpha_1 + \alpha_2 V_n h\left(A_n\right)},$$
$$A_{n+1} = \alpha_3\left(V_n + 1\right) A_n$$

where V_0 and A_0 are positive initial conditions, and the function h denotes either of the two functions h_1 or h_2 as follows:

$$h_1(A) = \frac{1}{1 + A^2},$$
$$h_2(A) = \exp(-A)$$

Powell et al. created a variety of mechanistic models, ranging from strategic population models of beetle outbreaks to tactical behavior models detailing how beetles chose host trees[13]. They analyzed the behavior of their system of equations heuristically and compared it with observations. One example of a qualitative heuristic comparison is Powell et al.'s diagram of the behavior of mountain pine beetles nesting population and Geiszler et al.'s observations (1980)[14]. While Geiszler et al. observed data on the cumulative number of successful Mountain Pine Beetles (MPB) attacks on a single focus tree, Powell et al. supplied data about the number of MPB nesting in a focus tree as a function of flight hours. The numbers in Powell et al.'s diagram and those in Geiszler et al.'s observations were very similar. Powell et al. integrated three mathematical approaches to create a geographical framework for assessing the danger of MPB attacks on individual hosts[15]. According to the preliminary results of the study, stand microclimate, which is the collection of climatic factors measured at specific locations close to the earth's surface, significantly impacts attack risk more than host immunity or stand age. Powell et al. investigated the quantitative modeling and

analysis of direct temperature control as well as how these models revealed adaptive seasonality to oviposition, or egg laying, dates for succeeding generations[16]. According to their study, a stable fixed point on the developmental circle map correlates with univoltinism. This is the condition of generating a single offspring throughout a season, especially one with eggs that could hibernate, which is associated with reproductive success in many species living in temperate environments. In broad temperature bands, univoltine fixed points were stable and robust, but suddenly lose stability at the edges of these bands due to maladaptive cycles. The temperature bands in their study were used when studying the quantitative modeling and analysis of direct temperature control and how these models highlighted adaptive seasonality.

Summers et al. studied effects of periodic forcing on four discrete-time ecosystem models[17]. A periodic force is one that repeats itself periodically. This particular force effect can be applied as a force feedback stimulus. Their results showed that it might cause chaotic behavior.

Li et al.,[18] studied a mathematical model that took plant toxicity into account when calculating the functional response of plant-herbivore interactions. The authors explored how differences in dynamical behavior could be attributed to inter-specific variations in plant biology, growth and defense strategies, as well as responses to toxins in herbivores. It was found that herbivores were able to promote plant coexistence by lowering competitive effects and thus contributing to biodiversity with realistic parameter values.

According to Sui et al., stoichiometry-based models highlighted the significance of plant nutrition for the dynamics of herbivore-plant interactions[19]. Stoichiometry refers to the correlation between reactant and product quantities prior to, during, and after chemical processes. A continuous stoichiometric plant-herbivore model was examined in their study. They then examined the dynamics of the continuous and discrete models after introducing the discrete analog.

In Kang et al.'s study, a model in the form of host-parasite interaction observed quasi-periodicity, period-doubling, and then chaos behavior. They showed that the interior equilibrium point was globally stable in their continuous model[20].

In Agiza et al.'s study, a discrete predator-prey model with Holling's Type II response function which led to chaotic dynamics[23]. They took into account predators' natural mortality rate. The

model was presented by

$$x_{n+1} = ax_n\left(1 - x_n\right) - \frac{bx_n y_n}{1 + \varepsilon x_n}$$
$$y_{n+1} = \frac{dx_n y_n}{1 + \varepsilon x_n},$$

where the nonnegative parameters are a, b, c, and d. Prey and predator densities are represented by x and y, respectively. a and ε stand for the intrinsic growth parameter of the prey and the restriction on the growth rate of the predator population as the number of prey increases, respectively.

According to research by Liu et al., interactions between boreal hares that mostly consume twigs in the winter might be impacted by the chemical defenses of woody plants[24]. The authors placed a lot of emphasis on how the concentration of toxin frequently fluctuates with the age of twig segments. Their model took into account the fact that the woody internodes of the youngest segments of the deciduous angiosperm species of twigs that those hares chose to consume were more protected by toxins than the woody internodes of the older segments that subtend and support the younger segments. They found a linear stability of the equilibrium in which the hare population was extinct and sufficient conditions for the global equilibrium to be stable. Analytical results confirmed by numerical simulations showed that woody vegetation was a reasonable browse site for hares in boreal ecosystems and that there were limited cycles in those ranges. They found new results, showing that hare–plant population cycles could be caused by aging-dependent chemical defenses within plants.

Kartal used differential and difference equations to study the behavior of a plant-herbivore model[25]. The model was presented by

$$x(n+1) = \frac{x(n)(r - \alpha y(n))}{(r - \alpha y(n) - rkx(n))e^{-(r-\alpha y(n)} + rkx(n)},$$
$$y(n+1) = y(n)e^{\beta x(n) - s}$$

The parameters were all positive. To examine the model's overall behavior, Kartal looked at the system's solution in a certain sub-interval, which gave a system of difference equations. His research identified the plant-herbivore system's boundedness traits, periodic nature, and both local

and global stability conditions. According to his numerical studies, there was a Neimark-Sacker bifurcation in certain system regions based on the parameters' values. As a side note, this system can be studied later to show the existence of Neimark-Sacker bifurcation might be proven theoretically as well.

In a different plant-herbivore model, Din et al. investigated bifurcation analysis and chaos control for a plant–herbivore model with weak predator functional response[26]. The classification of equilibria was examined topologically. They demonstrated that the boundary equilibrium experienced transcritical bifurcation, whereas the positive steady-state of the discrete-time plant-herbivore model underwent Neimark–Sacker bifurcation. The model was presented by

$$x_{n+1} = \frac{x_n}{\alpha\left(1+y_n^2\right)+\beta x_n},$$
$$y_{n+1} = \gamma y_n\left(1+x_n\right)$$

Where x_n represented the Grapevine (plant) population density and y_n represented the Apple Twig Borer (herbivore) population density. Moreover, the parameters α, β and γ were all positive.

After studying a few recent papers in the field of discrete dynamical systems and chaos, it is worth providing the typical framework for discrete-generation host-parasite models which may take the following form:

$$\begin{aligned} P_{n+1} &= \lambda P_n f\left(P_n, H_n\right) \\ H_{n+1} &= c\lambda P_n\left(1-f\left(P_n, H_n\right)\right) \end{aligned} \tag{1.1}$$

where P and H are the host (plant) and parasite (herbivore) population biomasses in consecutive generations n and $n+1$, respectively. The parameter λ denotes the host's inherent rate of rising in the absence of parasites and may be presented by $\lambda = e^r$ where r is the intrinsic rate of increase. Also, c is the biomass conversion constant, and f is the function determining the fractional survival of parasitized hosts. n acquires the non-negative integer values.

The basic version of this model is that of Nicholson[31] and Nicholson and Bailey[32], who investigated in depth a model in which the fraction of hosts escaping parasitism is given by the Poisson

distribution's zero-term, namely

$$f\left(P_n, H_n\right) = \mathrm{e}^{-aH_n} \tag{1.2}$$

where a represents the average number of contacts per host. As a result, the probability of a host being attacked is $1 - \mathrm{e}^{-aH_n}$. Substituting Equation (1.2) into Equations (1.1) gives:

$$\begin{aligned} P_{n+1} &= \lambda P_n \mathrm{e}^{-aH_n} \\ H_{n+1} &= c\lambda P_n \left(1 - \mathrm{e}^{-aH_n}\right) \end{aligned}$$

The Nicholson–Bailey model has a positive equilibrium that is unstable when $\lambda > 1$[34]. This may provide unbounded solutions which are not ecological.

The Nicholson-Bailey host-parasite model was then modified by Beddington et al. as follows:

$$\begin{aligned} P_{n+1} &= \lambda P_n \mathrm{e}^{r(1-P_n/P_{\max})-aH_n} \\ H_{n+1} &= c\lambda P_n \left(1 - \mathrm{e}^{-aH_n}\right) \end{aligned} \tag{1.3}$$

The form $e^{r(1-P_n/P_{\max})}$ is the host density dependence and growth[29]. According to this definition, $P_{\max}$ is the host's environment imposed carrying capacity when the parasite is absent. In system (1.3), the parasite density depends on the stage attacked by the parasites at a particular time in their life cycle. During density-dependent growth regulation, the H_n herbivores search for P_n hosts. It means that herbivores of the next generation depend on the initial host P_n population, before parasitism.

Now, we can consider the following system for a more realistic representation model

$$\begin{aligned} P_{n+1} &= P_n \exp\left(r\left(1 - \frac{P_n}{k}\right) - bH_n\right) \\ H_{n+1} &= P_n \left(1 - \exp\left(-aH_n\right)\right) \end{aligned} \tag{1.4}$$

Beddington et al studied the predator-prey model for the case where b equals a in the density-dependent case[29]. Choosing the appropriate family chart of coordinate changes (dependent upon

a set of parameters), assuming $b = r$, subsequently the three positive parameters a, r, and k determine the behavior of the two populations. In this system, the Ricker difference equation[11] $P_{n+1} = P_n \exp r\,(1 - P_n/k)$ is used to represent the dynamics for $H = 0$. Thus, the growth of the prey is limited and does not become unbounded if the Ricker difference equation is used. Using the same idea, we can develop models that are density dependent and may take the general form:

$$\begin{aligned} P_{n+1} &= P_n g\,(P_n)\, f\,(H_n) \\ H_{n+1} &= P_n\,(1 - f\,(H_n)) \end{aligned}$$

where a prey species' survival rate in each generation is given by f. We may be able to modify systems like (1.5) to exhibit features like Neimark-Sacker bifurcation[30]

$$\begin{aligned} P_{n+1} &= r P_n \exp\,(-b H_n) \\ H_{n+1} &= P_n\,(1 - \exp\,(-a H_n)) \end{aligned} \tag{1.5}$$

and the period-doubling bifurcations associated with the Ricker map.

Roughly speaking, Neimark–Sacker bifurcation of the model defines that both host and parasite populations oscillate around some mean values. The oscillations are stable and will continue indefinitely under appropriate conditions.

In addition to having an attracting invariant curve that undergoes Neimark-Sacker bifurcation, there is a nontrivial steady-state solution in system (1.5) where the parameter values are stable for a certain range, which can be explicitly determined. The steady state may exhibit repelling behavior in some parameter spaces or attracting dynamics in other parameter regions.

A general model for the interaction between plants and herbivores[20] can also be presented by

$$\begin{aligned} P_{n+1} &= P_n \mathrm{e}^{r(1-P_n/P_{\max}) - aH_n} \\ H_{n+1} &= P_n \mathrm{e}^{r(1-P_n/P_{\max})}\left(1 - \mathrm{e}^{-aH_n}\right) \end{aligned}$$

considering the following assumptions:

Assumption 1. P_n represents the plant population's (nutritious) biomass after the attacks by the herbivore population, but before its defoliation. At the end of the season n, H_n represents the biomass of herbivores before they die.

Assumption 2. In the absence of herbivores, biomass growth is governed by Ricker's model with constant growth rates r and plant carrying capacities $P_{\max}$. Ricker dynamics determine how much new foliage the herbivore can consume.

Assumption 3. It is assumed that herbivores search for food at random. A herbivore's total consumption of biomass is measured by a constant, a, that correlates with the leaf area consumed. It takes the herbivore one unit of time (year) to complete its life cycle, and the larger the parameter a, the faster the feeding rate.

Kang et al. studied the interactions between certain plants and herbivores[20]. They developed an interesting host-parasite model. Leaves and herbivore biomass considered as state variables were used in their two-dimensional discrete-time model. In their model, the parameter space consisted of two parameters, one representing the growth rate of the host population, the other representing the damage caused by herbivores. Bifurcation diagrams presented in the parameter space were insightful. The bistability result and the crisis of a strange attractor suggested two alternative strategies for controlling herbivore populations: decreasing the population below some threshold or increasing the growth rate of the plant leaves. The model was given by:

$$x_{n+1} = x_n \mathrm{e}^{r(1-x_n)-ay_n}$$
$$y_{n+1} = x_n \mathrm{e}^{r(1-x_n)} \left(1 - \mathrm{e}^{-ay_n}\right)$$

Asheghi analyzed the dynamics behavior of a discrete-time model for a two-dimensional map with four parameters[30]. He studied steady-state stability locally, period-doubling, and the Neimark –Sacker bifurcations. He found that the standard form of period-doubling bifurcation and Neimarck

Sacker bifurcation are sometimes stable or unstable. The plant–herbivore model was presented by:

$$f(x,y) = x\exp\left(r\left(1-\frac{x}{k}\right)-by\right)$$
$$g(x,y) = x(1-\exp(-ay)),$$

in the case where $x \geq 0$, $y \geq 0$, and all the real parameters a, b, r, and k were positive, and $a \neq b$.

Initial thoughts for our model came from the forest pests defoliating millions of acres of forest each year. This is one example of a larger group of plant-herbivore interactions[27;28]. This makes them one of the most serious natural and agricultural stability challenges. Posing a great threat to North America's forests, the European Gypsy Moth (Lymantria dispar or EGM), a European moth that came to Massachusetts in 1869, devoured more than 300 species of trees and shrubs in the forests of the northeastern part of the US. Caterpillars have only one goal in mind: to kill trees. To do this, they damage trees, defoliate them, and make them more susceptible to diseases, and other pests[27;28].

A gypsy moth develops from an egg into a larva (caterpillar), then a pupa, and eventually an adult[27;28]. 500 to 1,000 eggs of female gypsy moths rest beneath the bark of trees. The eggs hatch into caterpillars in the spring (April) and enter the pupal stage in the early summer (June to early July). Adult Gypsy moths can be spotted from July to August after emerging from pupae in 10 to 14 days. The Gypsy Moth has one generation every year, and its population fluctuates in cycles that continue to climb and drop[27;28].

This knowledge gives us the idea of developing a new model shown below. We plan to analyze the system's behavior to understand how this is occurring each year.

In this dissertation, we plan to investigate a different system of Nicholson-Bailey's discrete host-parasite model presented by:

$$f(x,y) = x\, e^{r(1-\frac{x}{k})}\frac{a}{a+by},$$
$$g(x,y) = x\left(1-\frac{a}{a+by}\right),$$

where the parameters r, k, a and b are positive and $a \neq b$. We study local and global stability analy-

ses of the model. We also analyze the stability of period-doubling bifurcation and Neimarck Sacker bifurcation. Subsequently, we add the Allee effect dynamics to the newly developed Nicholson-Bailey model. In biology, the Allee effect is a population dynamics phenomena that grows with increasing density. Warder Clyde Allee, American ecologist, described it for the first time in the 1930s[66]. A strong Allee effect can be understood as an attractor generated by the extinction equilibrium. The principal dynamics of the interaction between two species prone to the Allee effect can be described by a 'phase space core' of three or four equilibrium states.

Several studies have dealt with the Allee effect in different aspects. Liu et al. examined the host-parasite interaction in a discrete-time model[67]. When the Allee effect was added, they found that the parameter ranges in which population dynamics were chaotic were compressed. Furthermore, the sensitivity to initial conditions of the host-parasitoid system decreased once the Allee effect was added. Thirdly, they have observed two seemingly complicated dynamics, intermittent chaos, and supertransients, the transient phase's length, which normally increases rapidly as system size increases, supertransients, without the Allee effect. By including the Allee effect, however, these two phenomena were replaced by another type of phenomenon-period alternation, which eliminated chaos. Based on the three novel findings mentioned above, it can be concluded that the Allee effect may also reduce dynamic complexity. Liu et al. introduced and described a single-species model with Allee effect:

$$H_{t+1} = H_t \exp\left(\frac{r\left(1 - H_t/K\right)\left(H_t - c\right)}{H_t + m}\right) \tag{1.6}$$

where H_t represented the population size at time t, and r represented the intrinsic growth rate. The environment's carrying capacity was given by K. The term $\left(H_t - c\right) / \left(H_t + m\right)$ was the Allee effect added to the original system. The parameter c was the lower bound for the host, while m was known as the Allen effect constant.

To assess the synergistic effects of Allee effects and parasitism, Kang et al. analyzed population dynamics of discrete-time host-parasite systems with component Allee effects, which occurred when a decline in population size results in a reduction in the value of any component of individual fitness[64], generated by predation satiation in hosts, which indicated that predators with

a functional/numerical Holling type-II response may cause their prey to develop an Allee mechanism[65]. In fact, one of the most intriguing results suggested that, because of a substantial Allee effect and parasitism, it would be conceivable for hosts and parasites to coexist in such large concentrations. Under various parameter ranges, they showed that component Allee effects might also result in the loss of interior equilibrium. The model was presented by:

$$\begin{aligned} N_{t+1} = F(N_t) &= N_t \quad \times \underbrace{\mathrm{e}^{r(1-N_t)}}_{\text{growth term with intraspecific competition}} \times \underbrace{I(N_t)}_{\text{component Allee effects}} \\ &= N_t \mathrm{e}^{r\left(1-N_t-\frac{m}{1+bN_t}\right)}. \end{aligned} \tag{1.7}$$

In this model, r indicated the maximum birth rate of the species, m was the predation intensity, b indicated handling time, the time it takes for a predator to handle food, starting with when the predator finds its victim and ending when it is consumed, and $r, b,$ and m were all positive parameters.

Wu and Zhao investigated the qualitative behavior of a discrete host-parasite model with refuge, which is a term used in ecology to describe a location where an organism might hide from predators in order to avoid being discovered, and strong Allee effects on the host[68]. They discovered that the refuge may lead to the extermination of parasitoids while the hosts were still going strong or that the refuge may stabilize the hosts-parasitoids' interaction. If both refuge and Allee effects were present, they may have had a negative or positive effect on the coexistence of both populations. In a host-parasitoid model with the refuge and Allee effects in the host, they showed that the coexistence of two populations would depend on the starting population sizes:

$$\begin{cases} N_{t+1} = (1-\gamma)N_t \mathrm{e}^{r\left(1-\frac{N_t}{K}\right)} + \gamma N_t \mathrm{e}^{r\left(1-\frac{N_t}{K}\right)} \mathrm{e}^{-aP_t}, t = 0, 1, 2, \cdots, \\ P_{t+1} = \gamma\beta N_t \left(1-\mathrm{e}^{-aP_t}\right) \end{cases} \tag{1.8}$$

This model incorporated a host population density dependency and subjected each generation of hosts to a fixed percentage of refuges. γ, K, a, r, and β were all positive constants and $0 < \gamma < 1$. γ was the fixed proportion of hosts that the parasitoids had access to in each generation. a standed for searching effectiveness, and N_t and P_t represented the host and parasite population densities

at generation t, respectively. The carrying capacity, also known as the maximum population size that could be sustained by the currently available and potentially restricted resources, was represented by K. The average number of offspring a parasite may produce from a parasitized host was represented by β, while the host's intrinsic growth rate was given by r.

Elaydi and Saker investigated the development of several population models using Allee effects[70]. They created a number of fitness functions that result in models with Allee effects that correlate. Their work was focused on a new mathematical model that results from a reasonable fitness function. Dynamics of 2-periodic systems with Allee effects were then studied. Results indicated that there existed a 2-periodic carrying capacity that was asymptotically stable.

Luís et al. studied two species in a Ricker-type competition model[69]. In addition to complete analysis of stability and bifurcation, the authors identified stable and unstable centers of manifolds. Results of the autonomous Ricker competition showed bifurcation at subcritical points, bubbles, which may engage in transient behavior that involves splitting into two nearly equal bodies, which then experience symmetry break before recombining or splitting indefinitely, and period-doubling bifurcations, but no Neimark-Sacker bifurcations.

By analyzing sources of competition, mutualism, and predator-prey models, Livadiotis and Elaydi proposed a general framework for establishing the Allee effect[71]. Their study focused on the Allee effect caused by interspecific interaction. Additionally, they demonstrated how semistable equilibria resulted in a greater number of possible Allee effect cores. The model was presented by

$$\begin{aligned} x_{n+1} &= \frac{a_1 x_n^2}{1 + x_n^2 + b_1 y_n} \\ y_{n+1} &= \frac{a_2 y_n^2}{1 + y_n^2 + b_2 x_n} \end{aligned} \tag{1.9}$$

where $x_n > 0$, $y_n > 0$, $a_{1,2}$, $b_{1,2} > 0$. This model may have nine steady states.

For our Allee effect model, we analyze the local stability of its steady states and bifurcation theory. The model after adding the Allee effect dynamics to the newly developed Nicholson-Bailey

model takes the form:

$$
\begin{aligned}
f(x,y) &= x^{1+\alpha}\, e^{r(1-\frac{x}{k})}\frac{1}{1+\frac{b}{a}y},\\
g(x,y) &= x\left(1-\frac{1}{1+\frac{b}{a}y}\right),
\end{aligned}
\tag{1.10}
$$

The system then identifies regions where the Allee effect eventually leads to chaos. After that, it analyzes multiple bifurcation analyses of the system, including period-doubling behavior and Neimark-Sacker bifurcation.

This dissertation contains two scientific articles and the rest of the chapters are organized as follows. Chapter (2) presents an overview of discrete systems, stability, center manifold, and bifurcation theory for maps. Chapter (3) is the first scientific paper that shows the analysis of stability and bifurcations of a modified Nicholson-Bailey type model. In Chapter (4), using the modified model described in Chapter 2, we investigate the stability and bifurcation of the Nicholson-Bailey type model with an Allee effect, and the numerical computations have also confirmed our results. The final chapter provides a summary and comparison of the two scientific articles.

Chapter 2

Preliminaries

The first few questions this dissertation seeks to answer are: "Is the steady state stable or unstable? As the eigenvalue changes, how does it affect the stability or instability? Does it lead to chaos or not?". We answer these questions analytically and numerically in Chapters 3 and 4 for different boundary and interior steady states. This chapter recalls the historical case of stability analysis and bifurcation theory for maps. It provides some basic definitions and theorems which will be useful in the sequel. In addition, it presents some results which are inspired by some known theorems such as the Linearizesd Stability Theorem and Center Manifold Theory.

2.1 Stability of a Steady State

Consider the map $F : \mathbb{R}^m \to \mathbb{R}^m$ and the generation at time n: $X_n \in \mathbb{R}^m$ then we have the discrete system

$$X_{n+1} = F(X_n), \quad n = 0, 1, \ldots \tag{2.1}$$

Let the initial population be given by X_0, then the steady state can define as follow $X_{N+1} = F(X_N) = X_N$ for some N then $X_n = X_N$ for all $n \geq N$. This is called steady state of F. For simplicity, let X^* be steady state, that is, $X^* = F(X^*)$. If X_{N_0} is close to X^* and X_n remains close to, or within a neighborhood of, X^* for all $n \geq N_0$, we then say X^* is stable steady state. The following definition can define the stability in formal way.

Definition 2.1.1. The steady state X^* is called (locally) stable if for every $\varepsilon > 0$ there exists $\delta = \delta(\varepsilon) > 0$ such that $\|X_0 - X_n\| < \delta$ exists, then the solution satisfies $\|X^* - X_n\| < \varepsilon$ in $\mathbb{R}^m$. The steady state X^* is called asymptotically (locally) stable if it is (locally) stable and there exists a constant $c > 0$ such that, if $\|X_0 - X_n\| < c$ then $\lim_{n\to\infty} \|X^* - X_n\| = 0$. The steady state X^* is called unstable if it is not stable.

Theorem 2.1.2. *Stability of X^* can often be determined from Jacobin $J = DF(X^*)$ where D is the derivative.*

- *If all eigenvalues of J satisfy $|\lambda| < 1$, then X^* is stable.*
- *If some eigenvalues of J satisfy $|\lambda| > 1$ then X^* is unstable.*

Throughout this work, two different steady states will be shown, a hyperbolic steady state and a non-hyperbolic steady state. Here is the definition,

2.2 Hyperbolic and Non-Hyperbolic Steady States

Let $F(X^*) = X^*$ be a steady state of $X_{n+1} = F(X_n), X \in \mathbb{R}^m$. Then X^* is called a hyperbolic steady state if all eigenvalues of Jacobian derivative $DF(X^*)$ have modulus different from 1. The non-hyperbolic steady state if at least one of the eigenvalues obtained from the Jacobian derivative $DF(X^*)$ has modulus 1.

In this work applying transformations from trace and determinant plane to the other planes are one of the most important concepts in our analysis. Define the 2×2 matrix J by

$$J = \begin{pmatrix} a & b \\ c & d \end{pmatrix}.$$

determined from the Jacobin matrix $J = DF(X^*)$ and define the trace of J by $\mathrm{tr} = \mathrm{tr}(J)$ and the determinant of J by $\det = \det(J)$ and they are real numbers.

The following linearization theorem states the stability conditions for every initial condition

$X_0 = (x_0, y_0)$ of (2.1) for the following two dimensional system:

$$\begin{aligned} x_{n+1} &= f(x_n, y_n), \\ y_{n+1} &= g(x_n, y_n), \end{aligned} \tag{2.2}$$

Theorem 2.2.1. ***(Linearized Stability Theorem[35])***

(i) If both roots of the quadratic equation

$$\lambda^2 - \operatorname{tr}\lambda + \det = 0 \tag{2.3}$$

lie in the open unit disk $|\lambda| < 1$, then the steady state X^* of the discrete system (2.1) is locally asymptotically stable.

(ii) If at least one of the roots of equation (2.3) has absolute value greater than one, then the steady state X^* of the discrete system (2.1) is unstable.

(iii) A necessary and sufficient condition for both roots of discrete system (2.3) to lie in the open unit disk $|\lambda| < 1$ is

$$|\operatorname{tr}| < 1 + \det < 2. \tag{2.4}$$

In this case the locally asymptotically stable steady state point X^* of the discrete system (2.1) is called a sink.

(iv) A necessary and sufficient condition for both roots of equation (2.3) to have absolute value greater than one is

$$|\det| > 1 \quad \textit{and} \quad |\operatorname{tr}| < |1 + \det|\,. \tag{2.5}$$

In this case the steady state point X^* of discrete system (2.1) is called a repeller.

(v) A necessary and sufficient condition for one root of equation (2.3) to have absolute value less than one and the other root of equation (2.3) to have absolute value greater than one is

$$\operatorname{tr}^2 - 4\,\det > 0 \quad \textit{and} \quad |\operatorname{tr}| > |1 + \det|\,. \tag{2.6}$$

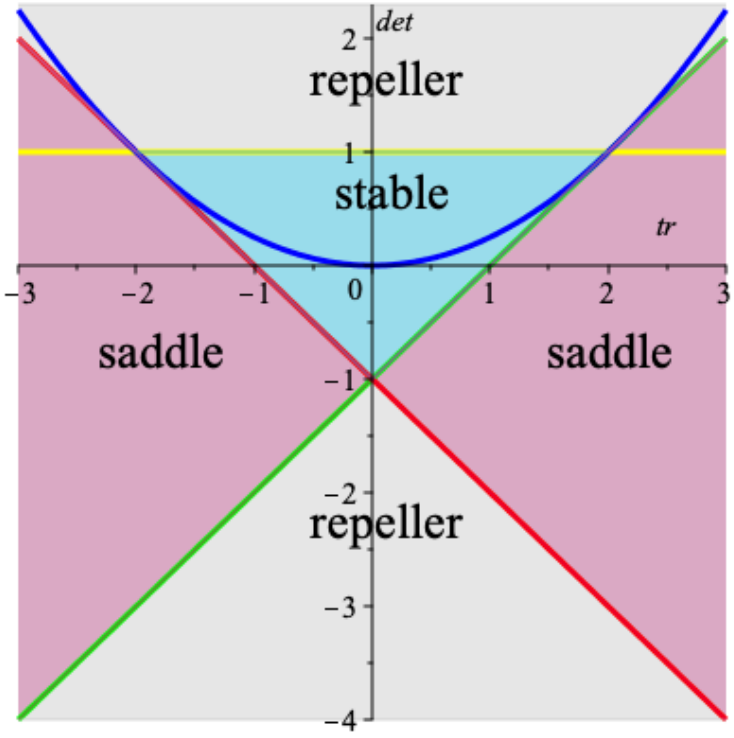

Figure 2.1: Different stability regions (stable, repelling, and saddle) in the trace-determinant (tr-det) plane.

In this case the unstable steady state X^* of the discrete system (2.1) is called a saddle point.

(vi) A necessary and sufficient condition for one root of equation (2.3) to have absolute value equal to one is

$$|\mathrm{tr}| = |1 + \det| .$$

Or

$$\det = 1 \quad \textit{and} \quad |\,\mathrm{tr}\,| \leq 2$$

In this case the steady state X^* of equation (2.3) is called a non-hyperbolic point.

Figure (2.1) provided a summary of regions from the Linearized Stability Theorem in the $\mathrm{tr} - \det$ plane.

We use Theorem 2.2.1 to obtain the stability conditions. From the inequality (2.4), we have the

stable condition as follows:

$$\begin{cases} \det < 1 \\ \det > \mathrm{tr} - 1 \\ \det > -\mathrm{tr} - 1 \end{cases} \tag{2.7}$$

because from the right hand side of the inequality (2.4) $\det > 0$, we obtain $\det < 1$. And from the left hand side, $|\,\mathrm{tr}\,| < 1 + \det$ gives $-1 - \det < \mathrm{tr} < 1 + \det$, meaning that $\det > \mathrm{tr} - 1$ and $\det > -\mathrm{tr} - 1$.

From the inequality (2.5), we have the repelling condition by

$$\begin{cases} \det > 1 \\ \det > \mathrm{tr} - 1 \\ \det > -\mathrm{tr} - 1 \end{cases} \quad \text{or} \quad \begin{cases} \det < \mathrm{tr} - 1 \\ \det < -\mathrm{tr} - 1 \end{cases} \tag{2.8}$$

Similarly, from the inequality (2.6), we have the saddle condition by

$$\begin{cases} \mathrm{tr} < 0 \\ \det > \mathrm{tr} - 1 \\ \det < -\mathrm{tr} - 1 \end{cases} \quad \text{or} \quad \begin{cases} \mathrm{tr} > 0 \\ \det < \mathrm{tr} - 1 \\ \det > -\mathrm{tr} - 1 \end{cases} \tag{2.9}$$

An invariant manifold is important to compute the center manifold, stable manifold, and unstable manifold for discrete systems or nonlinear maps.

2.3 Invariant Manifolds

Trajectories that are asymptotically departing or approaching an orbit called invariant manifolds.

2.3.1 Stable and Unstable Manifolds

W^s represents the set of trajectories that could take to reach the orbit's stable eigenvector. It can be written as

$$W^s(X^*) = \{X : F^n(X) \to X^*, n \to \infty\}$$

W^u represents the set of trajectories that depart the orbit as time moves forward. It can be written as

$$W^u(X^*) = \{X : F^{-n}(X) \to X^*, n \to \infty\}$$

.

E^s= span of eigenvectors coresponding to eigenvalues of modulus < 1

E^u= span of eigenvectors coresponding to eigenvalues of modulus > 1

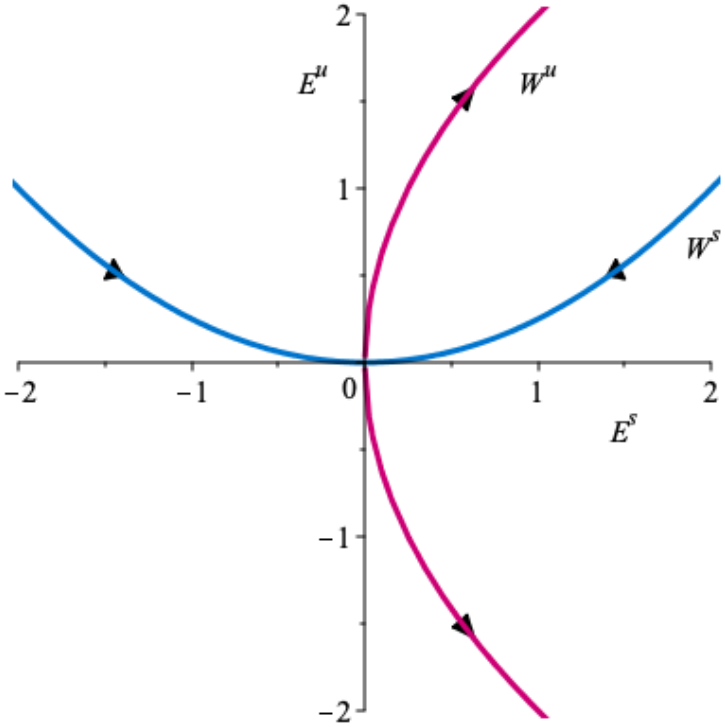

Figure 2.2: The local stable and unstable manifolds pass through 0.

Theorem 2.3.1. *(Invariant Manifold Theorem) Suppose that $F \in C^2$. Then there exist C^2 stable*

W^s and unstable W^u manifolds tangent to E^s and E^u, respectively, at $X = 0$ and C^1 center manifold W^c tangent to E^c at $X = 0$. Moreover, the manifolds W^c, W^s and W^u are all invariant[69].

Note that the definition of center manifold W^c is given below.

2.3.2 Center Manifolds

In this section, we provide the necessary definitions and theorems to analytically calculate the center manifold, as well as stable and unstable manifolds for any nonlinear. To present the center manifold theory for map, we start giving the following definition.

Definition 2.3.2. (wiggins[42]) Center manifold is an invariant manifold tangent at the steady-state in the direction of eigenvector with one of the eigenvalues of modulus 1.

By using a suitable change of variables, Suppose we have the map

$$\begin{aligned} X &\longmapsto AX + F(X,Y), \\ Y &\longmapsto BY + G(X,Y), \end{aligned} \tag{2.10}$$

where X is the center variable, and Y is the stable variable yes it is stable variable and you can see that $(X,Y) \in R^c \times R^s$, and $(X,Y) \in \mathbb{R}^c \times \mathbb{R}^s$. Moreover, F and G are $\mathbf{C}^t$ $(t \geq 2)$ nonlinear, second order or higher, map in some neighborhood of the origin, A is a $c \times c$ matrix having eigenvalues with modulus one, and B is an $s \times s$ matrix having eigenvalues with modulus less than one.

We can present the map as a system of difference equation such that

$$\begin{aligned} X_{n+1} &= AX_n + F\left(X_n, Y_n\right), \\ Y_{n+1} &= BY_n + G\left(X_n, Y_n\right), \end{aligned} \tag{2.11}$$

where the interesting dynamics can be studied for the stability of the origin $(0,0)$ where

$$\begin{aligned} F(0_c, 0_s) &= 0_c, \quad DF(0,0) = 0_{c\times(c+s)} \\ G(0_c, 0_s) &= 0_s, \quad DG(0,0) = 0_{s\times(c+s)} \end{aligned}$$

it presented locally as follow

$$W^c(0) = \{(X, Y) \in \mathbb{R}^c \times \mathbb{R}^s | Y = h(X), |X| < \delta, h(0) = 0, Dh(0) = 0\}$$

for δ sufficiently small and h can be found in the following.

Obviously $(X, Y) = (0, 0)$ is a steady state of (2.10), and the linear approximation is not sufficient for determining its stability since at least one of the eigenvalues has modulus 1. We then have the following theorem.

Theorem 2.3.3. *(Wiggins[42]) There exists a C^t center manifold for solutions of map (2.10). The dynamics of map (2.10) restricted to the center manifold is, for U sufficiently small, given by the following map*

$$U \longmapsto AU + F(U, h(U)), \quad U \in \mathbb{R}^c \tag{2.12}$$

Theorem 2.3.4. *(Stability[45])*

i) Suppose the steady state of (2.12) is stable, asymptotically stable or unstable; then the steady state of (2.10) is also stable, asymptotically stable, or unstable.

ii) Suppose the steady state of (2.12) is stable. Then if (X_n, Y_n) is a staedy state of (2.10) with (X_0, Y_0) sufficiently small, there is a solution U_n of (2.10) such that as $n \to \infty$, the (X, Y) coordinates of any point in $W^c(0)$ must satisfy

$$Y_{n+1} = h(X_{n+1}). \tag{2.13}$$

where the map h takes the following form to compute the center manifold

$$Y = h^c(X) = \alpha X^2 + \beta X^3 + \mathcal{O}\left(X^4\right) \equiv 0.$$

Differentiating (2.13) with respect to time implies that the (X, Y) coordinates of any point in

$W^c(0)$ must satisfy

$$Y_{n+1} = Dh(X)X_{n+1}. \tag{2.14}$$

As a results, any point in $W^c(0)$ must follow the dynamics generated by (2.11). Therefore, substituting

$$\begin{aligned} X_{n+1} &= AX_n + F(X_n, h(X_n)), \\ Y_{n+1} &= Bh(X_n) + G(X_n, h(X_n)) \end{aligned} \tag{2.15}$$

into (2.14) gives the map

$$Dh(X)[AX + f(X, h(X))] = Bh(X) + g(X, h(X))$$

We can now define $\mathcal{N}(h(X))$ to find the center manifold as follows:

$$\mathcal{N}(h(X)) \equiv Dh(X)[AX + F(X, h(X))] - Bh(X) - G(X, h(X)) = 0$$

Also, the center manifold for map can then find the stable manifold

$$W^s = \{(X, Y) \in \mathbb{R}^c \times \mathbb{R}^s : Y = h(X)\},$$

In this work, we use the cobweb diagram which is employed to assess the stability of center manifold's graphs. The cobweb diagram is one of the best graphical iteration techniques for assessing the stability of steady state. On the $v-u$ plane, we plot a diagonal line $u = v$ and the curve $u = h(v)$. We start at an initial point v_0. Then we move vertically once we hit the graph of h at the point $(v_0, h(v_0))$. We then move horizontally to meet the line $u = v$ at the point $(h(v_0), h(v_0))$. This determines $h(v_0)$ on the v axis. To find the second iteration $h(h(v_0)) = h^2(v_0)$, we move again vertically until we strike the graph of h at the point $(h(v_0), h^2(v_0))$, then we move horizontally to meet the line $v = u$ at the point $(h^2(v_0), h^2(v_0))$. Continuing this process, we can evaluate

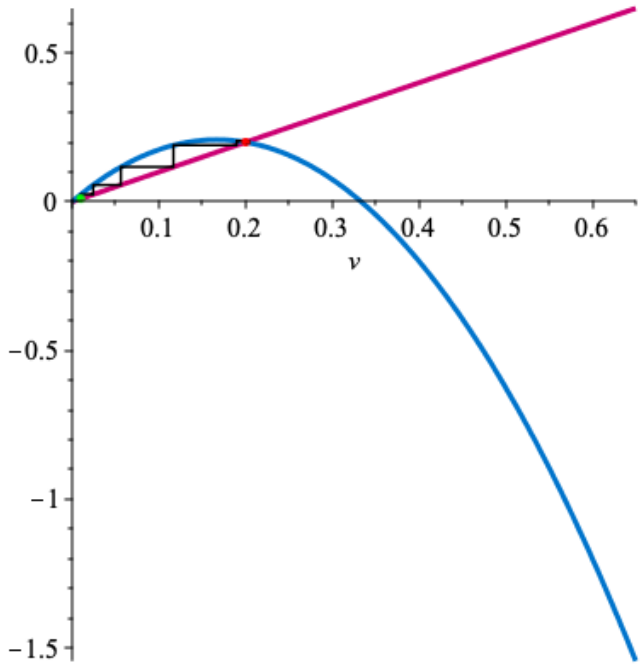

Figure 2.3: The cobweb diagram can show if the center manifold is stable or unstable.

all of the points in the orbit of v_0, namely, the set $\{v_0, h(v_0), h^2(v_0), \ldots, h^n(v_0), \ldots\}$.

2.4 Bifurcation

In this section, we present some of the main types of bifurcation theory. Bifurcation means topologically different behavior as the parameter changed, in other words, the dynamic changes as a particular parameter varies. The main objective of this section is that in the parameter space, we need to know how to find the bifurcation of the steady-state of the map. Then how can we determine its stability? In the following, we present the conditions and definitions that we will need to study our models in this work.

2.4.1 Properties of Bifurcation

Consider a discrete-time dynamical system depending on a parameter r

$$X \mapsto F(X; r), \quad X \in \mathbb{R}^m, r \in \mathbb{R}^1 \tag{2.16}$$

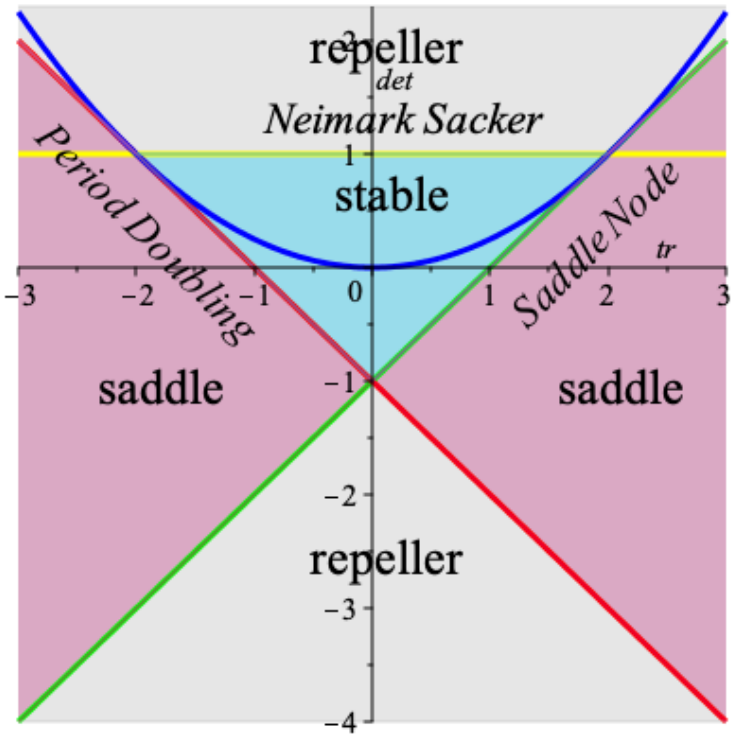

Figure 2.4: The incidence of the three main types of bifurcation in the trace-determinant (tr-det) plane. Neimark-Sacker bifurcation when det =1, Period-doubling bifurcation when $\det = -\operatorname{tr} -1$, and Saddle-Node bifurcation when $\det = \operatorname{tr} -1$.

where the map F is smooth with respect to both X and r. Consider $X = X_0$ to be a hyperbolic steady state of the system for $r = r_0$. Let us analyze this steady-state and its eigenvalues while the parameter r varies. We can observe that there are only three ways in which the hyperbolicity condition can be violated. Either a positive eigenvalues approaches the unit circle and we have $\lambda = 1$, or a negative eigenvalues approaches the unit circle and we have $\lambda = -1$, or a pair of complex eigenvalues reach the unit circle and we have $\lambda_{1,2} = e^{\pm i\theta_0}$, $0 < \theta_0 < \pi$, for some value of the parameter r. Figure (2.5) provided the three cases.

In the following, three main types of local bifurcations for maps will be presented. Local bifurcations of the system $X_{n+1} = F(X_n)$ is smooth and occurs at parameter values for which a steady-state or periodic orbit is non-hyperbolic. We also know that steady-states of a map are nonhyperbolic if one or more eigenvalues obtained from the Jacobin lie on the unit circle.

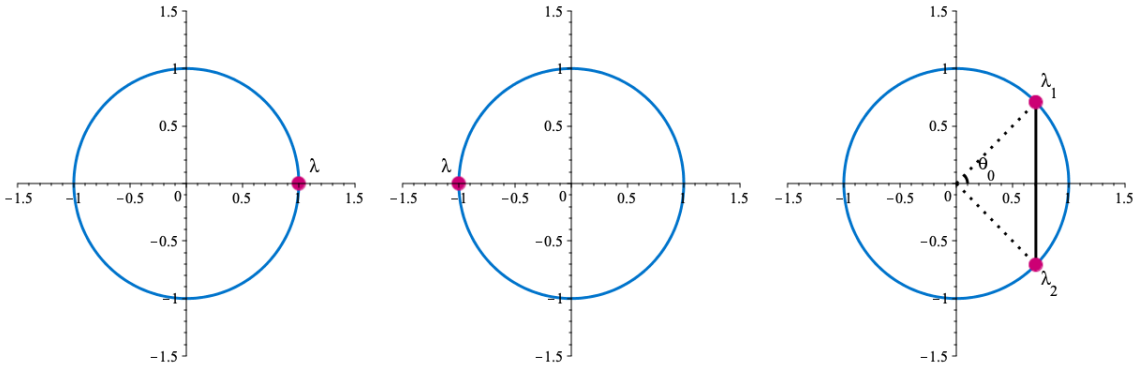

Figure 2.5: From left to right: a positive eigenvalue approaches the unit circle ($\lambda = 1$), a negative eigenvalue approaches the unit circle ($\lambda = -1$), or a pair of simple complex eigenvalues reach the unit circle ($\lambda_{1,2} = e^{\pm i\theta_0}$, $0 < \theta_0 < \pi$).

2.4.2 Period-Doubling Bifurcation

Consider a nonhyperbolic steady state and one of the eigenvalues associated with the linearization of the map about the steady state equals -1. This is associated with a bifurcation called period-doubling. The formal definition is stated as follows.

Definition 2.4.1. The bifurcation associated with the appearance of $\lambda_1 = -1$ is called a flip (or period-doubling) bifurcation.

Consider a one-parameter family of C^t $(t \geq 2)$ one-dimensional maps

$$x \mapsto f(x, r), \quad x \in \mathbb{R}^1, \quad r \in \mathbb{R}^1. \tag{2.17}$$

To compute the period-doubling bifurcation, there are some conditions sufficient for (2.17) that we should follow. These conditions are obtained from Wiggins[42]. It is sufficient for (2.17) to satisfy

$$f(0,0) = 0 \tag{2.18}$$

$$\frac{\partial f}{\partial x}(0,0) = -1 \tag{2.19}$$

$$\frac{\partial f^2}{\partial r}(0,0) = 0 \tag{2.20}$$

$$\frac{\partial^2 f^2}{\partial x^2}(0,0) = 0 \tag{2.21}$$

$$\frac{\partial^2 f^2}{\partial x \partial r}(0,0) \neq 0 \tag{2.22}$$

$$\frac{\partial^3 f^2}{\partial x^3}(0,0) \neq 0 \tag{2.23}$$

$$\tag{2.24}$$

The equation $\left(-\frac{\partial^3 f^2(0,0)}{\partial x^3}/\frac{\partial^2 f^2(0,0)}{\partial x \partial r}\right)$ shows on which side the period doubling bifurcation lies. In this case the bifurcation said to be stable if

$$\left(\frac{\partial^3 f^2}{\partial x^3}(0,0)/\frac{\partial^2 f^2}{\partial x \partial r}(0,0)\right) < 0$$

and it is unstable if

$$\left(\frac{\partial^3 f^2}{\partial x^3}(0,0)/\frac{\partial^2 f^2}{\partial x \partial r}(0,0)\right) > 0$$

.

2.4.3 Saddle-Node Bifurcation

Definition 2.4.2. A bifurcation associated with the appearance of $\lambda_1 = 1$ is called a fold, tangent or saddle-node bifurcation. It has a similar conditions to period-doubling bifurcation.

2.4.4 Neimark-Sacker Bifurcation

Definition 2.4.3. A bifurcation corresponding to the presence of $\lambda_{1,2} = e^{\pm i\theta_0}$, $0 < \theta_0 < \pi$, is called a Neimark-Sacker (or torus) bifurcation. This bifurcation require a two or higher dimensional map.

Let r be a parameter and $F_r : \mathbb{R}^2 \to \mathbb{R}^2$ with steady state $(0,0)$ where F_r smoothly depends on r and $-\varepsilon < r < \varepsilon$. Suppose for r close to 0 that $D\,F_r(0,0)$ has a complex pair of eigenvalues $\lambda(r)$, $\overline{\lambda(r)}$, $\lambda(r) \neq \overline{\lambda(r)}$ that means

(i) For $-\varepsilon < r < 0$, $|\lambda(r)| = |\overline{\lambda(r)}| < 1$.

(ii) For $r = 0$, $|\lambda(0)| = |\bar{\lambda}(0)| = 1$.

(iii) For $0 < r < \varepsilon$, $|\lambda(r)| = |\overline{\lambda(r)}| > 1$.

Then there are three cases:

(i') $r < 0$: $(0, 0)$ attractor.

(ii') $r = 0$: the dynamics is not clear.

(iii') $r > 0$: $(0, 0)$ repeller.

Theorems and a lemma utilized to calculate the Naimark-Sacker Bifurcation are discussed in the paragraphs that follow. Consider the system

$$X \mapsto F(X, r), X = (X_1, X_2)^T \in \mathbb{R}^2, r \in \mathbb{R}^1,$$

where F is a smooth function, which has at $r = 0$ the steady-state $X = 0$ with eigenvalues $\lambda_{1,2} = e^{\pm i\theta_0}$, $0 < \theta_0 < \pi$. By the implicit function theorem, the system has a unique steady-state $X_0(r)$ in some neighborhood of the origin for all sufficiently small r, because the eigenvalue is not on the unit disk $|\lambda| \neq 1$. Thus, the system may be expressed by

$$X \mapsto J(r)X + \mathcal{F}(X, r), \tag{2.25}$$

where $\mathcal{F}$ is a smooth vector function whose components $\mathcal{F}_{1,2}$ have Taylor expansions in X starting with at least quadratic terms, $\mathcal{F}(0, r) = 0$ for any sufficiently small r. There are two eigenvalues from the Jacobian matrix J

$$\lambda_{1,2}(r) = \mu(r)e^{\pm i\theta},$$

where $\mu(0) = 1$, $\theta(0) = \theta_0$. Thus $\mu(r) = 1 + \alpha(r)$, for some smooth function $\alpha(r)$, and $\alpha(0) = 0$. Suppose that $\alpha'(0) \neq 0$. Then, we can use α as a new parameter and express the eigenvalues in terms of α so we have $\lambda_1(\alpha) = \lambda(\alpha)$, $\lambda_2(\alpha) = \overline{\lambda(\alpha)}$, where

$$\lambda_{1,2}(\alpha) = (1 + \alpha)e^{\pm i\theta(\alpha)}$$

with a smooth function $\theta(\alpha)$ such that $\theta(0) = \theta_0$.

Lemma 2.4.4. *(Kuznetsov[49]) By complex variable analysis and defining a new parameter, system (2.25) can be transformed, for all sufficiently small r, into the following form:*

$$z \mapsto \lambda(\alpha)z + g(z, \bar{z}, \alpha),$$

where $\alpha \in \mathbb{R}^1, z \in \mathbb{C}^1, \lambda(\alpha) = (1+\alpha)e^{i\theta(\alpha)}$, and g is a complex-valued smooth function of $z, \bar{z}$, and α whose Taylor expansion with respect to $(z, \bar{z})$ contains quadratic and higher-order terms:

$$g(z, \bar{z}, \alpha) = \sum_{k+l\geq 2} \frac{1}{k!l!} g_{kl}(\alpha) z^k \bar{z}^l$$

with $k, l = 0, 1, \ldots$

Lemma 2.4.5. *The map*

$$z \mapsto \lambda z + \frac{g_{20}}{2} z^2 + g_{11} z\bar{z} + \frac{g_{02}}{2} \bar{z}^2 + O\left(|z|^3\right),$$

where $\lambda = \lambda(\alpha) = (1+\alpha)e^{i\theta(\alpha)}, g_{ij} = g_{ij}(\alpha)$, can be transformed by an invertible parameter-dependent change of complex coordinate.

$$z = w + \frac{h_{20}}{2} w^2 + h_{11} w\bar{w} + \frac{h_{02}}{2} \bar{w}^2,$$

for all sufficiently small $|\alpha|$, into a map without quadratic terms:

$$w \mapsto \lambda w + O\left(|w|^3\right)$$

provided that

$$e^{i\theta_0} \neq 1 \quad and \quad e^{3i\theta_0} \neq 1$$

Lemma 2.4.6. *The map*

$$z \mapsto \lambda z + \frac{g_{30}}{6} z^3 + \frac{g_{21}}{2} z^2\bar{z} + \frac{g_{12}}{2} z\bar{z}^2 + \frac{g_{03}}{6} \bar{z}^3 + O\left(|z|^4\right)$$

where $\lambda = \lambda(\alpha) = (1+\alpha)e^{i\theta(\alpha)}, g_{ij} = g_{ij}(\alpha)$*, can be transformed by an invertible parameter-dependent change of coordinates*

$$z = w + \frac{h_{30}}{6}w^3 + \frac{h_{21}}{2}w^2\bar{w} + \frac{h_{12}}{2}w\bar{w}^2 + \frac{h_{03}}{6}\bar{w}^3$$

for all sufficiently small α*, into a map with only one cubic term:*

$$w \mapsto \lambda w + c_1 w^2\bar{w} + O\left(|w|^4\right)$$

provided that

$$e^{2i\theta_0} \neq 1 \quad and \quad e^{4i\theta_0} \neq 1$$

Lemma 2.4.7. *(Normal form for the Neimark-Sacker bifurcation) The map*

$$\begin{aligned} z \mapsto \lambda z + \frac{g_{20}}{2}z^2 + g_{11}z\bar{z} + \frac{g_{02}}{2}\bar{z}^2 \\ + \frac{g_{30}}{6}z^3 + \frac{g_{21}}{2}z^2\bar{z} + \frac{g_{12}}{2}z\bar{z}^2 + \frac{g_{03}}{6}\bar{z}^3 \\ + O\left(|z|^4\right) \end{aligned}$$

where $\lambda = \lambda(\alpha) = (1+\alpha)e^{i\theta(\alpha)}, g_{ij} = g_{ij}(\alpha)$*, and* $\theta_0 = \theta(0)$ *is such that* $e^{ik\theta_0} \neq 1$ *for* $k = 1, 2, 3, 4$*, can be transformed by an invertible parameter dependent change of complex coordinate, which is smoothly dependent on the parameter,*

$$\begin{aligned} z = w + \frac{h_{20}}{2}w^2 + h_{11}w\bar{w} + \frac{h_{02}}{2}\bar{w}^2 \\ + \frac{h_{30}}{6}w^3 + \frac{h_{12}}{2}w\bar{w}^2 + \frac{h_{03}}{6}\bar{w}^3, \end{aligned}$$

for all sufficiently small $|\beta|$*, into a map with only the resonant cubic term:*

$$w \mapsto \mu w + c_1 w^2\bar{w} + O\left(|w|^4\right)$$

where $c_1 = c_1(\alpha)$.

The following theorem summarizes the collected results.

Theorem 2.4.8. *Suppose a two-dimensional discrete-time system*

$$X \mapsto F(X, r), \quad X \in \mathbb{R}^2, r \in \mathbb{R}^1$$

with smooth F *has, for all sufficiently small* $|r|$*, the steady-state* $x = 0$ *with eigenvalues*

$$\lambda_{1,2}(r) = \mu(r) e^{\pm i\theta(r)}$$

where $\mu(0) = 1$, $\theta(0) = \theta_0$

Let the following conditions be satisfied:

(i) $r'(0) \neq 0$

(ii) $e^{ik\theta_0} \neq 1$ *for* $k = 1, 2, 3, 4$

Then, there are smooth invertible coordinate and parameter changes transforming the system into

$$\begin{pmatrix} y_1 \\ y_2 \end{pmatrix} \longmapsto \begin{pmatrix} 1+\alpha \end{pmatrix} \begin{pmatrix} \cos\theta(\alpha) & -\sin\theta(\alpha) \\ \sin\theta(\alpha) & \cos\theta(\alpha) \end{pmatrix} \begin{pmatrix} y_1 \\ y_2 \end{pmatrix}$$
$$+ \begin{pmatrix} y_1^2 + y_2^2 \end{pmatrix} \begin{pmatrix} \cos\theta(\alpha) & -\sin\theta(\alpha) \\ \sin\theta(\alpha) & \cos\theta(\alpha) \end{pmatrix} \begin{pmatrix} A(\alpha) & -B(\alpha) \\ B(\alpha) & A(\alpha) \end{pmatrix} \begin{pmatrix} y_1 \\ y_2 \end{pmatrix} + O\left(\|y\|^4\right)$$

with $\theta(0) = \theta_0$ *and* $A(0) = \mathrm{Re}\left(e^{-i\theta_0} c_1(0)\right)$*, where* $c_1(0)$ *is given by the formula*

$$c_1(0) = \frac{g_{20}(0) g_{11}(0)\,(1 - 2\mu_0)}{2\,(\mu_0^2 - \mu_0)} + \frac{|g_{11}(0)|^2}{1 - \bar{\mu}_0} + \frac{|g_{02}(0)|^2}{2\,(\mu_0^2 - \bar{\mu}_0)} + \frac{g_{21}(0)}{2}.$$

where $\mu_0 = e^{i\theta_0}$

We can now come up with the following general conclusion.

Theorem 2.4.9. *(Generic Neimark-Sacker bifurcation) For any generic two-dimensional one-parameter system*

$$X \mapsto F(X, r),$$

having at $r = 0$ *the steady state* $X_0 = 0$ *with complex eigenvalues* $\lambda_{1,2} = e^{\pm i\theta_0}$*, there is a neighborhood of* X_0 *in which a unique closed invariant curve bifurcates from* X_0 *as* r *passes through zero.*

For more details see[49].

To determine the stability of Neimark-Sacker bifurcation, we need to determine the direction (the sign) of $a(0)$, where $a(0)$ can be computed by the following

$$a(0) = \mathrm{Re}\left(\frac{e^{-i\theta_0} g_{21}}{2}\right) - \mathrm{Re}\left(\frac{\left(1 - 2e^{i\theta_0}\right) e^{-2i\theta_0}}{2\left(1 - e^{i\theta_0}\right)} g_{20} g_{11}\right) - \frac{1}{2}\left|g_{11}\right|^2 - \frac{1}{4}\left|g_{02}\right|^2 \tag{2.26}$$

The result is summarized in the following lemma.

Lemma 2.4.10. *The invariant circle is asymptotically stable for* $a(0) < 0$ *and unstable for* $a(0) > 0$[42].

2.5 Persistence of Dynamical Systems

Definition 2.5.1 (Freedman[43])**.** *A* semiflow $\varphi : \Omega \times X \to X$ is called strongly ρ-persistent, if

$$\lim_{t\to\infty} \inf \rho\big(\varphi(t, x)\big) > 0 \ \ \forall x \in X, \ \rho(x) > 0$$

Definition 2.5.2 (Freedman[43])**.** *A* semiflow $\varphi : \Omega \times X \to X$ is called strongly uniformly ρ-persistent, if there exists some $\epsilon > 0$ such that

$$\lim_{t\to\infty} \inf \rho\big(\varphi(t, x)\big) > \epsilon \ \ \forall x \in X, \ \rho(x) > 0$$

Definition 2.5.3 (Massatt[44])**.** Let $\varphi : \Omega \times X \to X$ be a semiflow. Then, φ is called point-dissipative (or ultimately bounded) if there exists a bounded subset B of X which attracts all points in X.

2.6 Lambert W Function

In this section, we present $LambertW$ function and its properties. In this work, I will use the letter W as short written for $LambertW$.

2.6.1 Properties of Lambert W Function

The multivalued inverse of the mapping $W \mapsto We^W$ is the $LambertW$ function. The branches define by using the equations $W_k(k \in \mathbb{Z})$ as follows[46]

$$W_k(\mathsf{x}) \exp\left(W_k(\mathsf{x})\right) = \mathsf{x}$$

$$W_k(\mathsf{x}) \sim \ln_k \mathsf{x} \text{ as } \mathsf{x} \to \infty, \quad \forall \mathsf{x} \in \mathbb{R}$$

where $\ln x$ is the principal branch of natural logarithm. The properties that will be used in this work are

$$\mathsf{x} = W(\mathsf{x})\, e^{W(\mathsf{x})}, \tag{2.27}$$

$$W^{-1}(\mathsf{x}) = \mathsf{x}\, e^{\mathsf{x}}, \tag{2.28}$$

$$e^{W(\mathsf{x})} = \frac{\mathsf{x}}{W(\mathsf{x})}, \tag{2.29}$$

$$e^{-W(\mathsf{x})} = \frac{W(\mathsf{x})}{\mathsf{x}}. \tag{2.30}$$

2.6.2 Real Branches

For the real values, there are two branches $W_0(\mathsf{x})$ (or $W(0, \mathsf{x})$) and $W_{-1}(\mathsf{x})$ (or $W(-1, \mathsf{x})$). They are separately defined on the domains $\frac{-1}{e} \leq \mathsf{x} < \infty$ and $\frac{-1}{e} \leq \mathsf{x} < 0$, respectively. In addition, $W_0(\mathsf{x})$ maps the positive real axis onto itself with the lower bound at the origin, $W_0(\mathsf{x}) = 0$. $W_0(\mathsf{x})$ is a

monotone increasing function with the range of $[-1, \infty)$ while $W_{-1}(\mathrm{x})$ is a monotone decreasing function, with the range of $(-\infty, -1]$. We can observe the behaviour these two monotone functions in Figure (2.6).

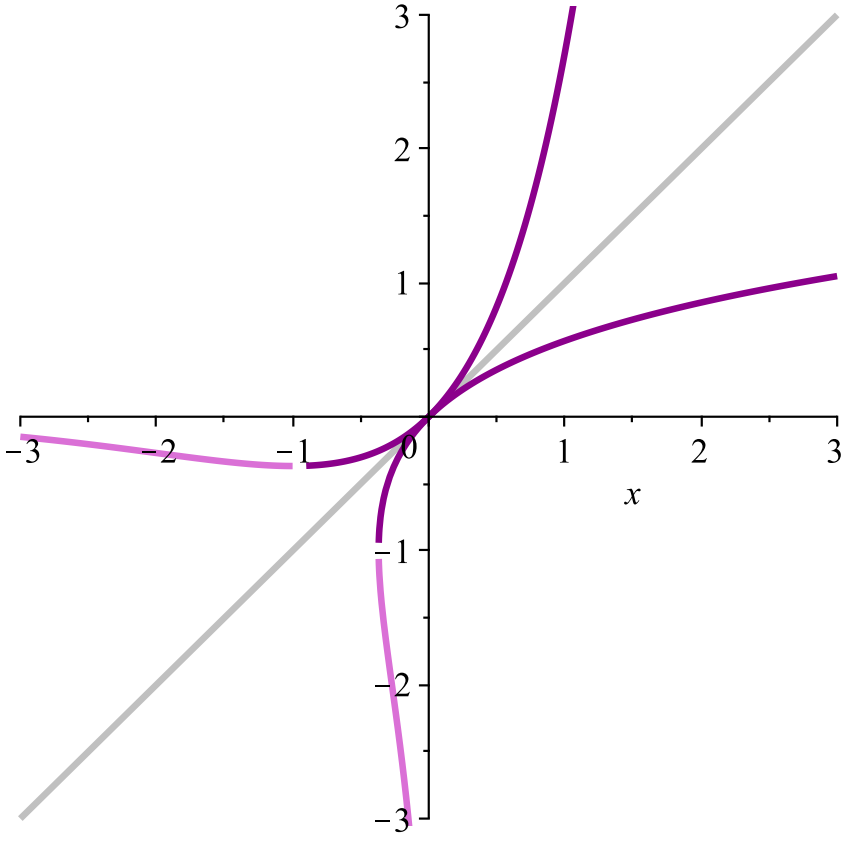

Figure 2.6: Real branches of the Lambert W and inverse functions for $W_0(\mathrm{x})$ (dark purple curve) and $W_{-1}(\mathrm{x})$ (purple curve).

Chapter 3

Stability Analysis and Bifurcations of a Modified Nicholson-Bailey Type Model

In this chapter, we investigate the dynamical behavior of a host-parasite model through the modification of a Nicholson-Bailey (MNB) model that contains four biological parameters in the first closed quadrant. By a re-scaling procedure, the MNB model is then reduced to a two-parameter system that almost entirely carries over the comprehensive dynamics of the original model. The new model always possesses two boundary steady states and we show that a third and unique interior steady state may exist under certain conditions imposed on one of the parameters.

We then analyze the local stability of each steady state for a different range of parameters by the linearization process of the model about each steady state. For specific values of the parameters in which a steady state is non-hyperbolic, the stability and dynamics of the steady state are studied by the application of bifurcation identities developed from the center manifold theory. Moreover, using the Jacobian matrix, we find thresholds for which the system is stable or unstable. We eventually study the stability analysis of a period-doubling bifurcation which may occur once we cross one of these thresholds, implying irregular dynamics which may lead to chaos. The results are supported by some simulations.

3.1 Introduction

The standard NB host- parasite model with three parameters was introduced in 1935[32]. The primary model is given by the following 2-dimensional map:

$$f(x,y) = d\,x\,e^{-a\,y}$$
$$g(x,y) = c\,x\,(1-e^{-a\,y})$$

where x represents the population of a host, y represents the population of a parasite, and parameters d, a, and c are reproductive host rate, searching efficiency, and the number of eggs of parasite which survive and feed over the hosts, respectively. In this model, the parameter d is assumed to be independent of x[32].

The MNB host-parasite model was then generalized more by different studies[33]. One of which takes into consideration the density dependence of the hosts, the parameter d, as a function of x and then the term d reduces the population of the hosts once it reaches a certain density level k using the first term of the Poisson distribution[20]. This model is then modified into the following map:

$$\begin{aligned} f(x,y) &= x\,e^{r\left(1-\frac{x}{k}\right)}e^{-a\,y} \\ g(x,y) &= c\,x\,(1-e^{-a\,y}) \end{aligned} \tag{3.1}$$

In general, if we modify the model by $f(x) = e^{r\left(1-\frac{x}{k}\right)}$ and $g(y) = e^{-a\,y}$, then map (3.1) can be presented by

$$\begin{aligned} F(x,y) &= x\,f(x)\,g(y) \\ G(x,y) &= c\,x\,\big(1-g(y)\big). \end{aligned} \tag{3.2}$$

In this article, we study a modified version of Nicholson-Bailey model (3.2) in the first closed

quadrant with the following functions f and g defined by

$$f(x) = e^{r\left(1-\frac{x}{k}\right)}, \quad \text{and} \quad g(y) = \frac{a}{a+by}$$

where the function g is related to the searching efficiency of a parasite population and reaches its maximum when there is no or a very limited number of parasite and a minimum level when there is an abundance of parasitoids. This is consistent with the definition g as the searching efficiency from the original model. Given the new host searching function, model (3.2) then yields the following form:

$$\begin{aligned} F(x,y) &= x\, e^{r\,\left(1-\frac{x}{k}\right)}\, \frac{a}{a+b\,y} \\ G(x,y) &= x\,\left(1-\frac{a}{a+by}\right). \end{aligned} \tag{3.3}$$

In the following, we will study the dynamics of the MNB model (3.3) and show that it always has two boundary steady states and a third interior steady state may appear when $b > 1$. For different parameter values, these steady states may evolve into hyperbolic or non-hyperbolic steady states. For the hyperbolic steady states, by the application of the Jury's test, we will characterize their (in)stability dynamics. However, for non-hyperbolic steady states, we determine the stability of steady states by the application of center manifold. For these, we first need to do some preliminary linear transformations of two-dimensional map (3.3) into its normal form. We will also provide two-dimensional diagrams in (x, r)-plane and (x, k)-plane for two types of codimension-one bifurcations of the discrete-time dynamical system and a codimension two bifurcation in (r, k)-plane, each of which indicates the regions where the system induced by our model is stable or unstable. Also, we will show where flip bifurcation and chaos may occur when traversing from a region to another. The results are also followed by some simulations for certain parameter values.

3.2 Steady States of the MNB Model

Consider the following two dimensional map in the first quadrant $\{(x, y) \mid x \geq 0,\ y \geq 0\}$ with non-negative parameters r, k, a and b such that $a \neq b$, since the case where $a = b$ can be easily reduced to the system shown in (3.7). Moreover, the case when the parameter a is 0 leads to a model that is not biologically and mathematically relevant to study, but when the parameter b is 0, it then becomes a Ricker model.

Map (3.3) can be rewritten by

$$\begin{aligned} F(x, y) &= x\, e^{r(1-\frac{x}{k})} \frac{1}{1+\frac{b}{a}y}, \\ G(x, y) &= x\left(1 - \frac{1}{1+\frac{b}{a}y}\right). \end{aligned} \tag{3.4}$$

From the two-dimensional map defined by equation (3.4), we obtain the following system of difference equation:

$$\begin{aligned} x_{n+1} &= x_n\, e^{r(1-\frac{x_n}{k})} \frac{1}{1+\frac{b}{a}y_n}, \\ y_{n+1} &= x_n\left(1 - \frac{1}{1+\frac{b}{a}y_n}\right). \end{aligned} \tag{3.5}$$

Using the change of variables $\mathrm{x}_n = \frac{b}{a}x_n$, $\mathrm{y}_n = \frac{b}{a}y_n$, and $\mathrm{k} = \frac{bk}{a}$ in MNB system (3.5), it then follows that

$$\begin{aligned} \mathrm{x}_{n+1} &= \mathrm{x}_n\, e^{r\left(1-\frac{\mathrm{x}_n}{\mathrm{k}}\right)} \frac{1}{1+\mathrm{y}_n}, \\ \mathrm{y}_{n+1} &= \mathrm{x}_n\left(1 - \frac{1}{1+\mathrm{y}_n}\right). \end{aligned} \tag{3.6}$$

For simplicity, we replace x_n, y_n and k in (3.6) by x_n, y_n and k respectively. It then leads to a

model that we will study in the sequel:

$$\begin{aligned} x_{n+1} &= x_n \, e^{r(1-\frac{x_n}{k})} \frac{1}{1+y_n}, \\ y_{n+1} &= x_n \Big(1 - \frac{1}{1+y_n}\Big), \end{aligned} \tag{3.7}$$

where $x_n \geq 0$, $y_n \geq 0$, and the terms x_n and y_n represent the densities of a host population and a parasitoid population following the original Nicholson-Bailey model definition at time point n, respectively. The intrinsic growth rate of the host population is denoted by r, and k is the environmental carrying capacity of the host population. It is also assumed that the biological process of reproduction may occur after generation n and before generation $n+1$[56].

It can be easily seen that system (3.7) attains two steady states, one is the origin $S_0 = (0, 0)$ and the other is a parasite free state $S_1 = (k, 0)$. In addition, for $k > 1$, an interior steady state for system (3.7) may appear, denoted by the point $S_2 = (x^*, y^*)$, which is obtained from the intersection of these two functions $f_1(y) = k - \frac{k}{r}\ln(y+1)$ and $f_2(y) = y + 1$ solved from the model given by system (3.7). These two functions, f_1 and f_2, are illustrated in Figure 3.1 for different values of the parameter k. Therefore, it follows that these two functions collide in the positive quadrant when $k > 1$.

Proposition 3.2.1. *For any $k > 1$, the functions $f_1(y) = k - \frac{k}{r}\ln(y+1)$ and $f_2(y) = y + 1$ have a unique intersection in the first quadrant.*

Proof. Let us first define $h(y) = f_1(y) - f_2(y)$. For $k > 1$, we observe that $h(0) = (f_1 - f_2)(0) = k-1$ is positive and $h(e^r-1) = (f_1-f_2)(e^r-1) = -e^r$ is negative. Moreover, $h'(y) = \frac{-k}{r(y+1)} - 1$ is negative for $y > -1$ hence h is decreasing on $(-1, \infty)$. Therefore, h has a unique root $y^* \in (0, \infty)$ for $k > 1$. □

From above, we also obtain that $x^* = y^* + 1 = f_1(y^*) \in (1, \infty)$ for $k > 1$.

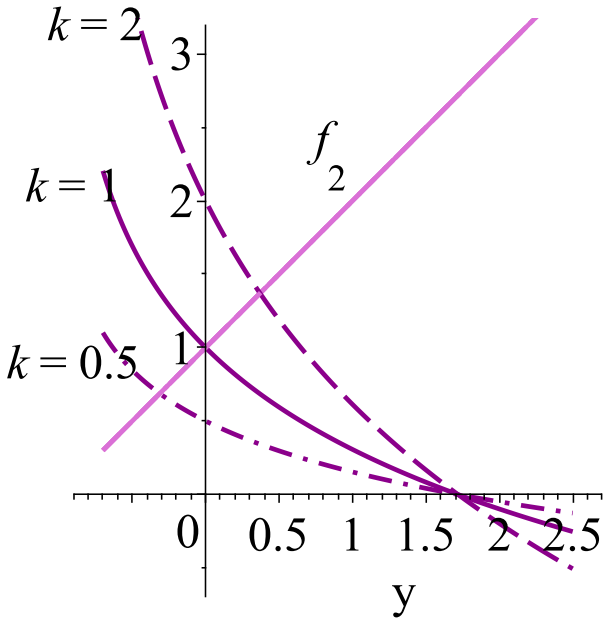

Figure 3.1: Three dark purple curves show the graph of function f_1 for different parameter values $k = 0.5, 1$ and 2, respectively. The function f_2, the light purple, is independent of k. The functions f_1 and f_2 have a positive intersection when $k > 1$.

3.3 Analysis of Local Stability

In this section, we study the local stability analysis of the model defined by system (3.7). In dynamical systems, local stability refers to the study of behavior of a dynamical system from small neighborhoods around each steady state. The stability of a system is determined by the calculation of its corresponding linearized system from a Jacobian matrix computed at each steady state.

The Jacobian matrix of the two dimensional model defined by system (3.7) is calculated by

$$J = \begin{pmatrix} \frac{\partial f}{\partial x} & \frac{\partial f}{\partial y} \\ \frac{\partial g}{\partial x} & \frac{\partial g}{\partial y} \end{pmatrix} = \begin{pmatrix} \frac{e^{r\left(1-\frac{x}{k}\right)}}{1+y} - \frac{x\, r\, e^{r\left(1-\frac{x}{k}\right)}}{k\,(1+y)} & -\frac{x\, e^{r\left(1-\frac{x}{k}\right)}}{(1+y)^2} \\ 1 - \frac{1}{1+y} & \frac{x}{(1+y)^2} \end{pmatrix}. \tag{3.8}$$

It then follows that Jacobian matrix (3.8) at the steady state $S_0 = (0, 0)$ is given by

$$J(S_0) = \begin{pmatrix} e^r & 0 \\ 0 & 0 \end{pmatrix}.$$

It is obvious that the eigenvalues of $J(0,0)$ are $\lambda_1 = e^r > 1$ and $\lambda_2 = 0 < 1$ with the corresponding eigenvectors $(1,0)^T$ and $(0,1)^T$, respectively. Since $\lambda_1 > 1$ and $\lambda_2 = 0$, the origin is a saddle point.

For the second steady state, the Jacobean matrix at the parasite free steady state $S_1 = (k,0)$ is given by

$$J(S_1) = \begin{pmatrix} 1-r & -k \\ 0 & k \end{pmatrix},$$

showing that the eigenvalues of $J(S_1)$ are $\lambda_1 = 1 - r$ and $\lambda_2 = k$, which depend on parameters r and k. To determine the stability of $S_1 = (k,0)$, one needs to study different cases which are stated by the following proposition:

Proposition 3.3.1. *According to different ranges of parameter values for r and k, the (in)stability analysis of the steady state $S_1 = (k,0)$ of the MNB model defined by system (3.7) is given as follows:*

(i) If $k < 1$ and $0 < r < 2$, then $S_1 = (k,0)$ is a stable.

(ii) If $k > 1$ and $r > 2$, then $S_1 = (k,0)$ is a repeller.

(iii) If $k < 1$ and $r > 2$, then $S_1 = (k,0)$ is a saddle.

(iv) If $k > 1$ and $0 < r < 2$, then $S_1 = (k,0)$ is a saddle.

A steady state S of a discrete-time dynamical system is said to be hyperbolic if all eigenvalues of the Jacobian matrix at p have a modulus different from 1. Moreover, the steady state S is non-hyperbolic if at least one of the eigenvalues obtained from the Jacobian matrix at S has modulus 1.

The stability of a non-hyperbolic steady state can be determined by the application of bifurcation formulae developed from center manifold theory. For system (3.7), stability of the steady state $S_1 = (k,0)$ for non-hyperbolic cases is discussed in the proposition below.

Proposition 3.3.2. *Consider sytem (3.7). Then the following statements hold true:*

(i) If $k = 1$ and $0 < r < 2$, then $S_1 = (k, 0)$ is half- stable non-hyperbolic steady state.

(ii) If $r = 2$ and $k < 1$, then the steady state $S_1 = (k, 0)$ is stable.

(iii) If $r = 2$ and $k = 1$, then the steady state $S_1 = (k, 0)$ is half-stable.

Proof. (i) Suppose $k = 1$ and $0 < r < 2$. To study the dynamics of the steady state $S_1 = (k, 0)$ in the first quadrant $Q_1 = \{(x, y) \mid x \geq 0,\ y \geq 0\}$, it is required to explicitly compute the local center manifold. For the sake of simplicity of calculation, we first translate the steady state $S_1 = (k, 0)$ of system (3.7) to origin S_0, which is done by the linear translation $(x, y) \mapsto (x + k, y)$. Then the map associated with sytem (3.7) translates to the following system:

$$\begin{aligned} f_1(x, y) =& (x + k)\, e^{r\left(1 - \frac{x+k}{k}\right)} \frac{1}{1 + y} - k, \\ g_1(x, y) =& (x + k) \left(1 - \frac{1}{1 + y}\right). \end{aligned} \tag{3.9}$$

The Taylor expansion of map (3.9) about the origin is given by

$$\begin{aligned} f_1(x, y) =& -(r - 1)\, x - k\, y + \frac{r\,(r - 2)\, x^2}{2\, k} + (r - 1)\, y\, x + k\, y^2 - \frac{r^2 (r - 3)\, x^3}{6\, k^2} \\ & - \frac{r\,(r - 2)\, y\, x^2}{2\, k} - (r - 1)\, x\, y^2 - k\, y^3 + \mathcal{O}(4), \\ g_1(x, y) =& k\, y^3 - k\, y^2 - x\, y^2 + k\, y + x\, y + \mathcal{O}(4). \end{aligned} \tag{3.10}$$

we can now consider the following change of variables from the span of eigenvectors when $k = 1$:

$$\begin{pmatrix} x \\ y \end{pmatrix} = \begin{pmatrix} 1 & -\frac{1}{r} \\ 0 & 1 \end{pmatrix} \begin{pmatrix} u \\ v \end{pmatrix} = \begin{pmatrix} u - \frac{v}{r} \\ v \end{pmatrix} \tag{3.11}$$

from which and map (3.9), it then follows that

$$\begin{pmatrix} u \\ v \end{pmatrix} \mapsto \begin{pmatrix} 1 - r & 0 \\ 0 & 1 \end{pmatrix} \begin{pmatrix} u \\ v \end{pmatrix} + \begin{pmatrix} \frac{r\,(r-2)}{2}\, u^2 + \left(1 + \frac{1}{r}\right)\, u\, v + \frac{r^2 - 2r - 2}{2r^2}\, v^2 + \mathcal{O}(3) \\ u\, v + \left(-1 - \frac{1}{r}\right) v^2 + \mathcal{O}(3) \end{pmatrix} \tag{3.12}$$

Assume that the map h takes the following form

$$u = h(v) = a\,v^2 + b\,v^3 + \mathcal{O}\left(v^4\right).$$

Now we can compute the constants a and b. The function h must satisfy the center manifold equation

$$h\left(\lambda_2 v + \tilde{g}(v, h(v))\right) - \lambda_1 h(v) - \tilde{f}(v, h(v)) = 0$$

from which the constants a and b can be found as

$$a = \frac{r^2 - 2r - 2}{2r^3},$$

$$b = \frac{6 + (18\,a - 2)r^2 + (18\,a + 3)r}{6\,r^3}.$$

Hence, the graph of $h(v)$ gives the center manifold

$$h(v) = \frac{(r^2 - 2\,r - 2)}{2\,r^3}\,v^2 + \mathcal{O}(3).$$

We then have the dynamics on the center manifold by the following map:

$$v \mapsto v + \left(-1 - \frac{1}{r}\right)\,v^2 + \mathcal{O}\left(v^3\right) \tag{3.13}$$

Thus, it follows that the steady state of (3.7) is unstable which can be seen in Figure (3.2). In the original coordinates system, the center manifold at $S_1 = (1, 0)$ takes the form

$$x = 1 - \frac{1}{r}\,y + \frac{r^2 - 2r - 2}{2r^3}\,y^2 + \mathcal{O}(y^3), \quad \text{as } y \to 0.$$

The center manifold behaves as a line near $(1, 0)$.

(ii) Similarly, suppose $r = 2$ and $k < 1$. To study the dynamics about the steady state $(k, 0)$ in the first quadrant $Q_1 = \{(x, y) \mid x \geq 0,\ y \geq 0\}$, it is required to explicitly compute the local

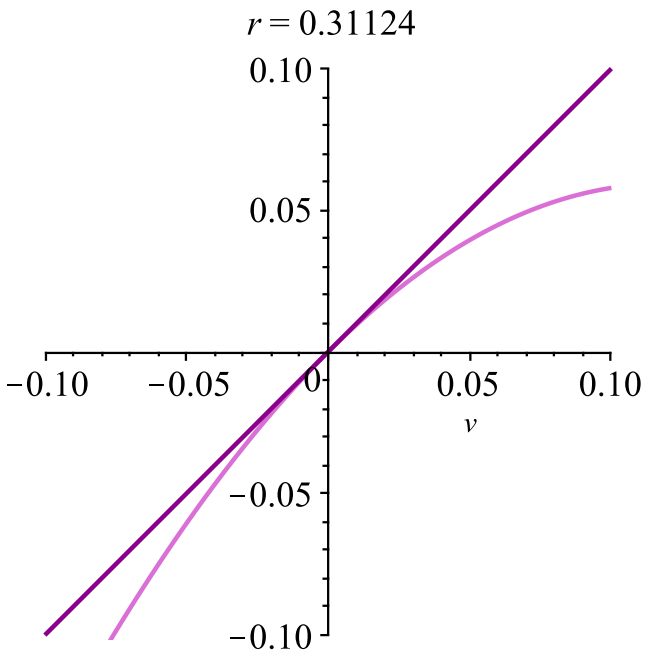

Figure 3.2: The center manifold is half-stable when $k = 1$ for $u = h(v)$.

center manifold. Here, we also translate the steady state $S_1 = (k, 0)$ of system (3.7) to origin S_0, which is done by the linear translation $(x, y) \mapsto (x + k, y)$. The map associated with sytem (3.7) translates to system (3.9), and the Taylor expansion of map (3.9) about the origin is given by (3.10). We can now consider the following change of variables when $r = 2$:

$$\begin{pmatrix} x \\ y \end{pmatrix} = \begin{pmatrix} 1 & -\frac{k}{1+k} \\ 0 & 1 \end{pmatrix} \begin{pmatrix} u \\ v \end{pmatrix} = \begin{pmatrix} u - \frac{k}{1+k} v \\ v \end{pmatrix} \tag{3.14}$$

from which and map (3.9), it then follows that

$$\begin{pmatrix} u \\ v \end{pmatrix} \mapsto \begin{pmatrix} -1 & 0 \\ 0 & k \end{pmatrix} \begin{pmatrix} u \\ v \end{pmatrix} + \begin{pmatrix} \left(1 + \frac{k}{1+k}\right) uv - \frac{k^2}{(1+k)^2} v^2 + \mathcal{O}(3) \\ uv + \left(-k - \frac{k}{1+k}\right) v^2 + \mathcal{O}(3) \end{pmatrix}. \tag{3.15}$$

Assume that the map h takes the following form and by some computation, we can obtain the center manifold by

$$v = h^c(u) = \alpha\, u^2 + \beta\, u^3 + \mathcal{O}\left(u^4\right) \equiv 0.$$

We then have the dynamics on the center manifold by the following map:

$$u \mapsto -u + \frac{2}{3\,k^2}\,u^3 + \mathcal{O}\left(u^4\right), \quad \text{as } u \to 0 \tag{3.16}$$

This shows that the behavior of the center manifold is asymptotically stable as u goes to 0. See Figure (3.3).

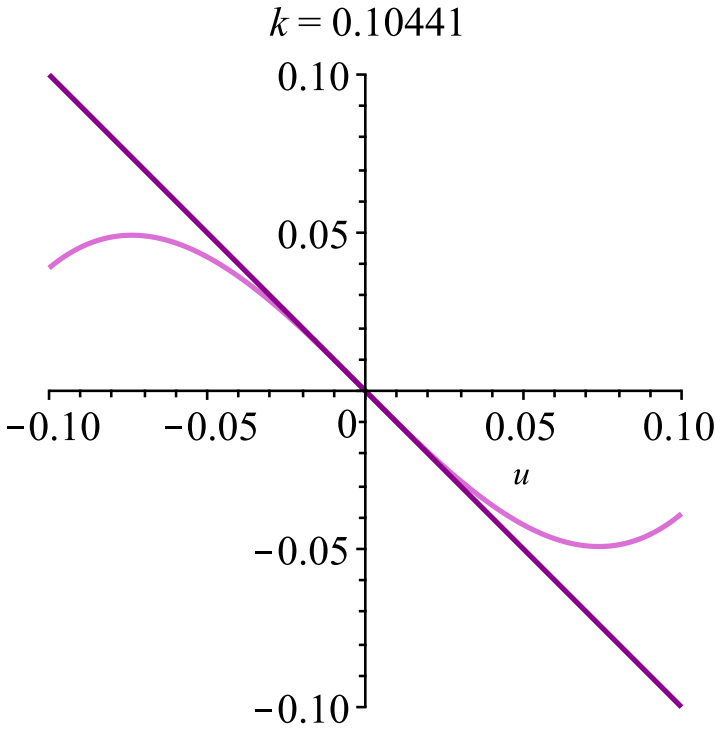

Figure 3.3: The center manifold is asymptotically stable when $r = 2$ for $v = h(u)$.

(iii) Suppose $k = 1$ and $r = 2$. Then the Jacobian matrix of this Taylor expansion gives two eigenvalues on the unit circle one and negative one. We can now consider the following change of variables:

$$\begin{pmatrix} x \\ y \end{pmatrix} = \begin{pmatrix} 1 & -\frac{1}{2} \\ 0 & 1 \end{pmatrix} \begin{pmatrix} u \\ v \end{pmatrix} = \begin{pmatrix} u - \frac{1}{2}\,v \\ v \end{pmatrix} \tag{3.17}$$

from which and map (3.9), it then follows that

$$\begin{pmatrix} u \\ v \end{pmatrix} \mapsto \begin{pmatrix} -1 & 0 \\ 0 & 1 \end{pmatrix} \begin{pmatrix} u \\ v \end{pmatrix} + \begin{pmatrix} \frac{3}{2}\, v\, u - \frac{1}{4}\, v^2 + \mathcal{O}(3) \\ v\, u - \frac{3}{2}\, v^2 + \mathcal{O}(3) \end{pmatrix}. \tag{3.18}$$

Assume that the map h takes the following form and by some computation, we get the center manifold as

$$u = h(v) = \alpha\, v^2 + \beta\, v^3 + \mathcal{O}\left(v^4\right) = -\frac{1}{8} v^2 + \mathcal{O}(3).$$

We then have the dynamics on the center manifold by the following map:

$$v \mapsto v - \frac{3}{2} v^2 + \mathcal{O}\left(v^3\right) \tag{3.19}$$

It follows that the steady state is unstable and that is made obvious by plotting it. In the original coordinates system, the center manifold at $S_1 = (1, 0)$ takes the form

$$x = 1 - \frac{1}{2}\, y - \frac{1}{8}\, y^2, \quad \text{as } y \to 0.$$

The center manifold behaves as a line near $(1, 0)$.

□

If $k > 1, r = 2$ or $k = 1, r > 2$, then the steady state $(k, 0)$ is non-hyperbolic and one of the eigenvalues of $J(k, 0)$ has a magnitude greater than 1, thus $(k, 0)$ is unstable.

Remark 1. : For parameter values $r = 2$ and $k = 1$, system (3.7) with initial condition $x_0 > 0$ and $y_0 > 0$ is bounded. To show this, we can see that system (3.7) is reduced to

$$\begin{aligned} x_{n+1} &= x_n\, e^{2(1-x_n)} \frac{1}{1 + y_n}, \\ y_{n+1} &= x_n \Big(1 - \frac{1}{1 + y_n}\Big), \end{aligned} \tag{3.20}$$

which has no interior steady state.

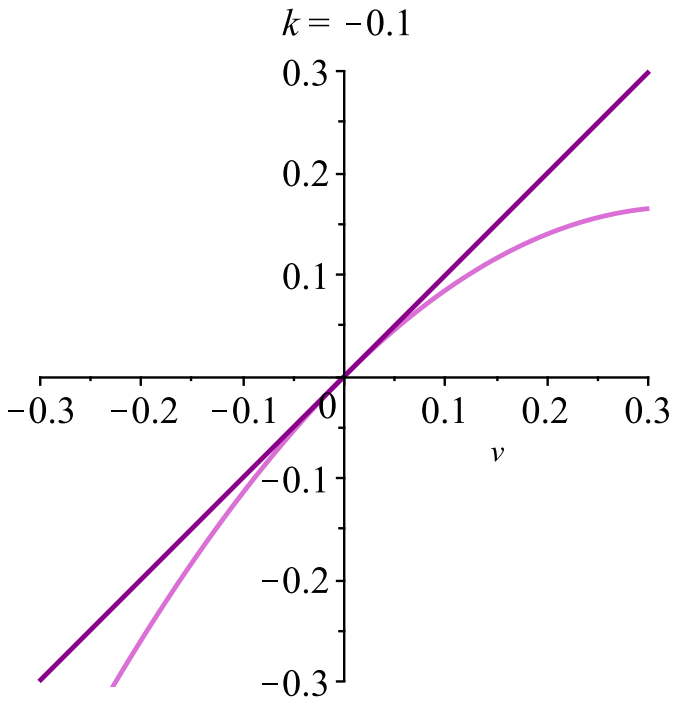

Figure 3.4: The center manifold is half-stable when $k = 1$ and $r = 2$ for $u = h(v)$.

The steady state $(0, 0)$ of system (3.20) is a hyperbolic saddle with eigenvalues $\lambda_1 = 0 < 1$ and $\lambda_2 = e^2 > 1$, and the steady state $(k, 0)$ is non-hyperbolic with eigenvalues $\lambda_{1,2} = \pm 1$. System (3.7) is bounded above on their domain by $\frac{e}{2}$ and 1 respectively. Therefore, after two iterations the orbit lies in the square region R defined as $R = [0, \frac{e}{2}] \times [0, \frac{e}{2}]$.

3.4 Global Stability of the Boundary Steady State S_1

In this section, we focus on the global stability and long-term behavior of solutions of the boundary steady state $S_1 = (k, 0)$. This means that all the solutions initiating away from the origin will not be trapped by S_0 and converges to S_1. In other words, its domain of attraction of system (3.7) is the entire positive quadrant.

Prior to providing the proof of global stability, we study the boundedness and persistence of (3.7) for the steady state $S_1(k, 0)$.

3.4.1 Persistence of the Model

First we provide some basic terminologies from Hal Smith[62] in the following. Also, throughout this section, $\Omega = (0, \infty)$ and X are a subset of Euclidean space.

What follows is indebted from the original idea of Kang et al.[20] For the persistence of the model at $S_1 = (k, 0)$, we define the following

$$\Gamma = \{(x, y) \mid x \geq 0,\ y \geq 0\}$$

$$\Gamma_{k,0} = \{(x, y) \in \Gamma \mid x > 0\}$$

$$\partial\Gamma_{k,0} = \Gamma \backslash \Gamma_{k,0}$$

Lemma 3.4.1. *System (3.7) is uniformly persistent with respect to* $(\Gamma_{k,0}, \partial\Gamma_{k,0})$.

Proof. For n large enough, we have

$$x_{n+1} < x_n e^{r\left(1-\frac{x_n}{k}\right)} < \frac{ke^{r-1}}{r} = M \quad \text{and,} \quad y_{n+1} < x_n = M,$$

where (x_n, y_n) is any positive solution of system (3.7).

Therefore, both x_n and y_n are bounded which means the system is point dissipative.

Let $M_\partial = \{(x_0, y_0) : (x_n, y_n)$ satisfy system (3.7) and $(x_n, y_n) \in \partial\Gamma_{k,0}, \forall n > 0\}$,

then we can see that $M_\partial = \{(0, y) : y \geq 0\} = \partial\Gamma_{k,0}$ with the unique steady state $(0, 0)$.

Let $W^S(0, 0)$ be the stable manifold of $(0, 0)$.

Claim:

$$W^S(0, 0) \cap \Gamma_{k,0} = \varnothing.$$

On the contrary, suppose that there exists a solution (x_n, y_n) of the system with $x_n > 0$ such that $(x_n, y_n) \to (0, 0)$ as $n \to \infty$. Then for large n, by sytem (3.7) we have

$$x_{n+1} > x_n e^{\frac{r}{2}}.$$

Since $r > 0$, it follows that $x_n \to \infty$ as $n \to \infty$, which is a contradiction. It is also clear that every orbit in M_∂ tends to $(0,0)$ as $n \to \infty$. Therefore, $(0,0)$ is an isolated invariant set in X and is acyclic in M_∂. From Thieme[60] and Hirsch et al.,[61] this means $\partial\Gamma(k,0)$ repels the solutions of system (3.7) uniformly with positive x_n. Therefore, there exists a $c > 0$ such that $x_n > c$ for n large enough. □

Theorem 3.4.2. *There exists a constant $c > 0$ such that for any $x_0 > 0$ we have the inequalities below*

$$c < x_n < \frac{ke^{r-1}}{r}$$

Proof. Obvious by the above proposition. □

Theorem 3.4.3. *System (3.7) is globally stable if $0 < r < 2$ and $0 < k < 1$.*

Proof. To show the global stability of the system, we start constructing the following conditions of system (3.7) when $0 < r < 2$ and $0 < k < 1$. For any initial condition $x_0 > 0, y_0 \geq 0$ we have

$$x_n + y_n = \frac{x_{n-1}e^{r\left(1-\frac{x_{n-1}}{k}\right)}}{1+y_{n-1}} + x_{n-1}\left(1 - \frac{1}{1+y_{n-1}}\right) \leqslant 2\,\frac{k\,e^{r-1}}{r}. \tag{3.21}$$

By adding the equations of system (3.7) for $n \geq 1$, we have

$$x_{n+1} + y_{n+1} = \frac{x_n\left(\mathrm{e}^{\frac{r\,(k-x_n)}{k}} + y_n\right)}{1+y_n}$$

$$\frac{y_{n+1}}{x_{n+1}} = \frac{y_n}{e^{\frac{r\,(k-x_n)}{k}}}$$

$$\frac{y_{n+1}}{y_n} = \frac{x_n}{1+y_n} \tag{3.22}$$

$$\ln\frac{x_{n+1}}{x_n} = \ln\left(\frac{e^{r\left(1-\frac{x_n}{k}\right)}}{1+y_n}\right)$$

$$= r\left(1 - \frac{x_n}{k}\right) + \ln\left(\frac{1}{1+y_n}\right).$$

In addition,

$$\begin{aligned}
\ln\left(\frac{x_{n+m}}{x_n}\right) &= \ln\left(\frac{x_{n+1}}{x_n} \cdot \frac{x_{n+2}}{x_{n+1}} \cdots \frac{x_{n+m}}{x_{n+m-1}}\right) \\
&= \ln\left(\frac{x_{n+1}}{x_n}\right) + \ln\left(\frac{x_{n+2}}{x_{n+1}}\right) + \cdots + \ln\left(\frac{x_{n+m}}{x_{n+m-1}}\right) \\
&= \sum_{j=n}^{n+m-1} \ln\left(\frac{x_{j+1}}{x_j}\right) \\
&= \sum_{j=n}^{n+m-1} \left(r\left(1 - \frac{x_j}{k}\right) + \ln\left(\frac{1}{1+y_j}\right)\right) \\
&= \sum_{j=n}^{n+m-1} r - \sum_{j=n}^{n+m-1} \left(r\left(\frac{x_j}{k}\right) - \ln\left(\frac{1}{1+y_j}\right)\right),
\end{aligned}$$

That is,

$$\ln\left(\frac{x_{n+m}}{x_n}\right) = mr - \sum_{j=n}^{m+n-1} \left(r\frac{x_j}{k} + \ln\left(1+y_j\right)\right)$$

or

$$\sum_{j=n}^{m+n-1} \left(r\frac{x_j}{k} + \ln\left(1+y_j\right)\right) = mr - \ln\left(\frac{x_{n+m}}{x_n}\right) \tag{3.23}$$

equivalently,

$$\sum_{j=n}^{m+n-1} \left(\frac{1}{m}\frac{x_j}{k} + \frac{1}{mr}\ln\left(1+y_j\right)\right) = 1 - \frac{1}{mr}\ln\left(\frac{x_{n+m}}{x_n}\right). \tag{3.24}$$

We also have

$$\frac{y_{n+m}}{y_n} \leq \prod_{j=n}^{n+m-1} \frac{x_j}{1+y_j}.$$

Since $k < 1$, then from equation (3.24) we have

$$\begin{aligned}
\frac{y_{n+m}}{y_n} &< \prod_{j=n}^{n+m-1} \frac{x_j}{k} \cdot \prod_{j=n}^{n+m-1} \frac{1}{1+y_j} \\
&< \prod_{j=n}^{n+m-1} \left[\frac{x_j}{k} + \frac{\ln(y_j+1)}{r}\right] \cdot \prod_{j=n}^{n+m-1} \frac{1}{1+y_j}
\end{aligned}$$

$$\leq \left(\frac{1}{m} \sum_{j=n}^{n+m-1} \left[\frac{x_j}{k} + \frac{\ln(y_j+1)}{r} \right] \right)^m \cdot \prod_{j=n}^{n+m-1} \frac{1}{1+y_j}$$

.

Using equation (3.24), we have

$$\frac{y_{n+m}}{y_n} \leq \left(1 - \frac{\ln \frac{x_{n+m}}{x_n}}{mr} \right)^m \cdot \left(\prod_{j=n}^{n+m-1} \frac{1}{1+y_j} \right). \tag{3.25}$$

Also, from Theorem 3.4.2, we have

$$c < x_n < M \qquad \text{and} \qquad c < x_{n+m} < M,$$

in addition,

$$\frac{1}{M} < \frac{1}{x_n} < \frac{1}{c},$$

then

$$\frac{c}{M} < \frac{x_{n+m}}{x_n} < \frac{M}{c},$$

also,

$$\ln \frac{c}{M} < \ln \frac{x_{n+m}}{x_n} < \ln \frac{M}{c},$$

then

$$-\ln \frac{M}{c} < -\ln \frac{x_{n+m}}{x_n} < -\ln \frac{c}{M},$$

it follows that

$$1 - \frac{\ln \frac{M}{c}}{mr} < 1 - \frac{\ln \frac{x_{n+m}}{x_n}}{mr} < 1 - \frac{\ln \frac{c}{M}}{mr}.$$

As a result, we have

$$\left(1 - \frac{\ln \frac{x_{n+m}}{x_n}}{mr} \right)^m < \max \left\{ \left| \left(1 - \frac{\frac{1}{C}}{mr} \right)^m \right|, \left| \left(1 - \frac{C}{mr} \right)^m \right| \right\},$$

where $\ln \frac{c}{M} = C$. We also know that

$$\lim_{m\to\infty} \left(1 + \frac{x}{m}\right)^m = e^x,$$

thus

$$\lim_{m\to\infty} \left(1 - \frac{C}{mr}\right)^m = e^{(\frac{-C}{r})}.$$

So we have

$$\left(1 - \frac{\ln \frac{x_{n+m}}{x_n}}{mr}\right)^m < \max\left\{\left|e^{(\frac{-1}{rC})}\right|, \left|e^{(\frac{-C}{r})}\right|\right\} := K.$$

We know that the sequence $\{y_n\}$ is bounded from above. Now we need to show that the sequence $\{y_n\}$ approaches zero. To the contrary, suppose that $\limsup_{n\to\infty} y_n \neq 0$, hence $\{y_n\}_{n\geq 1}$ has a sub-sequence $\{y_{n_k}\}_{k\geq 1}$ bounded away from zero. That is, there exists $\varepsilon > 0$ such that $\forall k \in \mathbb{N}$, $y_{n_k} > \varepsilon$. It then follows that

$$\begin{aligned}
\prod_{j=1}^{n+m-1} \frac{1}{1+y_j} &= \prod_{\substack{j=1 \\ y_j<\varepsilon}}^{n+m-1} \frac{1}{1+y_j} \cdot \prod_{\substack{j=1 \\ y_j\geq\varepsilon}}^{n+m-1} \frac{1}{1+y_j} \\
&\leqslant 1 \cdot \prod_{\substack{j=1 \\ y_j\geqslant\varepsilon}}^{n+m-1} \frac{1}{1+y_j} \\
&= 1 \cdot \prod_{1\leq n_k\leq n+m-1} \frac{1}{1+y_{n_k}},
\end{aligned}$$

hence

$$\prod_{j=1}^{n+m-1} \frac{1}{1+y_j} \leq \prod_{1\leq n_k\leq n+m-1} \frac{1}{1+\varepsilon},$$

also,

$$\frac{y_{n+m}}{y_n} < K \prod_{j=1}^{n+m-1} \frac{1}{1+y_j} \longrightarrow y_{n+m} < K \left(\prod_{j=1}^{n+m-1} \frac{1}{1+y_j}\right) y_n,$$

meaning that

$$y_{n+m} \leq K \left(\prod_{1\leq n_k\leq n+m-1} \frac{1}{1+\varepsilon}\right) y_n.$$

Thus

$$0 \leq \lim_{m\to\infty} y_{n+m} \leq \lim_{m\to\infty} K \left(\prod_{1\leq n_k \leq n+m-1} \frac{1}{1+\varepsilon} \right) y_n.$$

Therefore,

$$0 \leq \lim_{n\to\infty} y_n \leq K \frac{e\,k}{2} \lim_{n\to\infty} \beta^n.$$

Since $\beta = \frac{1}{1+\varepsilon} < 1$, then

$$\lim_{n\to\infty} y_n = 0,$$

which is a contradiction. Hence, $\lim_{n\to\infty} y_n \neq 0$ is false and

$$\lim_{n\to\infty} y_n = 0.$$

□

3.5 Stability of the Interior Steady State S_2

Now study the stability of the interior steady state by applying a transformation from $(\mathrm{tr}, \det)$-plane to (x, r)-plane when $k > 1$. System (3.7) has an interior steady state $S_2 = (x^*, y^*)$ in the first quadrant. Jacobian matrix (3.26) of system (3.7) at $S_2 = (x^*, y^*)$ can reduce to

$$J(S_2) = \begin{pmatrix} 1 - \frac{r\,x^*}{k} & -1 \\ 1 - \frac{1}{x^*} & \frac{1}{x^*} \end{pmatrix} = \begin{pmatrix} 1 - r + \ln(x^*) & -1 \\ 1 - \frac{1}{x^*} & \frac{1}{x^*} \end{pmatrix}. \tag{3.26}$$

The second matrix was obtained by replacing the identity $k = \frac{x\,r}{r-\ln(x)}$ which can be calculated from equation $e^{r\,(1-\frac{x}{k})} = x$. It then follows that

$$\mathrm{tr}(J) = 1 - r + \ln(x^*) + \tfrac{1}{x^*} \quad \text{and} \quad \det(J) = \tfrac{x^* - r + \ln(x^*)}{x^*}.$$

In the following theorems the stability will be determined using the conditions of stability in (2.7), (2.9) and (2.8).

Theorem 3.5.1. *Suppose $k > 1$, $r > 0$ and let $\Omega = \{(x, r) \mid r \geq 0,\ x \geq 1\}$. The stability region for the interior steady states in (x, r)-plane of dynamical system (3.7) is given by the following:*

(i) The region delimited between $r > \max\{0, \ln(x)\} = \ln(x)$ (yellow and orange curves in Figure (3.5)), and $r < f_3(x) = \frac{\ln(x)\,x+\ln(x)+3\,x+1}{1+x}$ (red curve in Figure (3.5)) is stable.

(ii) The region delimited between $r < f_1(x) = 0$ and $r > f_2(x) = \ln(x) - 1$ (green curve in Figure (3.5)) is repeller.

(iii) The region delimited below $r = f_2(x) = \ln(x) - 1$ or above $r = f_3(x) = \frac{\ln(x)\,x+\ln(x)+3\,x+1}{1+x}$ is saddle.

Proof. The solution of the equation $e^{r\,(1-\frac{x}{k})} = x$ for k is $k = \frac{x\,r}{r-\ln(x)}$, and $k > 1$. This means $r > f_5(x) = \ln(x)$ is the existence curve of the plane. The equations det $= 1$, det $=$ tr $- 1$ and det $=$ $-$tr -1 are equivalent to $r = f_1(x) = 0$, $r = f_2(x) = \ln(x) - 1$ and $r = f_3(x) = \frac{\ln(x)\,x+\ln(x)+3\,x+1}{1+x}$, respectively. For simplicity, we illustrated the curve associated with the equations det $= 1$, det $=$ tr $- 1$ and det $= -$tr $- 1$ by yellow, green and red curves in Figure (3.5), respectively.

Using (2.7), the stability regions for $x \geq 1$ is the region corresponding to inequality det < 1, or

$$\frac{x^* - r + \ln(x^*)}{x^*} < 1 \Longleftrightarrow r > \ln(x).$$

The region corresponding to inequality det $>$ tr -1 is

$$\frac{x^* - r + \ln(x^*)}{x^*} > 1 - r + \ln(x^*) + \frac{1}{x^*} - 1 \Longleftrightarrow r < \ln(x) - 1,$$

and the region corresponding to inequality det $> -$ tr -1 is

$$\frac{x^* - r + \ln(x^*)}{x^*} > -(1 - r + \ln(x^*) + \frac{1}{x^*}) - 1 \Longleftrightarrow r > \frac{(x+1)\,\ln(x) + 3\,x + 1}{x+1}.$$

Thus, the stable region corresponding to the solutions of the system from inequalities (2.7) is the region between $r > f_5(x) = \ln(x)$ (orange curve), and $r < f_3(x) = \frac{\ln(x)\,x+\ln(x)+3\,x+1}{1+x}$ (red curve). The repeller region corresponds to the solutions of the system based on inequalities in

(2.9). The inequalities of (2.9) correspond to the region between $r < f_1(x) = 0$ (yellow curve) and $r > f_2(x) = \ln(x) - 1$ (green curve), which is in the negative region. The saddle region correlates to the solutions of the system obtained from inequalities in (2.8), which correlates to the region $r > f_3(x) = \frac{\ln(x)\,x+\ln(x)+3\,x+1}{1+x}$ (red curve), or $r < f_2(x) = \ln(x) - 1$ (green curve). □

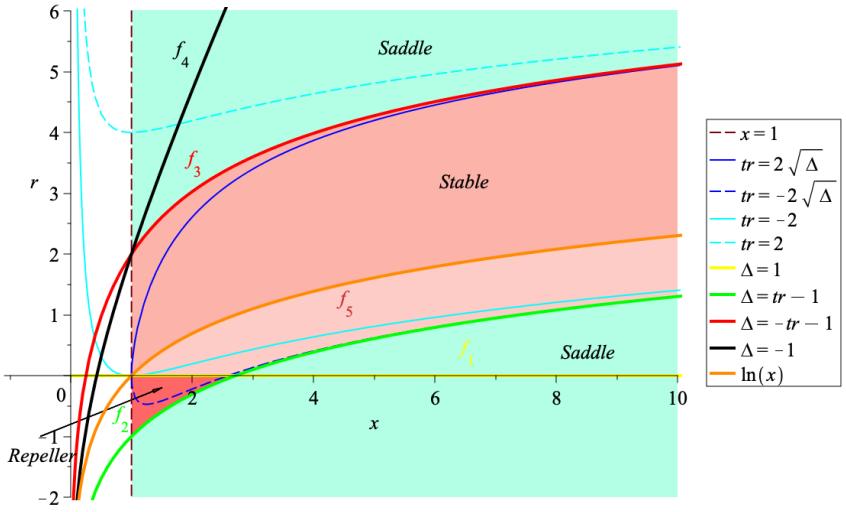

Figure 3.5: Stability regions of system (3.7) for different parameter values of r. The stable region is highlighted in orange, the green indicates the saddle region, and the red refers to the repeller region. The intersection point of the yellow with saddle curve occurs at $x = e$.

The same argument applies to the (x, k)-plane. Different stability regions can be showed as followed:

(a) The stable region occurs when $k > \max\{f_1, f_2\} = f_1$.

(b) The saddle region is delimited by $f_2 < k < f_1$, but the acceptable region is when $(x < k < f_1)$.

(c) The repeller region is when $f_3 < r < f_2$, but it is in the negative region. Since below the curve $x = k$, we can see that $r = \frac{\ln(x)k}{k-x} < 0$.

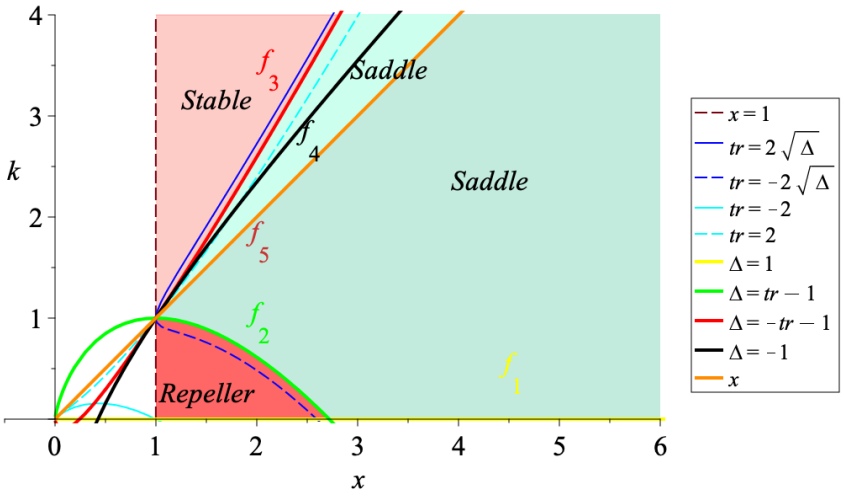

Figure 3.6: Stability regions of system (3.7) for $(x, k)-$plane. The curve $k = f_5(x) = x$ gives the existence regions, and under this curve, they are not acceptable regions.

3.6 Bifurcation Analysis

In this section, the plan is to locally analyze bifurcations of the interior steady-state for system (3.7). Listed in the following are the facts about Figure (3.5) bifurcation analysis.

Remark 2. From Theorem 3.5.1, the following statements are true for the Figure:

(a) The Neimark-Sacker bifurcation is given by the function f_1 where $1 < x < e$ (but that region is not acceptable because k is negative).

(b) The saddle node bifurcation is given by the function f_2 where $x > e$ (but that region is not acceptable because k is negative).

(c) The period doubling bifurcation is given by the function f_3 for any $x > 1$.

3.6.1 Period-Doubling Bifurcations (Flip Bifurcation)

The bifurcation associated with the appearance of $\lambda = -1$ is called a flip (or period-doubling) bifurcation. For $k > 1$ period doubling bifurcation happens when $J = J_{r=f_1(x)}(x^*, y^*)$, Jacobian matrix (3.26) of sytem (3.7) at the interior steady state for $r = f_1(x)$ has an eigenvalue of $\lambda = -1$. In other words, the flip bifurcation occurs as we cross the line det $= -\text{tr} - 1$. Consider the

function $r = f_1(x) = \frac{(x+1)\ln(x)+3x+1}{1+x}$ on $(1,\infty)$. f_1 is an increasing function starting from 2 for $x \in (1,\infty)$. To determine the stability of the period doubling bifurcation, whether it is stable or unstable, we first start by using the normal form for the steady state (x^*, y^*). That will show the dynamic behavior of the system in the case $r = r^*$ with $\lambda_2 \neq -1$. First apply a transformation for the system to make it simpler to calculate using the following change of variables

$$x = x^* + \bar{x},\ y = y^* + \bar{y},\ r = r^* + \bar{r}.$$

By this change of variables, system (3.7) transforms to the following two dimensional map

$$\begin{aligned} f(\bar{x},\bar{y}) &= (x^*+\bar{x})\, e^{(r^*+\bar{r})\left(1-\frac{x^*+\bar{x}}{k}\right)} \frac{1}{1+y^*+\bar{y}} - x^*, \\ g(\bar{x},\bar{y}) &= (x^*+\bar{x})\left(1-\frac{1}{1+y^*+\bar{y}}\right) - y^*. \end{aligned}$$

Then, the third order Taylor series of f and g are given by

$$\begin{aligned} f(\bar{x},\bar{y}) = &-\frac{2\,(y^*+1)\,\bar{x}\left(\frac{1}{2}\,\bar{r}\,y^*+k+\bar{r}\right)}{k\,(y^*+2)}\,\bar{x} - \bar{y} + \frac{(\bar{r}\,y^*+2\,k+2\,\bar{r})}{k\,(y^*+2)}\,\bar{x}\,\bar{y} \\ &+ \frac{\left(y^{*2}\,\bar{r}+3\,y^*k+3\,\bar{r}\,y^*+4\,k+2\,\bar{r}\right)\left(y^{*2}\,\bar{r}+y^*\,k+3\,\bar{r}\,y^*+2\,\bar{r}\right)}{2\,k^2(y^*+1)(y^*+2)^2}\,\bar{x}^2 + \frac{1}{y^*+1}\,\bar{y}^2 \\ &+ \frac{\left(y^{*2}\,\bar{r}+3\,y^*\,k+3\,\bar{r}y^*+4\,k+2\bar{r}\right)^2\left(-y^{*2}\bar{r}-3\,\bar{r}\,y^*+2\,k-2\,\bar{r}\right)}{6\,(y^*+1)^2\,(y^*+2)^3\,k^3}\,\bar{x}^3 - \frac{1}{(y^*+1)^2}\,\bar{y}^3 \\ &- \frac{\left(y^{*2}\,\bar{r}+\ y^*\,k+3\,\bar{r}\,y^*+4\,k+2\,\bar{r}\right)\left(y^{*2}\,\bar{r}+y^*\,k+3\,\bar{r}\,y^*+2\,\bar{r}\right)}{2\,k^2(y^*+2)^2\,(y^*+1)^2}\,\bar{x}^2\,\bar{y} \\ &- \frac{2\,\left(\frac{1}{2}\,\bar{r}\,y^*+k+\bar{r}\right)}{k\,(y^*+2)\,(y^*+1)}\,\bar{x}\,\bar{y}^2 + \mathcal{O}(4), \qquad (3.27) \\ g(\bar{x},\bar{y}) = &\frac{y^*}{y^*+1}\,\bar{x} + \frac{1}{y^*+1}\,\bar{y} + \frac{1}{(y^*+1)^2}\,\bar{x}\,\bar{y} + \frac{(-y^*-1)}{(y^*+1)^3}\,\bar{y}^2 - \frac{1}{(y^*+1)^3}\,\bar{x}\,\bar{y}^2 \\ &+ \frac{1}{(y^*+1)^3}\bar{y}^3 + \mathcal{O}(4). \end{aligned}$$

When $\bar{r} = 0$, we then have $\lambda_1 = -1$ which is an eigenvalue of the matrix J. The other eigenvalue is given by

$$\lambda_2 = -\frac{y^{*2}-2}{y^{*2}+3\,y^*+2},$$

which provides the matrix of eigenvectors as follows

$$P = \begin{pmatrix} -\frac{y^*+2}{y^*} & -\frac{y^*+1}{y^*+2} \\ 1 & 1 \end{pmatrix}.$$

We now use a diagonalizable matrix to analyze the steady state by the change of coordinates:

$$\begin{pmatrix} \bar{x} \\ \bar{y} \end{pmatrix} = \begin{pmatrix} -\frac{y^*+2}{y^*} & -\frac{y^*+1}{y^*+2} \\ 1 & 1 \end{pmatrix} \begin{pmatrix} u \\ v \end{pmatrix}.$$

Applying this change of coordinates to map (3.27), we obtain the following two dimensional map

$$\begin{pmatrix} u \\ v \end{pmatrix} \mapsto \begin{pmatrix} -1 & 0 \\ 0 & \lambda_2 \end{pmatrix} \begin{pmatrix} u \\ v \end{pmatrix} + \begin{pmatrix} \mathcal{F}(u,v,\bar{r}) \\ \mathcal{G}(u,v,\bar{r}) \end{pmatrix},$$

where the non-linear equations are provided by

$$\begin{aligned} \mathcal{F}(u,v,\bar{r}) &= \mathcal{F}_{200}u^2 + \mathcal{F}_{110}u\bar{r} + \mathcal{F}_{101}uv + \mathcal{F}_{011}v\bar{r} + \mathcal{F}_{020}\bar{r}^2 + \mathcal{F}_{002}v^2 + \mathcal{F}_{300}u^3 + \cdots, \\ \mathcal{G}(u,v,\bar{r}) &= \mathcal{G}_{200}u^2 + \mathcal{G}_{110}u\bar{r} + \mathcal{G}_{101}uv + \mathcal{G}_{011}v\bar{r} + \mathcal{G}_{020}\bar{r}^2 + \mathcal{G}_{002}v^2 + \cdots. \end{aligned} \tag{3.28}$$

Now we seek the center manifold on u and $\bar{r}$, which is

$$v = h^c(u,\bar{r}) = a\,u^2 + \mathcal{O}\left(|u,\bar{r}|^3\right).$$

By the substitution of v into equation (3.28), we get

$$\begin{aligned} \mathcal{F}(u,v,\bar{r}) &= \mathcal{F}_{002}u^4a^2 + \mathcal{F}_{011}u^2a\bar{r} + \mathcal{F}_{101}u^3a + \mathcal{F}_{300}u^3 + \mathcal{F}_{020}\bar{r} + \mathcal{F}_{110}u\bar{r} + \mathcal{F}_{200}u^2 + \cdots, \\ \mathcal{G}(u,v,\bar{r}) &= \mathcal{G}_{200}u^2 + \mathcal{G}_{011}u^2a\bar{r} + \mathcal{G}_{101}u^3a + \mathcal{G}_{020}\bar{r}^2 + \mathcal{G}_{110}u\bar{r} + \mathcal{G}_{002}u^4a^2 + \cdots. \end{aligned}$$

where some of these functions that will be needed below is given as follows

$$\begin{aligned}
\mathcal{G}_{200} &= \frac{(y^*+2)\,\left(y^{*2}-4\,y^*-8\right)}{6\,y^{*3}+14\,y^{*2}+8\,y^*}\\
\mathcal{F}_{200} &= \frac{-y^{*2}+2\,y^*+4}{6\,y^{*2}+14\,y^*+8}\\
\mathcal{F}_{110} &= -\frac{(y^*+1)(y^*+2)^2}{3\,y^*\,k+4\,k}\\
\mathcal{F}_{101} &= \frac{-y^{*3}+3\,y^{*2}+15\,y^*+12}{3\,y^{*3}+13\,y^{*2}+18\,y^*+8}\\
\mathcal{F}_{300} &= \frac{3\,y^{*4}+12\,y^{*3}+72\,y^{*2}+128\,y^*+64}{6\,y^{*2}(3\,y^*+4)\,(y^*+1)^2}.
\end{aligned}$$

By computing the center manifold, we then have

$$v = h^c(u,\bar{r}) = -\frac{\mathcal{G}_{200}u^2}{\lambda_2-1} + \mathcal{O}\left(|u,\bar{r}|^3\right).$$

We can now use the reduced map $u \mapsto \xi(u,\bar{r})$ defined by

$$\begin{aligned}
\xi(u,\bar{r}) = &-u + \mathcal{F}_{200}\,u^2 + \mathcal{F}_{110}u\,\bar{r} + \left(\mathcal{F}_{210} - \frac{\mathcal{F}_{011}\,\mathcal{G}_{200}}{\lambda_2-1}\right)\,\bar{r}\,u^2 +\\
&+\left(\mathcal{F}_{300} - \frac{\mathcal{F}_{101}\mathcal{G}_{200}}{\lambda_2-1}\right)u^3 + \mathcal{O}\left(|(u,\bar{r})|^4\right).
\end{aligned}$$

By using the conditions of period doubling bifurcation (2.18), we have

$$\begin{aligned}
\xi(\xi(u,\bar{r}),\bar{r}) =& u - 2\,\mathcal{F}_{110}\,u\,\bar{r} - 2\left(\mathcal{F}_{300} - \frac{\mathcal{F}_{101}\,\mathcal{G}_{200}}{\lambda_2-1} + \mathcal{F}_{200}^2\right)u^3\\
&-\left(\mathcal{F}_{200}\,\mathcal{F}_{110}\right)u^2\bar{r} + \left(\mathcal{F}_{110}\right)^2\,u\,\bar{r}^2 + \mathcal{O}(4).
\end{aligned}$$

Hence, the period doubling bifurcation can be calculated based on the following function

$$\mathcal{K} \equiv -2\,\mathcal{F}_{110}\left(-2\,\mathcal{F}_{300} + \frac{2\,\mathcal{F}_{101}\,\mathcal{G}_{200}}{\lambda_2-1} - 2\,\mathcal{F}_{200}^2\right) \neq 0.$$

Then by an easy computation, we can find that

$$-2\,\mathcal{F}_{300}+\frac{2\,\mathcal{F}_{101}\,\mathcal{G}_{200}}{\lambda_2-1}-2\,\mathcal{F}_{200}^2=-\frac{3y^{*4}+12y^{*3}+72y^{*2}+128y^*+64}{3y^{*2}(y^*+1)^2(3y^*+4)}$$
$$+\frac{2\left(-y^{*3}+3y^{*2}+15y^*+12\right)\left(y^*+2\right)\left(y^{*2}-4y^*-8\right)}{\left(3y^{*3}+13y^{*2}+18y^*+8\right)\left(6y^{*3}+14y^{*2}+8y^*\right)\left(\frac{-y^{*2}+2}{y^{*2}+3y^*+2}-1\right)}$$
$$-\frac{2\left(-y^{*2}+2y^*+4\right)^2}{\left(6y^{*2}+14y^*+8\right)^2}.$$

This can be seen using numerical simulations for different values of (r,k) in Figure (3.7) pdstable.png The result in Table 3.1 shows that the period doubling bifurcation $\mathcal{K}$ is stable.

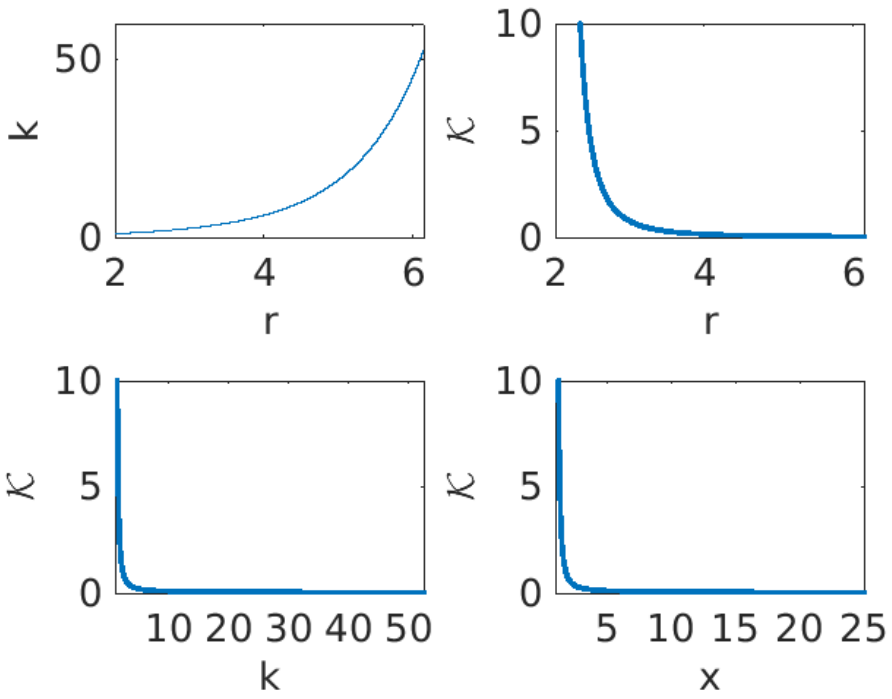

Figure 3.7: Stability of the period doubling bifurcation of system (3.7).

In summary, stability of steady state of this work is giving in the following. In this population model dynamics, there are three steady states in $\mathcal{Q}_1$.

(i) The origin steady state $S_0=(0,0)$.

(ii) The boundary steady states on the x axis $S_1=(k,0)$.

Table 3.1: Stability of the period doubling bifurcation for the given numerical values of $(r^*, \lambda_2, \mathcal{K})$.

k	r^*	λ_2	x	$\mathcal{F}_{200}$	$\mathcal{F}_{300}$	$\mathcal{F}_{110}$	$\mathcal{F}_{101}$	$\mathcal{K}$
1.0510	2.0149	0.9851	1.010000000	0.4938	2.6468	-0.9976	1.4851	6.63422
1.6127	2.5000	0.5502	1.397046267	0.3197	0.0013	-0.9588	1.0565	3.9651×10^{-3}
2.5336	3.0000	0.1841	1.963702289	0.1847	0.0002	-0.9879	0.7068	7.5621×10^{-4}
3.9538	3.5000	-0.1148	2.793343691	0.0834	0.0000	-1.0838	0.4304	2.8545×10^{-4}
6.2102	4.0000	-0.3559	4.041780333	0.0078	0.0000	-1.2604	0.2140	1.4766×10^{-4}
9.9035	4.5000	-0.5456	5.970944716	-0.0477	0.0000	-1.5491	-0.0481	9.2217×10^{-5}
16.1068	5.0000	-0.6896	9.021196436	-0.0875	0.0000	-2.0042	-0.0752	6.5322×10^{-5}
26.7300	5.5000	-0.7942	13.92893126	-0.1152	0.0000	-2.7144	-0.1634	5.0555×10^{-5}
45.1477	6.0000	-0.8671	21.91717936	-0.1339	0.0000	-3.8195	-0.2241	4.1674×10^{-5}
77.2791	6.5000	-0.9159	35.00689085	-0.1461	0.0000	-5.5395	-0.2644	3.5917×10^{-5}
133.4489	7.0000	-0.9475	56.52961736	-0.1539	0.0000	-8.2185	-0.2904	3.1932×10^{-5}

(iii) One interior steady state.

The origin steady state point $S_0 = (0, 0)$ is saddle and the stability of boundary steady-state $S_1 = (k, 0)$ is based on Proposition 3.3.1 and Figure (3.5):

(i) If $k < 1$ and $0 < r < 2$, then $S_1 = (k, 0)$ is an attracting node A. This means the discrete flow begins at infinity, passes asymptotically near saddle point S, and converges to the attractor point A. The bifurcation occurs when they approach $\lambda_1 = 1$.

(ii) If $k < 1$ and $r > 2$, then $S_1 = (k, 0)$ is a saddle point S.

(iii) If $k > 1$ and $0 < r < 2$, then $S_1 = (k, 0)$ is a saddle point S. Moreover, when $k > 1$ and $0 < r < 2$, the attractor A interior steady state appears. This means the discrete flow begins at infinity, passes asymptotically near the origin steady state point $S_0 = (0, 0)$, then passes asymptotically near boundary saddle point $S_1 = (k, 0)$, and converges to the attractor interior steady state point A.

(iv) If $k > 1$ and $r > 2$, then $S_1 = (k, 0)$ is a repelling node R. Moreover, when $k > 1$ and $r > 2$, the saddle point S interior steady state appears.

3.7 Concluding Remarks and Simulations

In this chapter, by a standard method we computed the period-doubling bifurcation without knowing the exact value of the positive steady state. The positive steady state falls in a different stability region depending on the parameter values k and r of the model. We also analyzed the local and global stability of the steady state point $(k, 0)$.

Moreover, we studied Neimarck-Sacker bifurcation and we showed that it is located in the negative region. On the other hand, the saddle node bifurcation with one of the eigenvalues equal to 1 also occurs in the negative region.

Future research will concentrate on the study of the other types of bifurcations and its dynamics for our model.

Below is an .mp4 movie that shows the transition of bifurcation diagram of sytem (3.7) when $0 < k < 5$.

Chapter 4

Dynamics of a Modified Nicholson-Bailey Model with Allee effect

In this chapter, we investigate the dynamical behavior of our host-parasitoid Nicholson-Bailey model by including an Allee effect term. The Allee effect is a population dynamics phenomenon that grows with increasing density. The Allee effect model contains six biological parameters in the first closed quadrant. By a re-scaling procedure, the model is then reduced to a three-parameter system that carries over the comprehensive dynamics of the original model. The new model always possesses three boundary steady states, and we show that the interior steady state may exist under certain conditions imposed on the parameters. We then use linearization of the model about each steady state to examine the local stability for a varied range of parameters. The stability and dynamics of each steady state are then examined using bifurcation identities obtained from the center manifold theory for non-hyperbolic values of the parameters. Furthermore, we can determine whether the system is stable or unstable using the Jury's test. Finally, we investigate the stability of a period-doubling bifurcation that may arise after one of these thresholds is crossed, exhibiting irregular dynamics that could lead to chaos. Simulations also support the results.

4.1 Introduction

The Allee effect is one of the interests in analyzing a biological process. This phenomenon in population dynamics attributed to the biologist W.C. Allee[50;51]. Allee[52], an ecologist, was one of the first to write extensively on the ecological relevance of animal aggregation; thus, the "Allee Effect" refers to the positive link between population density and individual fitness. This process has been modelled for various problems including mating selection that can trigger this impact, social dysfunction, inbreeding depression, food exploitation (e.g., host resistance can only be overcome by a large number of consumers), and predator avoidance or defense[52].

There are two types of Allee effects within the component domain and demographic Allee effects[53]. Component Allee effects occur at the level of individual fitness components, such as juvenile survival or litter size. On the other hand, demographic Allee effects are at the level of overall mean individual fitness and are almost generally viewed as the per capita population growth rate through the demography of the entire population[53]. Component Allee effects can lead to demographic Allee effects; hence the two are linked.

Allee proposed that low population densities result in a decline in the per capita birth rate. A population with low density may face extinction in such a circumstance. Allee discovered that the flour beetle population, Tribolium confusum, had the highest per capita growth rates at intermediate densities. Furthermore, when fewer mates were available, the females produced fewer eggs, which was an unexpected result. Allee did not give a clear and explicit definition of this new concept. Stephens, Sutherland, and Freckleton[54] describe the Allee effect as a positive correlation between any component of individual fitness and the number or density of conspecifics, or members of the same species. As density increases, fitness drops, so we have a negative density dependence in classical dynamics[70].

4.2 The Model

Throughout this work, $\mathcal{Q}_1 = \{(x, y) \in \mathbb{R}^2 \mid x \geq 0, y \geq 0\}$ denotes the first closed quadrant.

Consider the model defined by the following $2D$ map

$$
\begin{aligned}
f(x,y) &= x\ (\beta\, x)^{\alpha}\ e^{r\left(1-\frac{x}{k}\right)}\,\frac{a}{a+b\,y},\\
g(x,y) &= x\Big(1-\frac{a}{a+b\,y}\Big),
\end{aligned}
\tag{4.1}
$$

where the parameters a, b, r, k, α and β are positive. Map (4.1) can be written by

$$
\begin{aligned}
f(x,y) &= x\ (\beta\, x)^{\alpha}\ e^{r\left(1-\frac{x}{k}\right)}\,\frac{1}{1+\frac{b}{a}\,y},\\
g(x,y) &= x\,\Big(1-\frac{1}{1+\frac{b}{a}\,y}\Big).
\end{aligned}
\tag{4.2}
$$

The system induced by model (4.2) can then be given by

$$
\begin{aligned}
x_{n+1} &= x_n\ (\beta\, x_n)^{\alpha}\ e^{r\left(1-\frac{x_n}{k}\right)}\,\frac{1}{1+\frac{b}{a}\,y_n},\\
y_{n+1} &= x_n\,\Big(1-\frac{1}{1+\frac{b}{a}\,y_n}\Big).
\end{aligned}
\tag{4.3}
$$

By the new change of variables $X=\frac{b}{a}\,x$, $Y=\frac{b}{a}\,y$, system (4.3) becomes

$$
\begin{aligned}
X_{n+1} &= e^{\alpha\ln\left(\frac{\beta\,a}{b}\right)}\,X_n^{1+\alpha}e^{r\left(1-(\frac{a}{bk})X_n\right)}\,\frac{1}{1+Y_n},\\
Y_{n+1} &= X_n\Big(1-\frac{1}{1+Y_n}\Big).
\end{aligned}
\tag{4.4}
$$

Combine them by using the new variables $R=r+\alpha\ln(\frac{\beta\,a}{b})$, and $K=\frac{R\,b}{r\,a}\,k$. Then system (4.4) becomes

$$
\begin{aligned}
X_{n+1} &= X_n^{1+\alpha}e^{R\left(1-\frac{X_n}{K}\right)}\,\frac{1}{1+Y_n},\\
Y_{n+1} &= X_n\Big(1-\frac{1}{1+Y_n}\Big).
\end{aligned}
\tag{4.5}
$$

We note that R is not necessarily positive anymore but for the time being we assume α, a and b are so that $R>0$. For simplicity, we replace X_n, Y_n, R and K in (4.5) by x_n, y_n, r and k,

respectively.

$$\begin{aligned} x_{n+1} &= x_n^{1+\alpha} e^{r\left(1-\frac{x_n}{k}\right)} \frac{1}{1+y_n}, \\ y_{n+1} &= x_n\Big(1-\frac{1}{1+y_n}\Big). \end{aligned} \tag{4.6}$$

Then, the steady states of system (4.6) are solutions of the system of equations given by

$$\begin{cases} x^{1+\alpha} e^{r\left(1-\frac{x}{k}\right)} \frac{1}{1+y} = x, \\ x\left(1-\frac{1}{1+y}\right) = y, \end{cases} \tag{4.7}$$

which is equivalent to the solution of the following 3 steady states

$$O = \begin{cases} x = 0 \\ y = 0 \end{cases}, \quad B = \begin{cases} x^{\alpha} e^{r\left(1-\frac{x}{k}\right)} = 1 \\ y = 0 \end{cases}, \quad I = \begin{cases} x^{\alpha} e^{r\left(1-\frac{x}{k}\right)} = 1+y \\ x = 1+y \end{cases}. \tag{4.8}$$

Therefore, for any parameter value, origin O is always a steady state for dynamical system (4.6). The solutions of B in the second system of equations in (4.8) in $\mathcal{Q}_1$ gives the boundary steady state(s), and the third system I of equations gives the interior steady state(s) of the dynamical system (4.6).

The solution(s) of the second steady state B in (4.8), if exists, is equivalent to the solutions of the equations

$$\alpha \ln(x) = -r\left(1-\frac{x}{k}\right), \quad y = 0. \tag{4.9}$$

Also, the solution(s) of the third steady state I in (4.8), if exists, is equivalent to the solutions of the equations

$$(\alpha-1)\ln(x) = -r\left(1-\frac{x}{k}\right), \quad x = 1+y. \tag{4.10}$$

For different values of the parameters r, k, and α, the equations (4.9) and (4.10) may have no or several solutions in $\mathcal{Q}_1$. We note that in equation (4.10) since $x = y+1$ and $y \geq 0$, then the only valid solutions are in the region $x \geq 1$.

Model (4.6) can attain a maximum of five steady states; three of them are boundary steady

states and a maximum of two interior steady states may exist. The first boundary steady state is the origin $S_0 = (0, 0)$, and the second boundary steady state is the Allee effect given below

$$S_1 = (x_1^*, 0) = \left(e^{-W\left(-\frac{r\, e^{-\frac{r}{\alpha}}}{k\,\alpha}\right) - \frac{r}{\alpha}}, 0 \right) = \left(-\frac{k\,\alpha W\left(-\frac{r e^{-\frac{r}{\alpha}}}{k\,\alpha}\right)}{r}, 0 \right). \tag{4.11}$$

The third boundary steady state is k, which is carrying capacity parasite free state

$$S_2 = (x_2^*, 0) = \left(e^{-W\left(-1, -\frac{r\, e^{-\frac{r}{\alpha}}}{k\,\alpha}\right) - \frac{r}{\alpha}}, 0 \right) = \left(-\frac{k\,\alpha W\left(-1, -\frac{r e^{-\frac{r}{\alpha}}}{k\,\alpha}\right)}{r}, 0 \right).$$

The fourth steady state is the interior steady state that may appear when $x \geq 1$

$$\begin{aligned} S_3 = (z_1^*, z_1^* - 1) &= \left(e^{\frac{(-\alpha+1)\, W\left(-\frac{r\, e^{-\frac{r}{\alpha-1}}}{k\,(\alpha-1)}\right) - r}{\alpha-1}}, e^{\frac{(-\alpha+1)\, \mathrm{W}\left(-\frac{r\, e^{-\frac{r}{\alpha-1}}}{k\,(\alpha-1)}\right) - r}{\alpha-1}} - 1 \right) \\ &= \left(-\frac{k\,(\alpha-1) W\left(-\frac{r e^{-\frac{r}{(\alpha-1)}}}{k\,(\alpha-1)}\right)}{r}, -\frac{k\,(\alpha-1) W\left(-\frac{r e^{-\frac{r}{(\alpha-1)}}}{k\,(\alpha-1)}\right)}{r} - 1 \right). \end{aligned}$$

The fifth steady state is the second interior steady state that may appear when $x \geq 1$

$$\begin{aligned} S_4 = (z_2^*, z_2^* - 1) &= \left(e^{\frac{(-\alpha+1)\, \mathrm{W}\left(-1, -\frac{r\, e^{-\frac{r}{\alpha-1}}}{k\,(\alpha-1)}\right) - r}{\alpha-1}}, e^{\frac{(-\alpha+1)\, \mathrm{W}\left(-1, -\frac{r\, e^{-\frac{r}{\alpha-1}}}{k\,(\alpha-1)}\right) - r}{\alpha-1}} - 1 \right) \\ &= \left(-\frac{k\,(\alpha-1) W\left(-1, -\frac{r e^{-\frac{r}{(\alpha-1)}}}{k\,(\alpha-1)}\right)}{r}, -\frac{k\,(\alpha-1) W\left(-1, -\frac{r e^{-\frac{r}{(\alpha-1)}}}{k\,(\alpha-1)}\right)}{r} - 1 \right). \end{aligned}$$

Figure (4.1) provides the four boundary and interior steady states and zero as the first steady state given different range of parameter r. These are obtained numerically from the above Lambert W functions.

The following statements describe the dynamics of the boundary and interior steady states.

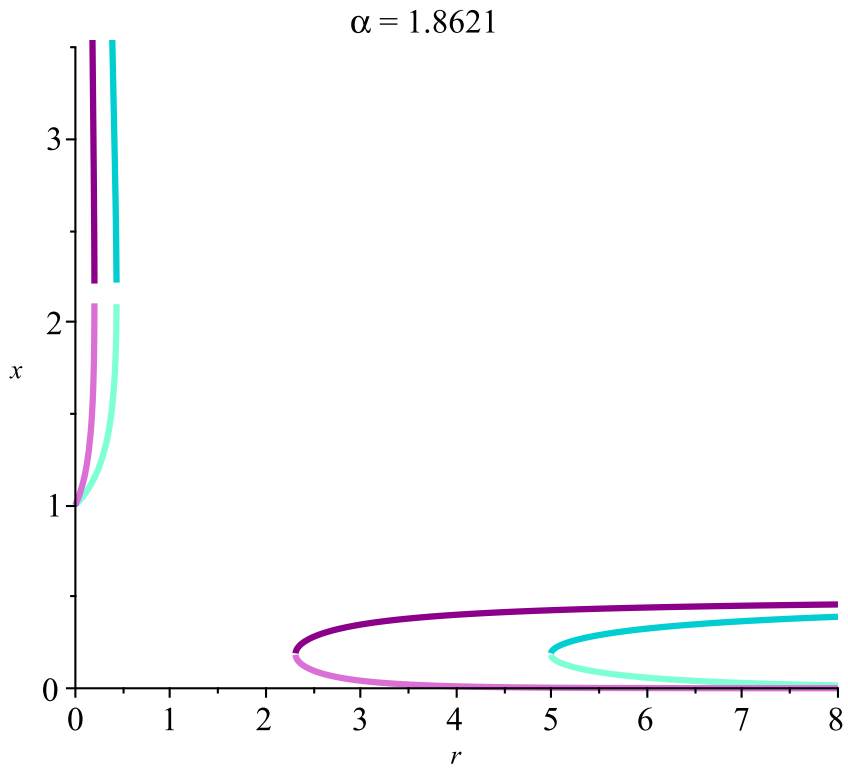

Figure 4.1: The two boundary steady states and the two interior steady states S_1, S_2, S_3 and S_4 with colors (green, dark green, purple, and dark purple) respectively. In the (r, x)-plane where the parameter $\alpha = 1.8621$ and $k = 0.5$.

Theorem 4.2.1. *Assume r, k, and α are positive parameters and let $(x^*, 0)$ be a solution of (4.9). For $k < 1$ in Ω_1, system (4.6) has:*

(i) No boundary steady state if $k < \frac{r}{\alpha} e^{1-\frac{r}{\alpha}}$.

(ii) One boundary steady state if $k = \frac{r}{\alpha} e^{1-\frac{r}{\alpha}}$. Moreover, $x^* = \frac{\alpha\, k}{r}$.

(iii) Two boundary steady states if $k > \frac{r}{\alpha} e^{1-\frac{r}{\alpha}}$. Moreover, $x_1^* < x_2^* < k$ if $\frac{\alpha\, k}{r} < 1$.

For $k > 1$, in Ω_1 system (4.6) always has two boundary steady states, $(x_1^*, 0)$ and $(x_2^*, 0)$ with $x_1^* < 1 < k < x_2^*$.

Proof. Let us use equation (4.9) to define $g(x) = r(1 - \frac{x}{k}) + \alpha \ln(x)$ with $g_1(x) = -r(1 - \frac{x}{k})$ and $g_2(x) = \alpha \ln(x)$. Take $g'(x) = 0$, then $x^* = \frac{k\alpha}{r}$ is the only critical point of g on $(0, \infty)$. Moreover,

$\lim_{x\to 0^+} g(x) = -\infty$ and $\lim_{x\to\infty} g(x) = -\infty$, therefore $x^* = \frac{k\,\alpha}{r}$ is the absolute maximum of g on $(0,\infty)$. We can now have the following cases:

(i) If $k < \frac{r}{\alpha}e^{1-\frac{r}{\alpha}}$, then $g < 0$ meaning g has no root on $(0,\infty)$. Therefore (4.9) has no solution.

(ii) If $k = \frac{r}{\alpha}e^{1-\frac{r}{\alpha}}$, then g has exactly one root at its absolute maximum.

(iii) If $k > \frac{r}{\alpha}e^{1-\frac{r}{\alpha}}$, then g has two positive roots x_1^* and x_2^*.

Claim: For $k < 1$, then either the two roots x_1^* and x_2^* are less than k, or the two roots x_1^* and x_2^* are larger than 1.

Proof by contradiction: Let us assume that g_1 and g_2 intersect at $x_1^* < k$ and $x_2^* > k$. It is then clear that the increasing function g_1 has a root at k and the other increasing function g_2 has a root at 1. Since g_2 is an increasing function and concave down, it means that g_2 must cross over the x-axis at a point less than k; otherwise, g_2 has to collide with g_1 at another point before k which is impossible by the assumption. This means that the root of g_2, which is 1, must occur before k or $1 < k$, which is a contradiction.

Moreover, the maximum of g occurs at $x^* = \frac{k\,\alpha}{r}$. We know that the two roots x_1^* and x_2^* are less than k, and that happens only if $\frac{k\,\alpha}{r} < k < 1$. The statement $\frac{k\,\alpha}{r} < k < 1$ is true because if $x_1^* < x_2^* < k$ it means $x^* < k < 1$. Furthermore, the two roots x_1^* and x_2^* are larger than 1, and that happens only if $\frac{k\,\alpha}{r} > k$. This statement $\frac{k\,\alpha}{r} > k$ is correct because if $1 < x_1^* < x_2^*$, it means that $x^* > k$.

Now assume $k > 1$. Similar to the previous case we can show that the function g has two positive roots x_1^* and x_2^* where $x_1^* < k$ and $x_2^* > 1$. □

To show which boundary steady state is larger in Q_1, consider B_1 as the exponent of the first boundary steady state x_1^* and B_2 as the exponent of the second boundary steady state x_2^* as follows:

$$B_1 = -W\left(-\frac{r\mathrm{e}^{-\frac{r}{\alpha}}}{k\,\alpha}\right) - \frac{r}{\alpha}, \qquad B_2 = -W\left(-1, -\frac{r\mathrm{e}^{-\frac{r}{\alpha}}}{k\,\alpha}\right) - \frac{r}{\alpha},$$

from the definition and Figure of Lambert W function (2.6)

$$W_0(\mathsf{x}) > W_{-1}(\mathsf{x}),$$

multiplying both sides by a negative

$$0 < -W_0(\mathsf{x}) < -W_{-1}(\mathsf{x}).$$

Therefore,

$$e^{-W\left(-\frac{re^{-\frac{r}{\alpha}}}{k\,\alpha}\right)-\frac{r}{\alpha}} < e^{-W\left(-1,-\frac{re^{-\frac{r}{\alpha}}}{k\,\alpha}\right)-\frac{r}{\alpha}}.$$

Thus, the first boundary steady state x_1^* is less than the second boundary steady state x_2^*. Below we demonstrate where these two boundary steady states $(x_1^*, 0)$ and $(x_2^*, 0)$ may exist and we identify their regions. Using the range of the largest boundary $W_{-1}(x)$ and solving it for k, it will give us the existence region. We know that

$$W\left(-1, -\frac{re^{-\frac{r}{\alpha}}}{k\,\alpha}\right) < -1,$$

that is

$$-\frac{1}{e} < -\frac{re^{-\frac{r}{\alpha}}}{k\,\alpha} < 0,$$

or

$$\frac{1}{e} > \frac{re^{-\frac{r}{\alpha}}}{k\,\alpha}.$$

Then the existence region is

$$k > \frac{re^{1-\frac{r}{\alpha}}}{\alpha}.$$

This is also shown in Figure (4.3).

Below we discuss the existence of the interior steady states.

Theorem 4.2.2. *Assume r, k, and α are positive parameters.*

For $k < 1$, the system has two cases in $\mathcal{Q}_1$: $\alpha < 1$ and $\alpha > 1$. For $\alpha < 1$, system (4.6) has only one root z_1^* with $k < z_1^* < 1$ which is not acceptable. For $\alpha > 1$, system (4.6) has three cases:

(i) No interior steady state exists if either $\frac{k\,(\alpha-1)}{r} < 1$ or $k < \frac{r}{\alpha-1} e^{1-\frac{r}{\alpha-1}}$.

(ii) One interior steady state exists if $\frac{k\,(\alpha-1)}{r} > 1$ and $k = \frac{r}{\alpha-1} e^{1-\frac{r}{\alpha-1}}$. Moreover, $x^* = \frac{k\,(\alpha-1)}{r}$.

(iii) Two interior steady states exist if $\frac{k\,(\alpha-1)}{r} > 1$ and $k > \frac{r}{\alpha-1} e^{1-\frac{r}{\alpha-1}}$. Moreover, $z_1^* < z_2^* < 1 < k$ if $\frac{(\alpha-1)\,k}{r} < 1$ and $k < 1 < z_1^* < z_2^*$ if $\frac{(\alpha-1)\,k}{r} > 1$.

For $k > 1$, in $\mathcal{Q}_1$ system (4.6) always has a unique interior steady state $(z_1^*, z_1^* - 1)$ with $1 < k < z_1^*$ for $\alpha > 1$. For $\alpha < 1$, similarly, system (4.6) always has a unique interior steady state $(z_2^*, z_2^* - 1)$ with $1 < z_2^* < k$.

Proof. Similar to the previous theorem and using equation (4.10), we can define $h(x) = r\,(1 - \frac{x}{k}) + (\alpha - 1)\,\ln(x)$, $h_1(x) = -r\,(1 - \frac{x}{k})$ and $h_2(x) = (\alpha - 1)\,\ln(x)$. Take $h'(x) = 0$, then $x^* = \frac{k\,(\alpha-1)}{r}$ is the only critical point of h on $(0, \infty)$. Moreover, if $\alpha > 1$, $\lim_{x\to 0^+} h(x) = -\infty$ and $\lim_{x\to\infty} h(x) = -\infty$, therefore $x^* = \frac{k\,(\alpha-1)}{r}$ is the absolute maximum of h on $(0, \infty)$. For $k < 1$, there are two cases:

When $\alpha < 1$, the only intersection steady state point of h_1 and h_2 is given by $0 < z_1^* < \infty$ $\forall r, k$ because z_2^* does not exist. However, the root is in the region $k < z_1^* < 1$ because h_1 is an increasing function that passes through k, and h_2 is a decreasing function that passes at point 1. Since $h_1(k) < h_2(k)$ and $h_2(1) < h_1(1)$, then there exists a unique intersection $z_1^* \in (k, 1)$ s.t $h_1(z_1^*) = h_2(z_1^*)$. But $z_1^* < 1$ corresponds to $y^* = z_1^* - 1 < 0$ and it does not exist either. Therefore, for $k < 1$ and $\alpha < 1$ there is no interior root.

When $\alpha > 1$, we have the following cases:

(i) If $k < \frac{r}{\alpha-1} e^{1-\frac{r}{\alpha-1}}$ then h has no root on $(0, \infty)$. Therefore (4.9) has no solution.

(ii) If $k = \frac{r}{\alpha-1} e^{1-\frac{r}{\alpha-1}}$ then h has exactly one root at its absolute maximum.

(iii) If $k > \frac{r}{\alpha-1}e^{1-\frac{r}{\alpha-1}}$ then h has maximum two positive roots z_1^* and z_2^*. Similar to the previous theorem, we can show that, for $k < 1$ and $\alpha > 1$, then either the two roots z_1^* and z_2^* are less than k, or the two roots z_1^* and z_2^* are larger than 1.

For $k > 1$, when $\alpha < 1$ there is only one root z_1^* with $1 < z_1^* \leq k$. The intersection point of h_1 and h_2 is given by the steady state $0 < z_1^* < \infty \; \forall r, k$. In addition, the root is in the region $1 < z_1^* < k$ because h_1 is an increasing function that passes through point k, and h_2 is a decreasing function that passes through the point 1. Since $h_1(k) < h_2(k)$ and $h_2(1) < h_1(1)$, then there exists $z_1^* \in (k, 1)$ s.t $h_1(z_1^*) = h_2(z_1^*)$.

For $\alpha > 1$, it is not difficult to show that the function h has two positive roots z_1^* and z_2^* where $z_1^* < k$ and $z_2^* > 1$. □

To illustrate which interior steady state is larger in Q_1, consider I_1 as the exponent of the first interior steady state z_1^* and I_2 as the exponent of the second interior steady state z_2^* as follows:

$$I_1 = -W\left(-\frac{r\mathrm{e}^{-\frac{r}{\alpha-1}}}{k(\alpha-1)}\right) - \frac{r}{\alpha-1}, \quad I_2 = -W\left(-1, -\frac{r\mathrm{e}^{-\frac{r}{\alpha-1}}}{k(\alpha-1)}\right) - \frac{r}{\alpha-1}.$$

Therefore,

$$e^{-W\left(-\frac{r\mathrm{e}^{-\frac{r}{\alpha-1}}}{k(\alpha-1)}\right)-\frac{r}{\alpha-1}} < e^{-W\left(-1,-\frac{r\mathrm{e}^{-\frac{r}{\alpha-1}}}{k(\alpha-1)}\right)-\frac{r}{\alpha-1}}.$$

Thus, the second interior steady state z_2^* is larger than the first interior steady state z_1^*. Below we look for the regions where those two interior steady states $(z_1^*, z_1^* - 1)$ and $(z_2^*, z_2^* - 1)$ exist. Using the domain of the largest boundary $W_{-1}(x)$ and solving it for k will give the existence region

$$-\frac{1}{e} < -\frac{r\mathrm{e}^{-\frac{r}{\alpha-1}}}{k(\alpha-1)} < 0,$$

if $\alpha > 1$, then

$$\frac{1}{e} > \frac{r\mathrm{e}^{-\frac{r}{\alpha-1}}}{k(\alpha-1)},$$

or

$$k > \frac{re^{1-\frac{r}{\alpha-1}}}{\alpha-1}.$$

However, if $\alpha < 1$, we only have W_0 for all r and k since

$$0 < -\frac{r\mathrm{e}^{-\frac{r}{\alpha-1}}}{k(\alpha-1)} < \infty.$$

Thus, solving them for k gives the existence region that is shown in Figure (4.2).

The results in theorems (4.2.1) and (4.2.2) can be summarized in the following:

Corollary 4.2.3. *Assume r, k, and α are positive parameters. System (4.6) has four cases in Ω_1.*

(i) Two boundary and one interior steady state for $k > 1$, $\forall\ \alpha, r$.

(ii) Two boundary and no interior steady state for $\frac{r}{\alpha}e^{1-\frac{r}{\alpha}} < k < 1$ with $0 < \alpha < r$ or $\frac{r}{\alpha}e^{1-\frac{r}{\alpha}} < k < \frac{r}{\alpha-1}e^{1-\frac{r}{\alpha-1}}$ with $\alpha > r$, or

$$-\frac{r}{W\left(-k\mathrm{e}^{-1}\right)} < \alpha < -\frac{r}{W\left(-k\mathrm{e}^{-1}\right)} + 1$$

with $\alpha < r < \alpha + 1$.

(iii) No boundary and no interior steady state for $k < \frac{r}{\alpha}e^{1-\frac{r}{\alpha}}$.

(iv) Two boundary and two interior steady states for $\frac{r}{\alpha-1}e^{1-\frac{r}{\alpha-1}} < k < 1$.

In the following we anlayze the stability of the boundary steady states and the interior steady states.

4.3 Stability of the Boundary Steady States

In this section we plan to prove the stability of the steady states for different parameter values, especially for k.

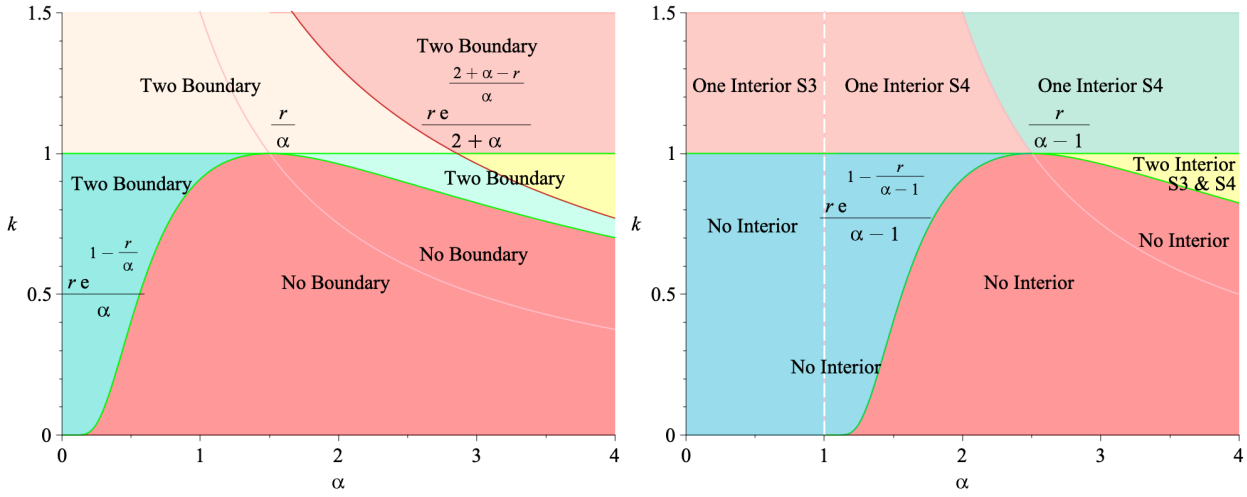

Figure 4.2: From left to right: The curves $k = \frac{r}{\alpha}e^{r(1-\frac{r}{\alpha})}$, $k = 1$, $k = \frac{r}{\alpha}$, $k = \frac{r}{\alpha+2}e^{1-\frac{2-r}{\alpha}}$ are green, green, pink, and orange respectively. The curves $k = \frac{r}{\alpha-1}e^{r(1-\frac{r}{\alpha-1})}$, $k = 1$, $k = \frac{r}{\alpha-1}$, $x = 1$ are green, green, pink, and white respectively. Contribution of number of boundary and interior steady states of system (4.6) in (α, k)-plane.

Theorem 4.3.1. *Assume r, k, and α are positive parameters, then the following statements hold for the stability of the boundary steady states of system (4.6) in $\mathcal{Q}_1$.*

1. *The steady state $S_0 = (0, 0)$ is stable.*

2. *The steady states $S_1 = (x_1^*, 0)$ and $S_2 = (x_2^*, 0)$ satisfy the following statements:*

   (a) *If $k < 1$ and $k < \frac{r}{\alpha}$, then $S_1 = (x_1^*, 0)$ is saddle and $S_2 = (x_2^*, 0)$ is stable.*

   (b) *If $k < 1$ and $k > \frac{r}{\alpha}$, then $S_1 = (x_1^*, 0)$ is repeller and $S_2 = (x_2^*, 0)$ is saddle, but it changes to repeller once it crosses $x_2^* > \frac{(\alpha+2)\,k}{r}$.*

   (c) *If $k > 1$ then $S_1 = (x_1^*, 0)$ is saddle and $S_2 = (x_2^*, 0)$ is saddle, but it changes to repeller once it crosses $x_2^* > \frac{(\alpha+2)\,k}{r}$.*

Proof. The Jacobian matrix of the map associated with system (4.6) is

$$J = \begin{pmatrix} \frac{x^\alpha\,(1+\alpha)}{(1+y)}\,\mathrm{e}^{r\left(1-\frac{x}{k}\right)} - \frac{r\,x^{1+\alpha}}{k\,(1+y)}\,\mathrm{e}^{r\left(1-\frac{x}{k}\right)} & -\frac{x^{1+\alpha}}{(1+y)^2}\,\mathrm{e}^{r\left(1-\frac{x}{k}\right)} \\ 1 - \frac{1}{1+y} & \frac{x}{(1+y)^2} \end{pmatrix}. \tag{4.12}$$

1. Jacobian matrix (4.12) at the steady state $S_0 = (0, 0)$ is given by

$$J(S_0) = \begin{pmatrix} 0 & 0 \\ 0 & 0 \end{pmatrix}.$$

The eigenvalues of $J(S_0)$ are both 0's, thus both have a magnitude less than 1, therefore S_0 is always stable.

2. Jacobian matrix (4.12) at the boundary steady state B is given by

$$J(B) = \begin{pmatrix} 1 + \alpha - \frac{r}{k}x^* & -x^* \\ 0 & x^* \end{pmatrix}. \tag{4.13}$$

The eigenvalues of $J(B)$ are $\lambda_1 = 1 + \alpha - \frac{r\,x^*}{k}$ and $\lambda_2 = x^*$. The stability of the steady state S_1 and S_2 satisfy the following conditions:

(a) Since $k < 1$ and $k < \frac{r}{\alpha}$, then from Theorem 4.2.1 we know that $x_1^* < x_2^* < k < 1$. Therefore $\lambda_2(x_1^*) = x_1^* < 1$ and $\lambda_2(x_2^*) = x_2^* < 1$. For $\lambda_1(x_1^*) = 1 + \alpha - \frac{r}{k}\,x_1^*$, since

$$W\left(\frac{-re^{-\frac{r}{\alpha}}}{k\alpha}\right) > -1 \Longrightarrow \alpha\left(1 + W\left(-\frac{re^{-\frac{r}{\alpha}}}{k\alpha}\right)\right) > 0 \Longrightarrow \alpha + \alpha\, W\left(-\frac{re^{-\frac{r}{\alpha}}}{k\alpha}\right) > 0,$$

using $W(\mathsf{x}) = e^{-W(\mathsf{x})}$ gives

$$\alpha - \frac{r}{k}e^{-\frac{r}{\alpha}}\frac{W\left(-\frac{re^{-\frac{r}{\alpha}}}{k\alpha}\right)}{\frac{-re^{-\frac{r}{\alpha}}}{k\alpha}} > 0 \Longrightarrow \alpha - \frac{r}{k}e^{-\frac{r}{\alpha}}e^{-W\left(\frac{-re^{-\frac{r}{\alpha}}}{k\alpha}\right)} > 0$$

$$\Longrightarrow 1 + \alpha - \frac{r}{k}e^{-W\left(\frac{-re^{-\frac{r}{\alpha}}}{k\alpha}\right)-\frac{r}{\alpha}} > 1.$$

Thus, $\lambda_1(x_1^*) = 1 + \alpha - \frac{r}{k}x_1^* > 1$. Therefore, $S_1 = (x_1^*, 0)$ is saddle.

Moreover, for $\lambda_1(x_2^*) = 1 + \alpha - \frac{r}{k}\,x_2^*$, since

$$W\left(-1, \frac{-re^{-\frac{r}{\alpha}}}{k\alpha}\right) < -1 \Longrightarrow \alpha\left(1 + W\left(-1, \frac{-re^{-\frac{r}{\alpha}}}{k\alpha}\right)\right) < 0$$
$$\Longrightarrow \alpha + \alpha W\left(-1, \frac{-re^{-\frac{r}{\alpha}}}{k\alpha}\right) < 0.$$

it means

$$\alpha - \frac{r}{k}e^{-\frac{r}{\alpha}} \frac{W\left(-1, -\frac{re^{-\frac{r}{\alpha}}}{k\alpha}\right)}{\frac{-re^{-\frac{r}{\alpha}}}{k\alpha}} < 0 \Longrightarrow 1 + \alpha - \frac{r}{k}e^{-W\left(-1, \frac{-re^{-\frac{r}{\alpha}}}{k\alpha}\right) - \frac{r}{\alpha}} < 1.$$

Thus, $\lambda_1(x_2^*) = 1 + \alpha - \frac{r}{k}x_2^* < 1$. Therefore, $S_2 = (x_2^*, 0)$ is stable.

(b) If $k < 1$ and $k > \frac{r}{\alpha}$, then from Theorem 4.2.1 $k < 1 < x_1^* < x_2^*$. This means $\lambda_2(x_1^*) = x_1^* > 1$ and $\lambda_2(x_2^*) = x_2^* > 1$. For $\lambda_1 = 1+\alpha-\frac{r}{k}x^*$ we know from part (a) that $\lambda_1(x_1^*) > 1$ and $\lambda_1(x_2^*) < 1$ always. Therefore, $S_1 = (x_1^*, 0)$ is repeller, and $S_2 = (x_2^*, 0)$ is saddle if $-1 < \lambda_1(x_2^*) < 1$. If, however, $\lambda_1(x_2^*) < -1$, it means $S_2 = (x_2^*, 0)$ is a repeller and $\lambda_1(x_2^*) = 1 + \alpha - \frac{r}{k}x_2^* < -1 \Longrightarrow 2 + \alpha < \frac{r}{k}x_2^* \Longrightarrow x_2^* > \frac{(\alpha+2)k}{r}$.

(c) Since $k > 1$ from Theorem 4.2.1 we know that $x_1^* < 1 < k < x_2^*$. That is, $\lambda_2(x_1^*) = x_1^* < 1$ and $\lambda_2(x_2^*) = x_2^* > 1$. For $\lambda_1 = 1 + \alpha - \frac{r}{k}x^*$, we know from part (a) that $\lambda_1(x_1^*) > 1$ and $\lambda_1(x_2^*) < 1$. Therefore, $S_1 = (x_1^*, 0)$ is saddle, and so is $S_2 = (x_2^*, 0)$, until it crosses -1, i.e., $\lambda_1(x_2^*) = 1 + \alpha - \frac{r}{k}x_2^* < -1 \Longrightarrow 2 + \alpha < \frac{r}{k}x_2^* \Longrightarrow x_2^* > \frac{(\alpha+2)k}{r}$ which means that now $\lambda_1(x_2^*) > 1$, that is, $S_2 = (x_2^*, 0)$ changes to a repeller.

□

This stability can be seen in Figure (4.3).

Note: $x^* = \frac{r}{2+\alpha}e^{\frac{2+\alpha-r}{\alpha}}$ means the first eigenvalue of matrix (4.13) is equal to -1, then we solve it for x as follows

$$1 + \alpha - \frac{r}{k}x^* = -1,$$

we get

$$x^* = \frac{(2+\alpha)k}{r}.$$

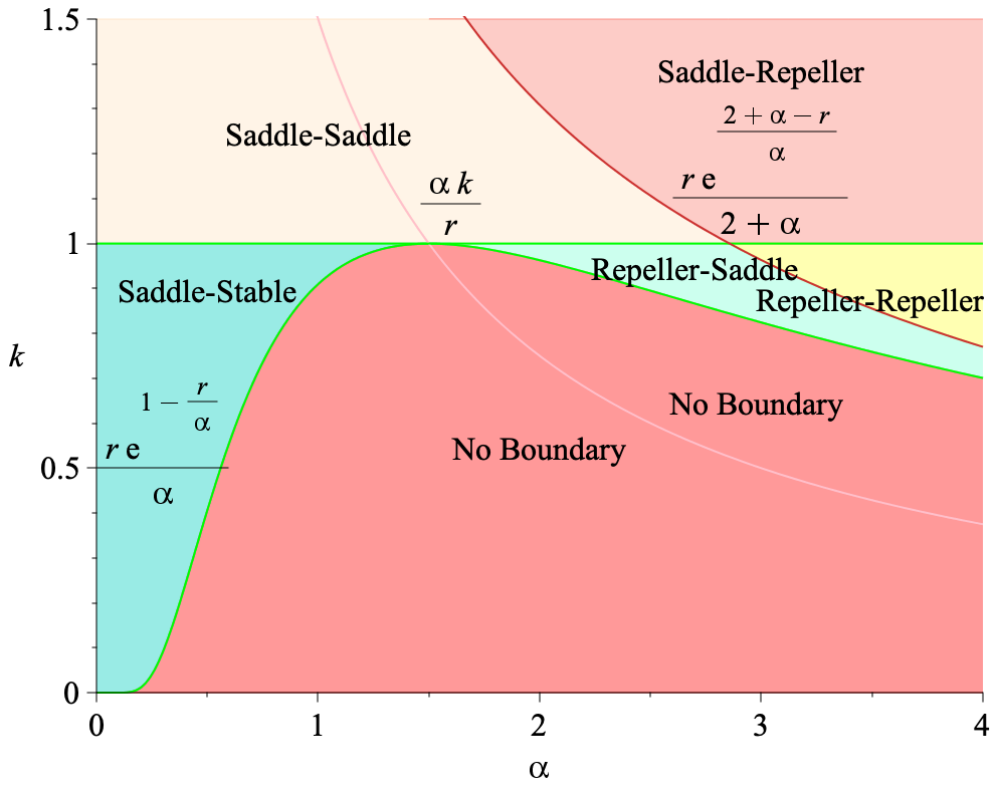

Figure 4.3: Stability regions of the boundary steady-states $(x_1^*, 0)$ and $(x_2^*, 0)$ where $r = 1.5$. The two green curves are $k = 1$ and $k = \frac{r\mathrm{e}^{\frac{\alpha-r}{\alpha}}}{\alpha}$. The pink curve is $k = \frac{r}{\alpha}$ and the orange curve is $k = \frac{r\mathrm{e}^{\frac{2+\alpha-r}{\alpha}}}{2+\alpha}$.

We know that x^* is the Allee effect steady state S_1 in (4.11), so we can substitute it by

$$\mathrm{e}^{-\frac{\mathrm{w}\left(-\frac{r\,\mathrm{e}^{-\frac{r}{\alpha}}}{k\,\alpha}\right)\alpha+r}{\alpha}} = \frac{(2+\alpha)\,k}{r},$$

rewrite it by

$$\mathrm{e}^{-\mathrm{w}\left(-\frac{r\,\mathrm{e}^{-\frac{r}{\alpha}}}{k\,\alpha}\right)-\frac{r}{\alpha}} = \frac{(2+\alpha)\,k}{r},$$

then solve it for k we get

$$k = \frac{r}{2+\alpha}\,\mathrm{e}^{\frac{-r}{\alpha}}\,\mathrm{e}^{-\mathrm{w}\left(-\frac{r\,\mathrm{e}^{-\frac{r}{\alpha}}}{k\alpha}\right)}.$$

By using the property (2.30) for the W function, we have

$$k = \frac{r}{2+\alpha}\, \mathrm{e}^{\frac{-r}{\alpha}} \frac{\mathrm{W}\left(-\frac{r\mathrm{e}^{-\frac{r}{\alpha}}}{k\alpha}\right)}{-\frac{re^{-\frac{r}{\alpha}}}{k\alpha}} = -\frac{k\alpha}{2+\alpha}\, W\left(-\frac{r\mathrm{e}^{-\frac{r}{\alpha}}}{k\alpha}\right),$$

or

$$k\left(1 + \frac{\alpha}{2+\alpha}\, W\left(-\frac{r\mathrm{e}^{-\frac{r}{\alpha}}}{k\alpha}\right)\right) = 0,$$

simplifying it

$$\frac{\alpha}{2+\alpha}\, W\left(-\frac{r\mathrm{e}^{-\frac{r}{\alpha}}}{k\alpha}\right) = -1,$$

then

$$W\left(-\frac{r\mathrm{e}^{-\frac{r}{\alpha}}}{k\alpha}\right) = -\frac{2+\alpha}{\alpha}.$$

Applying the inverse of the W function to both sides gives

$$-\frac{r\mathrm{e}^{-\frac{r}{\alpha}}}{k\alpha} = -\frac{2+\alpha}{\alpha}\mathrm{e}^{-\frac{2+\alpha}{\alpha}},$$

solving it for k, then

$$k = \frac{r\,\mathrm{e}^{\frac{2+\alpha-r}{\alpha}}}{2+\alpha}. \tag{4.14}$$

The stability of the second boundary steady-state changed from saddle to repeller once it crossed this curve $k = \frac{r\,\mathrm{e}^{\frac{2+\alpha-r}{\alpha}}}{2+\alpha}$, as we can see in Figure (4.3). Similarly, let the first eigenvalue of matrix (4.13) be equal to 1 and solve it for x^*.

$$1 + \alpha - \frac{r}{k}x^* = 1,$$

which gives

$$x^* = \frac{\alpha k}{r}.$$

Then substitute x^* and solve for k as follows

$$\mathrm{e}^{-\frac{\mathrm{w}\left(-\frac{r\mathrm{e}^{-\frac{r}{\alpha}}}{k\alpha}\right)\alpha+r}{\alpha}} = \frac{\alpha k}{r},$$

or

$$k = \frac{r}{\alpha}\,\mathrm{e}^{\frac{-r}{\alpha}}\mathrm{e}^{-\mathrm{w}\left(-\frac{r\,\mathrm{e}^{-\frac{r}{\alpha}}}{k\alpha}\right)} = \frac{r}{\alpha}\,\mathrm{e}^{\frac{-r}{\alpha}}\frac{\mathrm{W}\left(-\frac{r\mathrm{e}^{-\frac{r}{\alpha}}}{k\alpha}\right)}{-\frac{r\mathrm{e}^{-\frac{r}{\alpha}}}{k\alpha}} = -\frac{k\alpha}{\alpha}\,W\left(-\frac{r\mathrm{e}^{-\frac{r}{\alpha}}}{k\alpha}\right),$$

then

$$k\left(1 + W\left(-\frac{r\mathrm{e}^{-\frac{r}{\alpha}}}{k\alpha}\right)\right) = 0.$$

It then follows that

$$W\left(-\frac{r\mathrm{e}^{-\frac{r}{\alpha}}}{k\alpha}\right) = -1,$$

equivalently,

$$-\frac{r\mathrm{e}^{-\frac{r}{\alpha}}}{k\alpha} = -\frac{1}{e} \Longrightarrow -r\mathrm{e}^{-\frac{r}{\alpha}} = -\frac{\alpha\, k}{e} \Longrightarrow k = \frac{r\mathrm{e}^{\frac{\alpha-r}{\alpha}}}{\alpha}.$$

Now, the stability of the non-hyperbolic steady state $(x_2^*, 0)$ can be presented by the center manifold theory for system (4.6). The theorem below provides all the possibilities needed to apply center manifold theory to determine the local stability.

Theorem 4.3.2. *Assume r, k, and α, are positive parameters, then the following statements hold for the stability of the boundary steady states of system (4.6) in Ω_1.*

(i) If $k = 1$ and $r \neq \alpha$, then S_2 is unstable non-hyperbolic steady state.

(ii) If $k = 1$ and $r = \alpha$, then S_2 is unstable non-hyperbolic steady state.

(ii) If $k \neq 1$ and $x^* = \frac{\alpha\, k}{r}$, then $S_1 = S_2$ is stable non-hyperbolic steady state.

Proof. (i) Suppose $k = 1$, $r \neq \alpha$ and $\lambda_1(x_2^*) = 1 + \alpha - \frac{r}{k}x_2^* = 1$. Then solve it for r, it gives $r = \frac{\alpha\, k}{x_2^*}$. Substitute the value of r in $x_2^* = e^{-\frac{\mathrm{w}\left(-\frac{re^{-\frac{r}{\alpha}}}{k\alpha}\right)\alpha+r}{\alpha}}$, which gives $x_2^* = -\frac{k}{\mathrm{W}\,(-k\,\mathrm{e}^{-1})}$, and since $k = 1$ then that gives $x_2^* = 1$ because $W(-\frac{1}{e}) = -1$. To study the dynamics about the steady state S_2 in $\Omega_1 = \left\{(x, y) \in \mathbb{R}^2 \mid x \geq 0, y \geq 0\right\}$, it is required to explicitly

compute the local center manifold. For the sake of simplicity of calculation, we first bring the steady state S_2 of system (4.6) to the origin S_0, which is done by the linear translation $(x, y) \mapsto (x + x^*, y)$. Then the map associated with system (4.6) translates to the following system:

$$\begin{aligned} f_1(x,y) =& (x+x^*)^{1+\alpha}\, e^{r\left(1-\frac{x+x^*}{k}\right)} \frac{1}{1+y} - x^*, \\ g_1(x,y) =& (x+x^*)\left(1-\frac{1}{1+y}\right). \end{aligned} \tag{4.15}$$

The Taylor series expansion of map (4.15) is given by

$$\begin{aligned} f_1(x,y) =& \frac{(k\alpha - rx^* + k)}{k}\, x - x^* y - \frac{(k\alpha - rx^* + k)}{k} xy \\ &+ \frac{\left((\alpha^2+\alpha)\,k^2 - 2r(1+\alpha)x^*k + r^2x^{*2}\right)}{2x^*k^2} x^2 + x^* y^2 \\ &- \frac{\left((\alpha^2+\alpha)\,k^2 - 2r(1+\alpha)x^*k + r^2x^{*2}\right)}{2x^*k^2} x^2 y + \frac{(k\alpha - rx^* + k)}{k} xy^2 \\ &+ \frac{\left((\alpha^3-\alpha)\,k^3 - 3(1+\alpha)\alpha r k^2 x^* + 3r^2x^{*2}(1+\alpha)k - r^3x^{*3}\right)}{6x^{*2}k^3} x^3 - x^* y^3 + \mathcal{O}(4), \\ g_1(x,y) =& x^*\, y^3 - x^*\, y^2 - x\, y^2 + x^*\, y + x\, y + \mathcal{O}(4). \end{aligned} \tag{4.16}$$

The linear part of equation (4.16) is

$$J = \begin{pmatrix} \alpha + 1 - \frac{r\,x^*}{k} & -x^* \\ 0 & x^* \end{pmatrix}. \tag{4.17}$$

The eigenvalues $\lambda_{1,2}$ and the eigenvectors P of those eigenvalues for matrix (4.17) are

$$\lambda_{1,2} = \begin{pmatrix} 1+\alpha-r \\ 1 \end{pmatrix}, P = \begin{pmatrix} 1 & \frac{1}{\alpha - r} \\ 0 & 1 \end{pmatrix}.$$

Consider the change of coordinates

$$\begin{pmatrix} x \\ y \end{pmatrix} = \begin{pmatrix} 1 & \frac{1}{\alpha - r} \\ 0 & 1 \end{pmatrix} \begin{pmatrix} u \\ v \end{pmatrix} = \begin{pmatrix} u + \frac{1}{\alpha - r} v \\ v \end{pmatrix}.$$

The computation shows that the equation $D = P^{-1}JP$ and the nonlinear part indeed hold.

$$\begin{pmatrix} u \\ v \end{pmatrix} \mapsto \begin{pmatrix} 1 + \alpha - r & 0 \\ 0 & 1 \end{pmatrix} \begin{pmatrix} u \\ v \end{pmatrix} + P^{-1} \begin{pmatrix} \tilde{f}(u, v) \\ \tilde{g}(u, v) \end{pmatrix},$$

where

$$P^{-1} = \begin{pmatrix} 1 & -\frac{1}{\alpha - r} \\ 0 & 1 \end{pmatrix}.$$

The nonlinear part is

$$\begin{aligned} \tilde{f}(u, v) =& \frac{(\alpha^2 + (-2r + 1)\alpha + r^2 - 2r)}{2} u^2 + \frac{(r + 1)}{r - \alpha} u\, v \\ &+ \frac{(\alpha^2 + (-2r + 1)\alpha + r^2 - 2r - 2)}{2(r - \alpha)^2} v^2 + \mathcal{O}(3) \\ \tilde{g}(u, v) =& u\, v - \frac{(r - \alpha + 1)}{-\alpha + r} v^2 + \mathcal{O}(3). \end{aligned}$$

Since the invariant manifold is tangent to the corresponding eigenspace, and the second eigenvalue λ_2 is the one we need to examine its local stability, we assume the form $u = h(v)$.

$$u = h(v) = a\, v^2 + b\, v^3 + \mathcal{O}\left(v^4\right), \quad a, b \in \mathbb{R}$$

Now to compute the constants a and b, the function h must satisfy the center manifold equation

$$h(\lambda_2\, v + \tilde{g}(v, h(v))) - \lambda_1\, h(v) - \tilde{f}(v, h(v)) = 0. \tag{4.18}$$

Calculating (4.18), we get

$$a = \frac{\alpha^2 + (-2r+1)\alpha + r^2 - 2r - 2}{2(-\alpha + r)^3},$$

$$b = \frac{1}{6(-\alpha+r)^3}\Big[(-12a+2)\alpha^3 + ((42a-6)r + 18a + 3)\alpha^2 + (-5 + (-48a+6)r^2 + (-36a-6)r)\alpha + (18a-2)r^3 + (18a+3)r^2 + 6r\Big]. \quad (4.19)$$

Hence,

$$h(v) = \frac{\alpha^2 + (-2r+1)\alpha + r^2 - 2r - 2}{2(r-\alpha)^3}\, v^2 + \mathcal{O}(3).$$

We then have the dynamics on the center manifold by the map:

$$v \mapsto v + \frac{r - \alpha + 1}{\alpha - r} v^2 + \mathcal{O}\left(v^3\right) \quad (4.20)$$

It then follows that the steady state is half-stable as demonstrated in Figure (4.4). In the original coordinates system, the center manifold at $S_2 = (x_2^*, 0)$ then takes the form

$$x = x^* + \frac{1}{\alpha - r}\, y + \frac{\alpha^2 + (-2r+1)\alpha + r^2 - 2r - 2}{2(r-\alpha)^3}\, y^2, \quad \text{as } y \to 0.$$

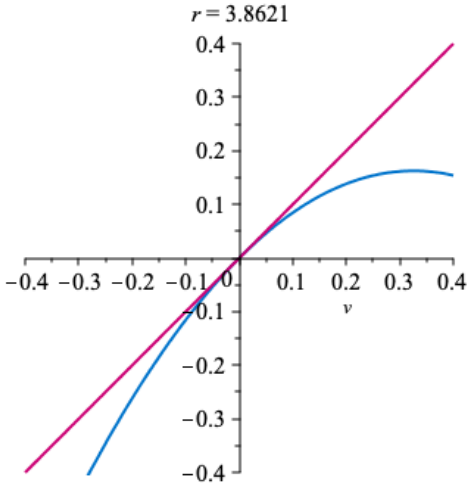

Figure 4.4: Center manifold is half-stable or semi-stable for $r = 3.8621$ and $u = h(v)$.

Similar results for the proof of the case $k = 1$ and $r \neq \alpha$ can be found because when we cross the curve $k = 1$ in Figure (4.4) upward, the system shows changing dynamic behavior from stable to saddle as well as crossing horizontally when $k = 1$ and $\alpha = r$.

(ii) Suppose $k = 1$ and $\alpha = r$, then both eigenvalues are one. In this case, use normal form by letting $\alpha = r + \alpha_1$, and consider the change of coordinates that provide the following,

$$\begin{pmatrix} x \\ y \end{pmatrix} = \begin{pmatrix} 1 & \frac{1}{\alpha_1} \\ 0 & 1 \end{pmatrix} \begin{pmatrix} u \\ v \end{pmatrix} = \begin{pmatrix} u + \frac{1}{\alpha_1} v \\ v \end{pmatrix}.$$

It then follows that

$$\begin{pmatrix} u \\ v \end{pmatrix} \mapsto \begin{pmatrix} 1 + \alpha_1 & 0 \\ 0 & 1 \end{pmatrix} \begin{pmatrix} u \\ v \end{pmatrix} + P^{-1} \begin{pmatrix} f(u, v) \\ g(u, v) \end{pmatrix},$$

where

$$\begin{aligned} \tilde{f}(u, v) =& \frac{(\alpha_1^2 + \alpha_1 - r)}{2} u^2 - \frac{(r + 1)}{\alpha_1} uv + \frac{(\alpha_1^2 + \alpha_1 - r - 2)}{2\alpha_1^2} v^2 + \mathcal{O}(3) \\ \tilde{g}(u, v) =& u\, v - \frac{(\alpha_1 - 1)}{\alpha_1} v^2 + \mathcal{O}(3). \end{aligned}$$

Assume the map h takes the following form, and by some computation we get the center manifold by

$$u = h(v) = \alpha\, v^2 + \beta\, v^3 + \mathcal{O}\left(v^4\right) = -\frac{(\alpha_1^2 + \alpha_1 - r - 2)}{2\alpha_1^3} v^2 + \mathcal{O}(3).$$

Thus, the dynamics of the center manifold is given by the map:

$$v \mapsto v - \frac{(\alpha_1 - 1)}{\alpha_1} v^2 + \mathcal{O}\left(v^3\right)$$

It follows that the steady state is half-stable or semi-stable as demonstrated in Figure (4.5).

In the original coordinates system, the center manifold at $S_2 = (x^*, 0)$ takes the form

$$x = x^* + \frac{1}{\alpha_1}\, y + \frac{(-\alpha_1^2 - \alpha_1 + r + 2)}{2\alpha_1^3}\, y^2, \quad \text{as } y \to 0.$$

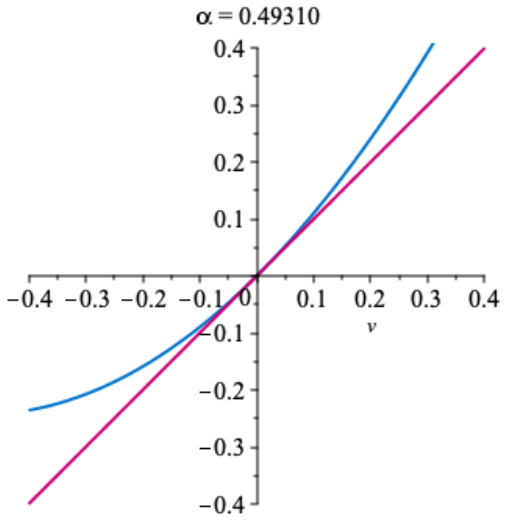

Figure 4.5: The center manifold is half-stable or semi-stable. Here $\alpha = 0.43$ for $u = h(v)$.

(iii) If $k \neq 1$ and $x^* = \frac{\alpha\, k}{r}$, consider the change of coordinates,

$$\begin{pmatrix} x \\ y \end{pmatrix} = \begin{pmatrix} 1 & -\frac{\alpha\, k}{\alpha\, k - r} \\ 0 & 1 \end{pmatrix} \begin{pmatrix} u \\ v \end{pmatrix} = \begin{pmatrix} u - \frac{\alpha\, k}{\alpha\, k - r}\, v \\ v \end{pmatrix}.$$

It follows that

$$\begin{pmatrix} u \\ v \end{pmatrix} \mapsto \begin{pmatrix} 1 & 0 \\ 0 & \frac{\alpha\, k}{r} \end{pmatrix} \begin{pmatrix} u \\ v \end{pmatrix} + \begin{pmatrix} -\frac{r}{2k} u^2 + \frac{r\,(\alpha+1)}{\alpha\, k - r} uv - \frac{(2k+r)k\alpha^2}{2(k\alpha - r)^2} v^2 + \mathcal{O}(3) \\ u\, v - \frac{\alpha^2 k^2}{(\alpha k - r) r} v^2 + \mathcal{O}(3) \end{pmatrix}.$$

Assume that the map h takes the following form and by some computation, the center manifold is attained as follows

$$v = h(u) = \alpha\, u^2 + \beta\, u^3 + \mathcal{O}\left(u^4\right) \equiv 0.$$

Then the dynamics of the center manifold is given by the following map:

$$u \mapsto -u - \frac{r}{2k}u^2 + \mathcal{O}\left(u^3\right)$$

Therefore, it follows that the steady state is stable and is provided by Figure (4.6).

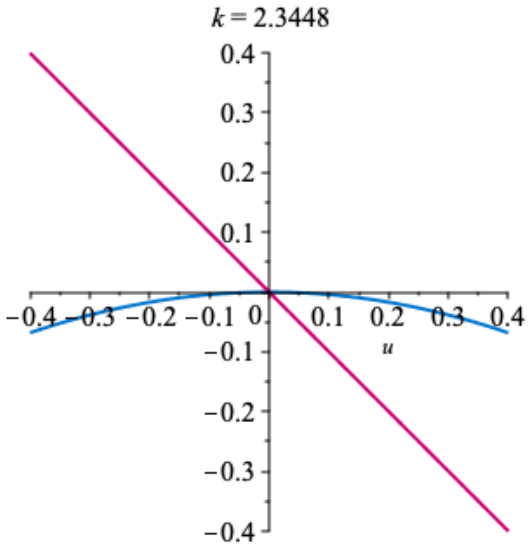

Figure 4.6: Center manifold is stable when $k = 2.3448$ and $r = 2$ for $v = h(u)$.

□

4.4 Stability Regions of the Interior Steady-States

In this section, we estimate the stability regions of the interior steady states S_3 and S_4 for co-dimension one (x, r), (x, k) and (x, α) planes. For co-dimension two, (α, k), (r, k) and (r, α) planes in $\mathcal{Q}_1$, the largest interior steady state S_4 is used. Moreover, the region in this section being considered is $x \geq 1$, because $x = y + 1$ and $y \geq 0$. We started first by getting Jacobian matrix (4.12) of system (4.6) at the interior steady-state $x^{\alpha}\ \mathrm{e}^{r\left(1-\frac{x}{k}\right)} = 1 + y$ and $x = 1 + y$, which is reduced to

$$J^* = \begin{pmatrix} 1 + \alpha - \frac{x^* r}{k} & -1 \\ 1 - \frac{1}{x^*} & \frac{1}{x^*} \end{pmatrix}. \tag{4.21}$$

4.4.1 One Parameter Bifurcation (Co-Dimension 1)

In order to study the stability of the interior steady states, we start by transforming the $(\mathrm{tr}, \det)$ plane to other one co-dimension using the linearization theorem and stability conditions (2.2.1). The stability regions for the (x, r)-plane is presented as follows,

Theorem 4.4.1. *Suppose $k > 0$, $\alpha > 0$ and let $\Omega = \{(x, r) \mid r \geq 0,\ x \geq 1\}$. The stability regions of dynamical system (4.6) in (x, r)-plane is given by the following statements:*

(i) The region delimited between $r > f_1(x) = \alpha + \ln(x)(1-\alpha)$ and $r < f_3(x) = \frac{-(\alpha-1)(x+1)\ln(x)+(\alpha+3)x+\alpha+1}{x+1}$ is stable.

(ii) The region delimited between $r > f_2(x) = \ln(x)(1-\alpha)+\alpha-1$ and $r < f_1(x) = \alpha + \ln(x)(1-\alpha)$ is repelling.

(iii) The region below $r < f_2(x) = \ln(x)(1-\alpha)+\alpha-1$ or above $r > f_3(x) = \frac{-(\alpha-1)(x+1)\ln(x)+(\alpha+3)x+\alpha+1}{x+1}$ is saddle.

Also the acceptable (positive) region is the region where $r > \ln(x)(1-\alpha)$ (shown by the orange curve in Figure (4.7)).

Proof. Solving the equation $x^{\alpha}\ e^{r(1-\frac{x}{k})} = x$ for k gives $k = \frac{r\,x}{r-\ln(x)+\alpha\,\ln(x)} > 0$, that is $r > -\alpha\,\ln(x) + \ln(x)$ (orange curve). Substituting k in Jacobin matrix (4.21) gives the determinant and trace

$$\mathrm{tr} = 1 + \alpha - r + \ln(x) - \alpha\,\ln(x) + \frac{1}{x} \qquad \text{and} \qquad \det = \frac{-\alpha\,\ln(x) + \ln(x) + \alpha - r + x}{x}.$$

For simplicity, we drop asterix from the steady state x^*. The region delimited between the three curves from inequalities (2.4) $\det = 1$, $\det = \mathrm{tr} - 1$ and $\det = -\mathrm{tr} - 1$ provides stable region and is equivalent to $r = f_1(x) = \alpha + \ln(x)(1-\alpha)$, $r = f_2(x) = \ln(x)(1-\alpha)+\alpha-1$, $r = f_3(x) = \frac{-(\alpha-1)(x+1)\ln(x)+(\alpha+3)x+\alpha+1}{x+1}$ in (x, r)-plane, respectively. For simplicity, the color of the curves corresponding to the equations $\det = 1$, $\det = \mathrm{tr} - 1$ and $\det = -\mathrm{tr} - 1$ are shown in yellow, green and red curves, respectively. We can see that $\lim_{x\to 0^+} f_i(x) = \mathrm{sign}(\alpha - 1)\infty$, and

$\lim_{x\to\infty} f_i(x) = -\text{sign}(\alpha-1)\infty$ for $i = 1, 2, 3$. Moreover $f_1(x) - f_2(x) = 1 > 0$ and $f_3(x) - f_2(x) = \frac{3x+1}{x+1}$, therefore, $f_2 < f_1 < f_3$ in Ω_1 as can be seen in Figure (2.5).

The region corresponding to the inequality det < 1 and det > 1 is, respectively, equivalent to

$$\begin{cases} r > \alpha + \ln(x)(1-\alpha), \\ r < \alpha + \ln(x)(1-\alpha). \end{cases}$$

Similarly, the region corresponding to the inequality det $<$ tr $- 1$ and det $>$ tr $- 1$ is, respectively, equivalent to

$$\begin{cases} r < \ln(x)(1-\alpha) + \alpha - 1, \\ r > \ln(x)(1-\alpha) + \alpha - 1. \end{cases}$$

Finally, the region corresponding to the inequality det $< -\text{tr} - 1$ and det $< -\text{tr} - 1$ is, respectively, equivalent to

$$\begin{cases} r > \frac{-(-1+\alpha)\,(x+1)\,\ln(x)+(\alpha+3)\,x+\alpha+1}{x+1}, \\ r < \frac{-(-1+\alpha)\,(x+1)\,\ln(x)+(\alpha+3)\,x+\alpha+1}{x+1}. \end{cases}$$

The stable region corresponding to the solutions of the system of inequalities (2.7) is the region when $r < f_3(x)$ and $r > f_1(x)$. From which and using inequalities (2.8), it can be seen that the repeller region corresponding to the solutions of the system is given by the region $r < f_3(x)$ and $r > f_2(x)$. The second system of inequality has no solution in Ω. Also, inequalities given by (2.9) gives the saddle region corresponding to the solutions of the system which corresponds to the regions $r > f_3(x) > f_2(x)$ curves, or $r < f_2(x) < f_3(x)$. Thus, the saddle region is either $r > f_3(x)$ or $r < f_2(x)$.

Note that, the only existence region is the region where $r > -\alpha\,\ln(x) + \ln(x)$ (orange curve). It is shown in Figure (4.7).

□

Theorem 4.4.2. *Suppose $r > 0$, $k > 0$ and let $\Omega = \{(x, \alpha) \mid \alpha \geq 0,\ x \geq 1\}$. The stability regions for the interior steady states in (x, α)-plane of dynamical system (4.6) is given by the following statements:*

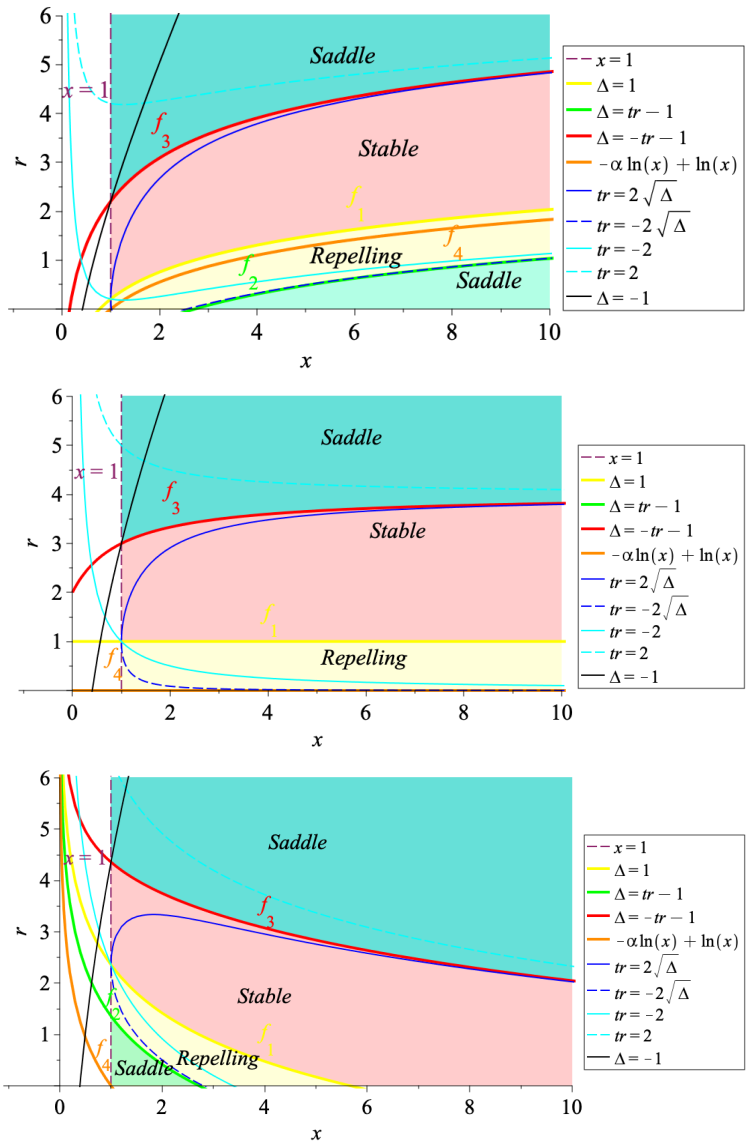

Figure 4.7: Stability regions of $(x, r)-$ plane for different values of α where $\alpha = 0.20513$, $\alpha = 1$, and $\alpha = 2.3590$.

(i) The region delimited between $\alpha > f_1(x) = \frac{\ln(x)-r}{\ln(x)-1}$ *and* $\alpha < f_3(x) = \frac{\ln(x)\,x-x\,r+\ln(x)-r+3\,x+1}{\ln(x)\,x+\ln(x)-x-1}$ *is stable.*

(ii) The region delimited between $\alpha > f_2(x) = \frac{\ln(x)-r-1}{\ln(x)-1}$ *and* $\alpha < f_1(x) = \frac{\ln(x)-r}{\ln(x)-1}$ *is repelling.*

(iii) The region below $\alpha < f_2(x) = \frac{\ln(x)-r-1}{\ln(x)-1}$ *or above* $\alpha > f_3(x) = \frac{\ln(x)\,x-x\,r+\ln(x)-r+3\,x+1}{\ln(x)\,x+\ln(x)-x-1}$ *is saddle.*

Also the acceptable (positive) region is the region where $\alpha > f_4 = \frac{\ln(x)-r}{\ln(x)}$ *(orange curve).*

Proof. Solving the equation $x^{\alpha}\, e^{r(1-\frac{x}{k})} = x$ for k gives $k = \frac{r\, x}{r-\ln(x)+\alpha\, \ln(x)}$, meaning that $\alpha > \frac{\ln(x)-r}{\ln(x)}$ (orange curve). Similar to the previous theorem, the region corresponding to inequality $\det < 1$ is equivalent to

$$\begin{cases} \alpha < \frac{\ln(x)-r}{\ln(x)-1} & \& \quad x < e, \\ \alpha > \frac{\ln(x)-r}{\ln(x)-1} & \& \quad x > e. \end{cases}$$

In addition, the region corresponding to the inequality $\det > 1$ is specified by

$$\begin{cases} \alpha > \frac{\ln(x)-r}{\ln(x)-1} & \& \quad x < e, \\ \alpha < \frac{\ln(x)-r}{\ln(x)-1} & \& \quad x > e. \end{cases}$$

The region corresponding to inequality $\det < \mathrm{tr} - 1$ is also equivalent to

$$\begin{cases} \alpha > \frac{\ln(x)-r-1}{\ln(x)-1} & \& \quad x < e, \\ \alpha < \frac{\ln(x)-r-1}{\ln(x)-1} & \& \quad x > e. \end{cases}$$

In addition, the region corresponding to the inequality $\det > \mathrm{tr} - 1$ is specified by

$$\begin{cases} \alpha < \frac{\ln(x)-r-1}{\ln(x)-1} & \& \quad x < e, \\ \alpha > \frac{\ln(x)-r-1}{\ln(x)-1} & \& \quad x > e. \end{cases}$$

In addition, the region corresponding to inequality $\det < -\mathrm{tr} - 1$ is equivalent to

$$\begin{cases} \alpha < \frac{\ln(x)\, x - x\, r + \ln(x) - r + 3\, x + 1}{\ln(x)\, x + \ln(x) - x - 1} & \& \quad x < e, \\ \alpha > \frac{\ln(x)\, x - x\, r + \ln(x) - r + 3\, x + 1}{\ln(x)\, x + \ln(x) - x - 1} & \& \quad x > e. \end{cases}$$

Finally, the region corresponding to the inequality $\det > -\mathrm{tr} - 1$ is equivalent to

$$\begin{cases} \alpha > \frac{\ln(x)\, x - x\, r + \ln(x) - r + 3\, x + 1}{\ln(x)\, x + \ln(x) - x - 1} & \& \quad x < e, \\ \alpha < \frac{\ln(x)\, x - x\, r + \ln(x) - r + 3\, x + 1}{\ln(x)\, x + \ln(x) - x - 1} & \& \quad x > e. \end{cases}$$

The stable region that corresponds to the solutions of the system is the region when $f_1(x) < \alpha <$

$f_3(x)$ for $x > e$ or $f_3(x) < \alpha < f_1(x)$ for $x < e$. The repeller region that corresponds to the solutions is given by the region under yellow curve and above the green curve for $x > e$, and it is under the green curve and above the yellow curve for $x < e$. The saddle region corresponds to the region above green and red curve, or below green and below red curve.

The results are shown in Figure (4.8).

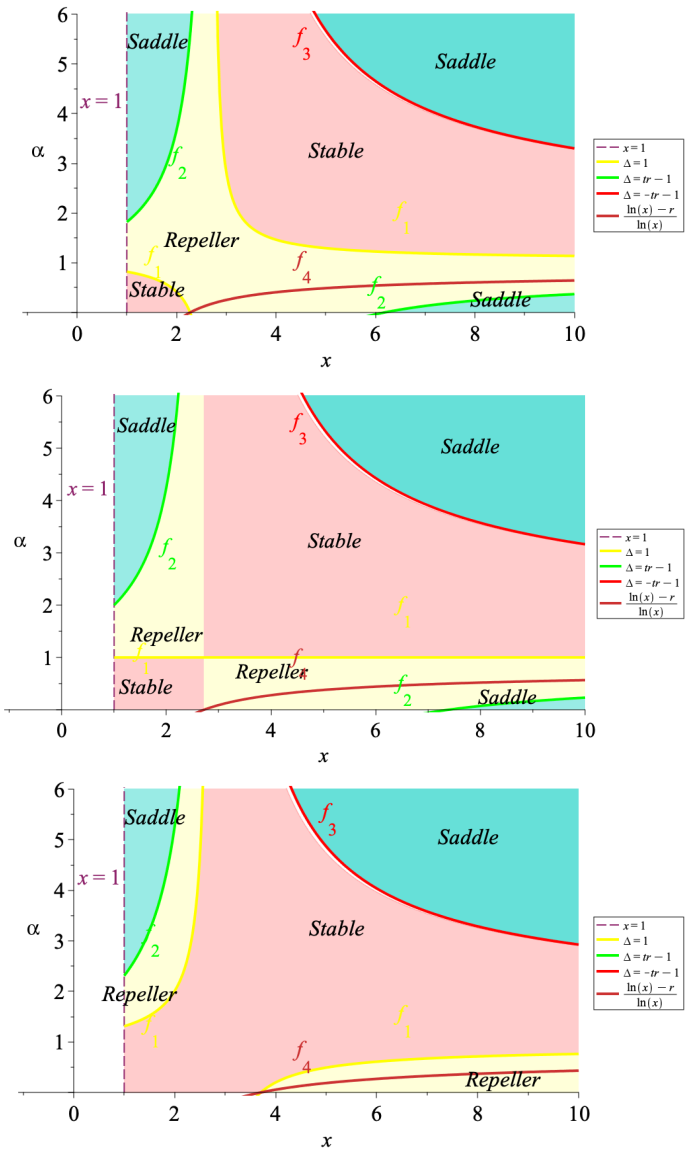

Figure 4.8: The stability regions of the $(x, \alpha)-$plane interior steady-states points $(z_1^*, z_1^* - 1)$ and $(z_2^*, z_2^* - 1)$ where $r = 0.82051$, $r = 1$, and $r = 1.3097$.

□

Theorem 4.4.3. *Suppose* $r > 0$, $\alpha > 0$ *and let* $\Omega = \{(x, k) \mid k \geq 0, \ x \geq 1\}$. *The stability*

regions for the interior steady states of the dynamical system (4.6) *in* Ω *is given by the following statements:*

(i) The region delimited between $k > f_1(x) = \frac{\left(-rx^2+2\,k\,x+k\right)\ln(x)-r\,x(k-x)}{\ln(x)k\,x}$ *and* $k < f_3(x) = \frac{r\,x\,(x+(x+1)\,\log(x)-1)}{r\,(x-1)+(4\,x+2)\,\log(x)}$ *is stable.*

(ii) The region delimited between $k > f_2(x) = x - x\,\ln(x)$ *and* $k < f_1(x) = \frac{\left(-rx^2+2\,k\,x+k\right)\ln(x)-r\,x(k-x)}{\ln(x)k\,x}$ *is repelling.*

(iii) The region below $k < f_2(x) = x - x\,\ln(x)$ *or above* $k > f_3(x) = \frac{r\,x\,(x+(x+1)\,\log(x)-1)}{r\,(x-1)+(4\,x+2)\,\log(x)}$ *is saddle.*

Also the acceptable (positive) region is the region where $k > f_4(x) = -\frac{rx}{\ln(x)-r}$ *(orange curve).*

Proof. Solving the equation $x^\alpha\, e^{r(1-\frac{x}{k})} = x$ for α gives $\alpha = \frac{\ln(x)\,k-r\,k+r\,x}{\ln(x)\,k}$, as a result, $k > f_4(x) = -\frac{rx}{\ln(x)-r}$. By substituting α where $y = x - 1$ in the Jacobin matrix (4.21) we attain the trace and determinant as follows

$$\text{tr} = \frac{(-rx^2 + 2\,k\,x + k)\ln(x) - r\,x\,(k-x)}{\ln(x)\,k\,x} \qquad \text{and} \qquad \det = \frac{((x+1)\;k - r\,x)\ln(x) - r\,(k-x)}{\ln(x)\,k\,x}.$$

The region delimited between the three curves in (2.4) $\det = 1$, $\det = \text{tr} - 1$ and $\det = -\text{tr} - 1$ is stable and they can be expressed by $k = f_1(x) = \frac{r\,x\,(\ln(x)-1)}{\ln(x)-r}$, $k = f_2(x) = -(\ln(x) - 1)\,x$ and $k = f_3(x) = \frac{r\,x(\ln(x)\,x+\ln(x)-x-1)}{4\,\ln(x)\,x-r\,x+2\,\ln(x)-r}$, respectively.

The region corresponding to inequality $\det < 1$ is given by

$$\begin{cases} k < \frac{r\,x\,(\ln(x)-1)}{\ln(x)-r} & \& \quad x \le e \quad \& \quad r < \ln(x), \\ k > \frac{r\,x\,(\ln(x)-1)}{\ln(x)-r} & \& \quad x \le e \quad \& \quad r > \ln(x), \\ k < \frac{r\,x\,(\ln(x)-1)}{\ln(x)-r} & \& \quad x > e \quad \& \quad r < \ln(x), \\ k > \frac{r\,x\,(\ln(x)-1)}{\ln(x)-r} & \& \quad x > e \quad \& \quad r > \ln(x). \end{cases}$$

When $r = 1$, it then follows that

$$\begin{cases} k < x & \& \quad x > e, \\ k > x & \& \quad 1 < x < e. \end{cases}$$

In addition, the region corresponding to the inequality det > 1 is specified by

$$\begin{cases} k > \frac{r\,x\,(\ln(x)-1)}{\ln(x)-r} & \& \quad x < e & \& \quad r < \ln(x), \\ k < \frac{r\,x\,(\ln(x)-1)}{\ln(x)-r} & \& \quad x < e & \& \quad r > \ln(x), \\ k > \frac{r\,x\,(\ln(x)-1)}{\ln(x)-r} & \& \quad x \geq e & \& \quad r < \ln(x), \\ k < \frac{r\,x\,(\ln(x)-1)}{\ln(x)-r} & \& \quad x \geq e & \& \quad r > \ln(x). \end{cases}$$

When $r = 1$, we have

$$\begin{cases} k > x & \& \quad x > e, \\ k < x & \& \quad 1 < x < e. \end{cases}$$

The region corresponding to inequality det $< \mathrm{tr} - 1$ is equivalent to

$$k < x - x\,\ln(x) \quad \& \quad r > 0.$$

When $r = 1$, we have

$$k < x - x\log(x) \quad \& \quad x > 1.$$

In addition, the region corresponding to the inequality det $> \mathrm{tr} - 1$ is specified by

$$k > x - x\,\ln(x) \quad \& \quad r > 0.$$

When $r = 1$, we have

$$k > x - x\log(x) \quad \& \quad x > 1.$$

Finally, the region corresponding to inequality det $< -\operatorname{tr} -1$ is given by

$$\begin{cases} k < \frac{r\,x\,(x+(x+1)\,\log(x)-1)}{r\,(x-1)+(4\,x+2)\,\log(x)} & \& \quad x < e \quad \& \quad r < \frac{2\,(2\,x+1)\,\log(x)}{1+x}, \\ k > \frac{r\,x\,(x+(x+1)\,\log(x)-1)}{r\,(x-1)+(4\,x+2)\,\log(x)} & \& \quad x < e \quad \& \quad r > \frac{2\,(2\,x+1)\,\log(x)}{1+x}, \\ k < \frac{r\,x\,(x+(x+1)\,\log(x)-1)}{r\,(x-1)+(4\,x+2)\,\log(x)} & \& \quad x \geq e \quad \& \quad r < \frac{2\,(2\,x+1)\,\log(x)}{1+x}, \\ k > \frac{r\,x\,(x+(x+1)\,\log(x)-1)}{r\,(x-1)+(4\,x+2)\,\log(x)} & \& \quad x \geq e \quad \& \quad r > \frac{2\,(2\,x+1)\,\log(x)}{1+x}. \end{cases}$$

When $r = 1$ and $x = x^0 \approx 1.37266$, we have

$$\begin{cases} k < \frac{(x\cdot(x+1)(\log(x)-1))}{(-x+(4x+2)\log(x)-1)} & \& \quad x > x^0, \\ k > \frac{(x\cdot(x+1)(\log(x)-1))}{(-x+(4x+2)\log(x)-1)} & \& \quad 1 < x < x^0. \end{cases}$$

In addition, the region corresponding to the inequality det $> -\operatorname{tr} -1$ is specified by

$$\begin{cases} k > \frac{r\,x\,(x+(x+1)\,\log(x)-1)}{r\,(x-1)+(4\,x+2)\,\log(x)} & \& \quad x < e \quad \& \quad r < \frac{2\,(2\,x+1)\,\log(x)}{1+x}, \\ k < \frac{r\,x\,(x+(x+1)\,\log(x)-1)}{r\,(x-1)+(4\,x+2)\,\log(x)} & \& \quad x < e \quad \& \quad r > \frac{2\,(2\,x+1)\,\log(x)}{1+x}, \\ k > \frac{r\,x\,(x+(x+1)\,\log(x)-1)}{r\,(x-1)+(4\,x+2)\,\log(x)} & \& \quad x \geq e \quad \& \quad r < \frac{2\,(2\,x+1)\,\log(x)}{1+x}, \\ k < \frac{r\,x\,(x+(x+1)\,\log(x)-1)}{r\,(x-1)+(4\,x+2)\,\log(x)} & \& \quad x \geq e \quad \& \quad r > \frac{2\,(2\,x+1)\,\log(x)}{1+x}. \end{cases}$$

When $r = 1$ and $x = x^0 \approx 1.37266$, we have

$$\begin{cases} k > \frac{(x\cdot(x+1)(\log(x)-1))}{(-x+(4x+2)\log(x)-1)} & \& \quad x > x^0, \\ k < \frac{(x\cdot(x+1)(\log(x)-1))}{(-x+(4x+2)\log(x)-1)} & \& \quad 0 < x < x^0. \end{cases}$$

Therefore, there are three different cases and regions to study and determine the stability for this $(x, k)-$plane. The regions are $r < \ln(x) < \frac{2\,(2\,x+1)\,\log(x)}{1+x}$, $r > \frac{2\,(2\,x+1)\,\log(x)}{1+x} > \ln(x)$, and $\ln(x) < r < \frac{2\,(2\,x+1)\,\log(x)}{1+x}$. For these cases, there are also three different values of r: $r < 1$, $r = 1$ and $r > 1$.

Case 1: For $r < 1$, the stable regions correspond to the solutions of inequalities (2.7) give as follows: the region where $r < \ln(x) < \frac{2\,(2\,x+1)\,\log(x)}{1+x}$ is given by $f_1(x) < k < f_3(x)$; but the region

where $r > \frac{2\,(2\,x+1)\,\log(x)}{1+x} > \ln(x)$ does not exists since $k > f_1(x)$ and $k > f_3(x)$. When $\ln(x) < r < \frac{2\,(2\,x+1)\,\log(x)}{1+x}$, we then have $f_3(x) < k < f_1(x)$. In addition, the saddle regions correspond to the solution's inequalities (2.9) which is given by: $k > f_3(x)$ if $r < \ln(x) < \frac{2\,(2\,x+1)\,\log(x)}{1+x}$. However, when $r > \frac{2\,(2\,x+1)\,\log(x)}{1+x} > \ln(x)$, the saddle region does not exist because $k > f_2(x)$ and $k < f_3(x)$. When $\ln(x) < r < \frac{2\,(2\,x+1)\,\log(x)}{1+x}$, the region is $k < f_3(x)$. In addition, for the saddle regions if $r < \ln(x) < \frac{2\,(2\,x+1)\,\log(x)}{1+x}$, then $k < f_2(x)$, or if $r > \frac{2\,(2\,x+1)\,\log(x)}{1+x} > \ln(x)$, then $k < f_2(x)$, however when $\ln(x) < r < \frac{2\,(2\,x+1)\,\log(x)}{1+x}$, it does not exist since $f_1(x) < k < f_2(x)$. The repeller region corresponds to $f_2(x) < k < f_1(x)$ if $r < \ln(x) < \frac{2\,(2\,x+1)\,\log(x)}{1+x}$, or $f_2(x) < k < f_1(x)$ if $r > \frac{2\,(2\,x+1)\,\log(x)}{1+x} > \ln(x)$, or $k > f_2(x)$ if $\ln(x) < r < \frac{2\,(2\,x+1)\,\log(x)}{1+x}$.

Case 2: For $r > 1$, the result is similar to $r < 1$ and that shows in Figure (4.9).

Case 3: For $r = 1$, there are three different regions $x < x^0 \approx 1.37266$, $x^0 < x < e$ and $x > e$. The stable regions are given by: $f_1(x) < k < f_3(x)$ when $x < x^0$; however, when $x^0 < x < e$ it does not exist because $k > f_3(x) > f_2(x) > f_1(x)$; and when $x > e$ the stable region is delimited between $f_2(x) < k < f_1(x)$. The saddle regions is given by: $k > f_3(x)$ when $x < x^0$; the saddle region does not exist when $x^0 < x < e$; or $k < f_3(x)$ when $x > e$. For the other condition, the saddle regions are given by: $k < f_2(x)$ when $x < x^0$; $k < f_2(x)$ when $x^0 < x < e$; and when $x > e$ the saddle region does not exist because $f_3(x) < k < f_2(x)$. The repeller region corresponds to the regions $f_2(x) < k < f_1(x)$ when $x < x^0$, or $f_2(x) < k < f_1(x)$ when $x^0 < x < e$, and it does not exist when $x > e$.

Figure (4.9) provides the three cases of r.

□

4.4.2 Two Parameter Bifurcation (Co-Dimension 2)

We demonstrate the stability region for positive steady state points in parameter space the first and second interior steady states of (α, k), (r, k), and (α, r)-planes for certain values of parameters r, k and α.

We start by computing the region where $\alpha > 1$ for the interior steady state S_4. For this purpose,

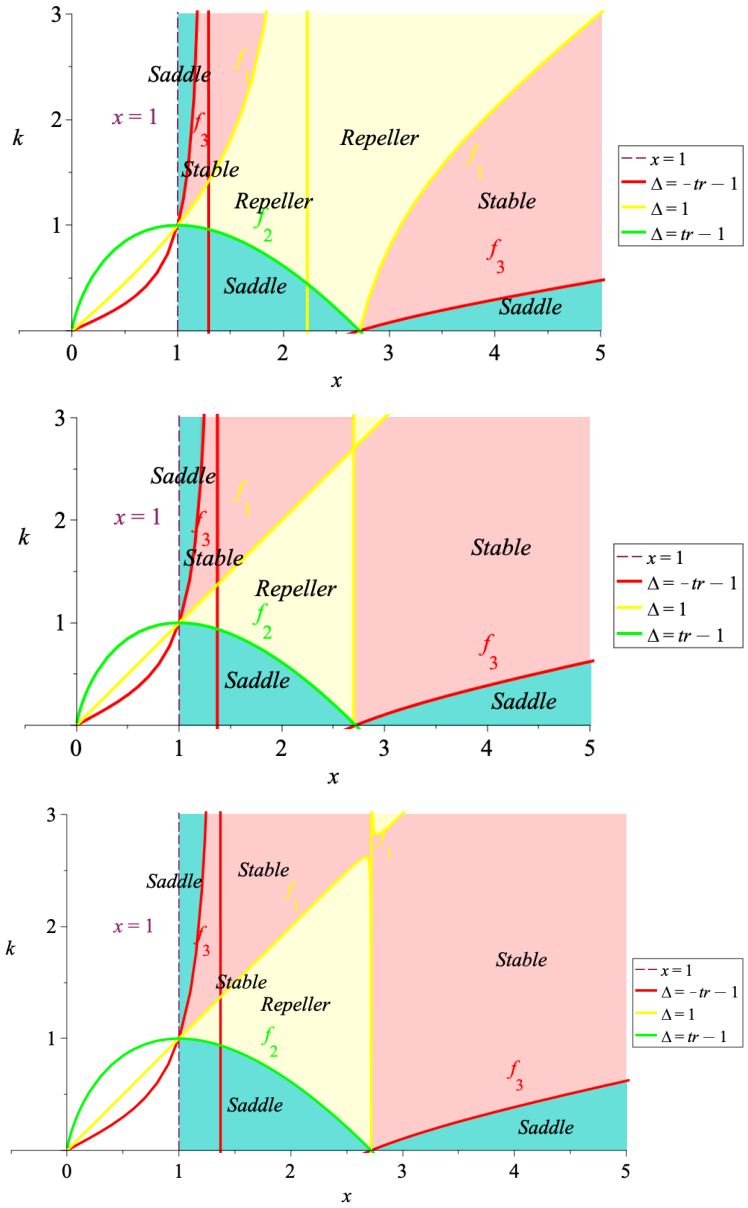

Figure 4.9: Stability regions of $(x, k)-$plane for the interior steady-states points where $r = .8$, $r = 1$, and $r = 1.0345$.

we use the range of $W_{-1}(\mathsf{x})$

$$W\left(-1, -\frac{re^{-\frac{r}{\alpha-1}}}{k(\alpha-1)}\right) < -1, \tag{4.22}$$

and from the domain of $W_{-1}(\mathsf{x})$, we can rewrite (4.22) as

$$-\frac{1}{e} \leq -\frac{re^{-\frac{r}{\alpha-1}}}{k(\alpha-1)} < 0. \tag{4.23}$$

Solving (4.23) for k provides the existence curve for (α, k)-plane and (r, k)-plane

$$k \geq \frac{r\, \mathrm{e}^{1-\frac{r}{\alpha-1}}}{(\alpha-1)}.$$

Also, solving (4.23) for r provides the existence curve of (α, r)-plane as

$$r \leq (1-\alpha) W\left(-\frac{k}{e}\right).$$

This is shown in Figure (4.12).

Figure (4.10) shows the stability of W_{-1} and W_0 for different α values and different k values can be stable, repeller, or saddle.

Theorem 4.4.4. *Suppose $r > 0$, $\alpha > 0$, $k > 0$ and $x \geq 1$ then the following statements are true for system (4.6) for (α, k)-plane:*

(i) The stable region is delimited between $f_1(\alpha) < k < f_3(\alpha)$.

(ii) The repeller region is delimited between $f_2(\alpha) < k < f_1(\alpha)$.

(iii) The saddle region is either delimited between $f_3(\alpha) < k < \infty$ or $0 < k < f_2(\alpha)$.

The acceptable region is given by $k > f_4(\alpha) = \frac{\frac{\alpha-r-1}{\alpha-1}\, r}{\alpha-1}$ (orange curve) for the existence region based on the parameter k.

Proof. The proof depends on three steps based on the conditions established for stability (2.2.1). First, we obtain the trace tr and determinant $\det$ of Jacobin matrix (4.21). After substituting the largest interior steady state $z_2^* = e^{\frac{(-\alpha+1)\,\mathrm{W}\left(-1, -\frac{r\, e^{-\frac{r}{\alpha-1}}}{k\,(\alpha-1)}\right) - r}{\alpha-1}}$ into matrix (4.21), it then follows that

$$\mathrm{tr}(J^*) = \frac{1}{k}\left(-r\, \mathrm{e}^{\frac{(-\alpha+1)W\left(-1, -\frac{r\, \mathrm{e}^{-\frac{r}{\alpha-1}}}{k\,(\alpha-1)}\right) - r}{\alpha-1}} + k\left(\alpha + e^{(\alpha-1)W\left(-1, -\frac{r\, \mathrm{e}^{-\frac{r}{\alpha-1}}}{k\,(\alpha-1)}\right) + r} + 1\right)\right),$$

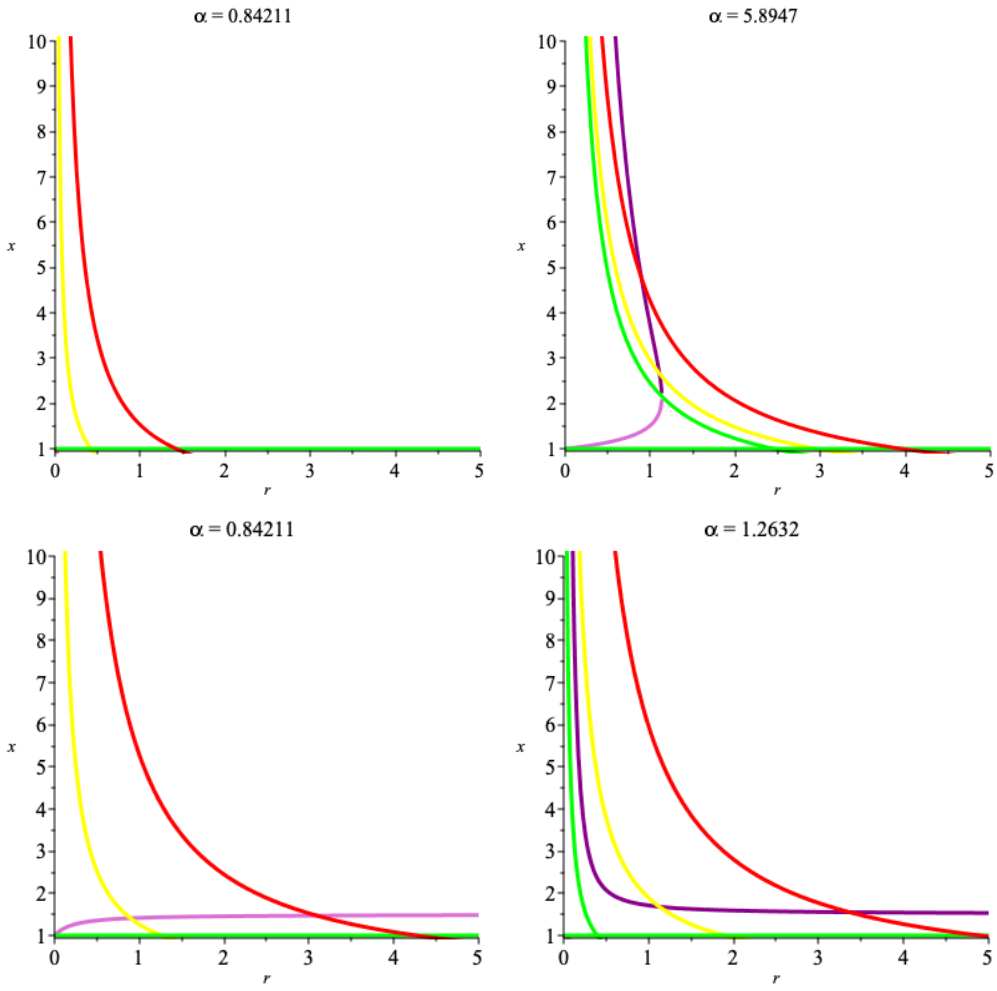

Figure 4.10: Top Left: No interior steady states exist when $\alpha < 1$. Top right: when $\alpha > 1$, the steady state W_0 is saddle (purple curve below the green curve), however, W_{-1} changes its stability for different values of parameter r (dark purple curve is: repeller between the green and yellow curves, stable between the yellow and red curves, and saddle above red). In the top row, we have $k = 0.5$. Bottom Left: Only W_0 exists in different regions (repeller, stable, and saddle, similar to the top left case) when $\alpha < 1$. However, we will only have W_{-1} for different (in)stability regions (repeller, stable, and saddle) when $\alpha > 1$. For the bottom panels, we assume $k = 1.5$.

and

$$\det(J^*) = \frac{1}{k}\left(\alpha\, k\, e^{\frac{(\alpha-1)W\left(-1,-\frac{r\,e^{-\frac{r}{\alpha-1}}}{k\,(\alpha-1)}\right)+r}{\alpha-1}} + k - r\right).$$

The identities det $= 1$ and det $=$ tr $- 1$ are equivalent to $k = f_1 = \frac{r}{\alpha\, e^{-\frac{\alpha-r}{\alpha-1}}}$ (yellow curve), $k = f_2 = 1$ or $\frac{\frac{\alpha-r-1}{\alpha-1}\,r}{\alpha-1}$ (green curve), respectively. However, for det $= -$tr $- 1$, we can only find an upper bound $k = f_3 \leq \beta = -\frac{re^{-\frac{r}{\alpha-1}-\frac{-\alpha-3}{\alpha-1}}}{-\alpha-3}$ (red curve), where β is the upper bound of the red

curve when $\alpha > 1$. As a result, to find the dynamics of the steady state S_4, we need to check the following statements. The other cases are similarly obtained for saddle or repeller regions.

(i) First assume that $\alpha > 1$. Also, we know that the stable region corresponds to the solutions of the system of inequalities given by (2.7). This means that we should first have det < 1, it then follows that

$$\alpha\, e^{W\left(-1,-\frac{r\, e^{-\frac{r}{\alpha-1}}}{k\,(\alpha-1)}\right)+\frac{r}{\alpha-1}} - \frac{r}{k} < 0 \Longrightarrow e^{W\left(-1,-\frac{r\, e^{-\frac{r}{\alpha-1}}}{k(\alpha-1)}\right)} < \frac{r\, e^{-\frac{r}{\alpha-1}}}{\alpha\, k}.$$

Now we use the appropriate properties of W function (2.29) below. For $\alpha > 1$, we can then multiply both sides by the decreasing function W that reverses the inequality

$$\frac{-\frac{r\, \mathrm{e}^{-\frac{r}{\alpha-1}}}{k\,(\alpha-1)}}{W\left(-1,-\frac{r\, \mathrm{e}^{-\frac{r}{\alpha-1}}}{k\,(\alpha-1)}\right)} < \frac{r}{k\,\alpha}\, \mathrm{e}^{-\frac{r}{\alpha-1}} \Longrightarrow -\frac{\alpha}{(\alpha-1)} > W\left(-1,-\frac{re^{-\frac{r}{\alpha-1}}}{k(\alpha-1)}\right).$$

We know that the domain of W_{-1} is $-\frac{1}{e} < x < 0$. We also know that the inverse of decreasing W function is decreasing so that the inequality reverses and that $W^{-1}(-\frac{\alpha}{(\alpha-1)}) = -\frac{\alpha}{(\alpha-1)}e^{-\frac{\alpha}{(\alpha-1)}}$. Take the inverse of W function from both sides then solve it for k, it then follows that

$$\max\left\{-e^{-1}, -\frac{\alpha\, e^{-\frac{\alpha}{\alpha-1}}}{\alpha-1}\right\} < -\frac{r\, e^{-\frac{r}{\alpha-1}}}{k(\alpha-1)} < 0.$$

Since

$$\max\left\{-e^{-1}, -\frac{\alpha\, e^{-\frac{\alpha}{\alpha-1}}}{\alpha-1}\right\} = -\frac{\alpha\, e^{-\frac{\alpha}{\alpha-1}}}{\alpha-1},$$

we then have

$$\alpha\, e^{-\frac{\alpha}{\alpha-1}} > \frac{r\, e^{-\frac{r}{\alpha-1}}}{k}.$$

As a result, the stable region corresponding to inequality $det < 1$ is equivalent to $k > \frac{r}{\alpha}\mathrm{e}^{\frac{\alpha-r}{\alpha-1}}$ for $\alpha > 1$. This can be shown similarly for $\alpha < 1$, we can then summarize it by

$$\begin{cases} k > \frac{r}{\alpha}\mathrm{e}^{\frac{\alpha-r}{\alpha-1}} & \& \quad \alpha > 1, \\ k < \frac{r}{\alpha}\mathrm{e}^{\frac{\alpha-r}{\alpha-1}} & \& \quad \alpha < 1. \end{cases}$$

For $\det > \mathrm{tr} - 1$, it then follows that

$$\frac{r}{k}\, e^{\frac{(-\alpha+1)W\left(-1,-\frac{r\, e^{-\frac{r}{\alpha-1}}}{k\,(\alpha-1)}\right)-r}{\alpha-1}} + \frac{k\,(\alpha-1)}{k}\, e^{\frac{(\alpha-1)W\left(-1,-\frac{r\, e^{-\frac{r}{\alpha-1}}}{k\,(\alpha-1)}\right)+r}{\alpha-1}} + \frac{(-\alpha+1)\,k}{k} - \frac{r}{k} > 0,$$

simplifying it, we obtain

$$\frac{r}{k}\, e^{-W\left(-1,-\frac{r\, e^{-\frac{r}{\alpha-1}}}{k\,(\alpha-1)}\right)-\frac{r}{\alpha-1}} + (\alpha-1)\, e^{W\left(-1,-\frac{r\, e^{-\frac{r}{\alpha-1}}}{k\,(\alpha-1)}\right)+\frac{r}{\alpha-1}} + (-\alpha+1) - \frac{r}{k} > 0,$$

using the properties of W function (2.27) and (2.29) we have

$$\frac{r}{k}\frac{W\left(-1,-\frac{r\,\mathrm{e}^{-\frac{r}{\alpha-1}}}{k\,(\alpha-1)}\right)}{\left(-\frac{r\,\mathrm{e}^{-\frac{r}{\alpha-1}}}{k\,(\alpha-1)}\right)\, e^{\frac{r}{\alpha-1}}} + \frac{(\alpha-1)\left(-\frac{r\,\mathrm{e}^{-\frac{r}{\alpha-1}}}{k\,(\alpha-1)}\right)}{W\left(-1,-\frac{r\,\mathrm{e}^{-\frac{r}{\alpha-1}}}{k\,(\alpha-1)}\right)}\, e^{\frac{r}{\alpha-1}} + (-\alpha+1) - \frac{r}{k} > 0,$$

simplifying them again gives us

$$\frac{1}{\alpha-1}\left(-\,\mathrm{W}\left(-1,-\frac{r\,\mathrm{e}^{-\frac{r}{\alpha-1}}}{k\,(\alpha-1)}\right)(\alpha-1) + \frac{\left(-\frac{r}{k}\right)}{\mathrm{W}\left(-1,-\frac{r\,\mathrm{e}^{-\frac{r}{\alpha-1}}}{k\,(\alpha-1)}\right)} + (-\alpha+1) - \frac{r}{k}\right) > 0,$$

more simplifications after dividing each term by $(\alpha-1)$ gives

$$-\,W\left(-1,-\frac{r\,\mathrm{e}^{-\frac{r}{\alpha-1}}}{k\,(\alpha-1)}\right) + \frac{\left(-\frac{r}{k\,(\alpha-1)}\right)}{W\left(-1,-\frac{r\,\mathrm{e}^{-\frac{r}{\alpha-1}}}{k\,(\alpha-1)}\right)} - 1 - \frac{r}{k\,(\alpha-1)} > 0. \tag{4.24}$$

Let us now consider $u = W\left(-1,-\frac{r\,\mathrm{e}^{-\frac{r}{\alpha-1}}}{k\,(\alpha-1)}\right)$, we can rewrite (4.24) as follows

$$-u + \frac{\left(-\frac{r}{k\,(\alpha-1)}\right)}{u} - 1 - \frac{r}{k\,(\alpha-1)} > 0.$$

It is clear that there are two solutions: $u = -1$ and $u = -\frac{r}{k(\alpha-1)}$. Since the above inequality is quadratic, this means that u must be between the two roots to satisfy the inequality. As a result, because W_{-1} is a monotone decreasing function with the range $(-\infty, -1]$, then those

two roots must be written as $-\frac{r}{k(\alpha-1)} < u < -1$ (the other case $-1 < u < -\frac{r}{k(\alpha-1)}$ is not within the range of W_{-1}). Let us first compute the right hand side, $u < -1$. Using the properties of W_{-1} being a monotone decreasing function and the domain W_{-1}, thus we can write $u < -1$ as follows

$$-\frac{1}{e} \leq -\frac{r\,\mathrm{e}^{-\frac{r}{\alpha-1}}}{k\,(\alpha-1)} < 0.$$

Multiplying by k and then solving for k gives

$$-\frac{k}{e} \leq -\frac{r\,\mathrm{e}^{-\frac{r}{\alpha-1}}}{(\alpha-1)} \Longrightarrow \frac{k}{e} \geq \frac{r\,e^{-\frac{r}{\alpha-1}}}{(\alpha-1)} \Longrightarrow k \geq \frac{r\,e^{1-\frac{r}{\alpha-1}}}{(\alpha-1)}.$$

Also, for the left hand side, we can show that

$$u > \frac{-r}{k(\alpha-1)} \Longrightarrow W\left(-\frac{r\,\mathrm{e}^{-\frac{r}{\alpha-1}}}{k\,(\alpha-1)}\right) > -\frac{r}{k(\alpha-1)}.$$

Applying the inverse of W function to both sides and using the property (2.28) gives

$$-\frac{r\mathrm{e}^{-\frac{r}{\alpha-1}}}{k(\alpha-1)} > -\frac{r}{k(\alpha-1)}e^{-\frac{r}{k(\alpha-1)}} > \frac{-1}{e} \Longrightarrow \frac{r\mathrm{e}^{-\frac{r}{\alpha-1}}}{k(\alpha-1)} < \frac{r\mathrm{e}^{-\frac{r}{k(\alpha-1)}}}{k(\alpha-1)},$$

or

$$\mathrm{e}^{-\frac{r}{\alpha-1}} < \mathrm{e}^{-\frac{r}{k(\alpha-1)}} \Longrightarrow k > 1.$$

As a result, the region corresponding to the inequality $\det > \mathrm{tr} - 1$ is given by

$$\begin{cases} k > \frac{r\,e^{1-\frac{r}{\alpha-1}}}{(\alpha-1)} & \& \quad \alpha > 1, k > 1, \\ k < \frac{r\,e^{1-\frac{r}{\alpha-1}}}{(\alpha-1)} & \& \quad \alpha < 1, k < 1. \end{cases}$$

For the inequality $\det > -\mathrm{tr} - 1$, we have

$$-r\,\mathrm{e}^{\frac{(-\alpha+1)\,\mathrm{W}\left(-1,-\frac{r\,\mathrm{e}^{-\frac{r}{\alpha-1}}}{k\,(\alpha-1)}\right)-r}{\alpha-1}} + k\,(1+\alpha)\,\mathrm{e}^{\frac{(\alpha-1)W\left(-1,-\frac{r\,\mathrm{e}^{-\frac{r}{\alpha-1}}}{k\,(\alpha-1)}\right)+r}{\alpha-1}} + (\alpha+3)\,k > r.$$

To solve this inequality we define $r := t\,(\alpha - 1)$

$$-t(\alpha-1)e^{\frac{(-\alpha+1)W\left(-\frac{te^{-t}}{k}\right)-t(\alpha-1)}{\alpha-1}} + k(1+\alpha)e^{\frac{(\alpha-1)W\left(-\frac{te^{-t}}{k}\right)+t(\alpha-1)}{\alpha-1}} + (\alpha+3)k > t(\alpha-1).$$

Simplifying it using the properties of W function (2.29) and (2.30), that is, $e^{W(\mathsf{x})} = \frac{\mathsf{x}}{W(\mathsf{x})}$ $e^{-W(\mathsf{x})} = \frac{W(\mathsf{x})}{\mathsf{x}}$, we obtain

$$\frac{k\,(\alpha-1)W\left(-1,-\frac{t\,\mathrm{e}^{-t}}{k}\right)^2 + k\,(\alpha+3)W\left(-1,-\frac{t\,\mathrm{e}^{-t}}{k}\right) - (1+\alpha)\,t}{W\left(-1,-\frac{t\,\mathrm{e}^{-t}}{k}\right)} > t\,(\alpha-1).$$

Multiply both sides by $W\left(-1,-\frac{t\,\mathrm{e}^{-t}}{k}\right)$, and for $\alpha > 1$ we have

$$k\,(\alpha-1)\,W\left(-1,-\frac{t\,\mathrm{e}^{-t}}{k}\right)^2 + k\,(\alpha+3)W\left(-1,-\frac{t\,\mathrm{e}^{-t}}{k}\right) - (1+\alpha)\,t - \left(t\,(\alpha-1)W\left(-1,-\frac{t\,\mathrm{e}^{-t}}{k}\right)\right) < 0. \quad (4.25)$$

Now in order to get the roots of this inequality, let's consider for simplicity that $u = W\left(-1,-\frac{t\,\mathrm{e}^{-t}}{k}\right)$ where $t = \frac{r}{\alpha-1}$, so we have

$$k\,(\alpha-1)\,u^2 + k\,(\alpha+3)\,u - (1+\alpha)\,t - t\,(\alpha-1)\,u < 0. \quad (4.26)$$

Assume that $\alpha > 1$ and then solving the equality we got two solutions: u_1 and u_2 that are given by

$$u_1 = \frac{-\alpha k + t\alpha - 3k - t + \sqrt{\alpha^2k^2 + 2\alpha^2kt + \alpha^2t^2 + 6\alpha k^2 - 4\alpha kt - 2\alpha t^2 + 9k^2 + 2kt + t^2}}{2k(\alpha-1)},$$

$$u_2 = -\frac{\alpha k - t\alpha + \sqrt{\alpha^2k^2 + 2\alpha^2kt + \alpha^2t^2 + 6\alpha k^2 - 4\alpha kt - 2\alpha t^2 + 9k^2 + 2kt + t^2} + 3k + t}{2k(\alpha-1)}.$$

Since $t = \frac{r}{\alpha-1}$, then those two roots simplify to

$$u_1 = \frac{-\alpha\, k - 3\, k + r + \sqrt{\alpha^2\, k^2 + 6\, \alpha\, k^2 + 2\, \alpha\, k\, r + 9\, k^2 - 2\, k\, r + r^2}}{2\, k\, (\alpha - 1)},$$

$$u_2 = -\frac{\alpha\, k + \sqrt{\alpha^2\, k^2 + 6\, \alpha\, k^2 + 2\, \alpha\, k\, r + 9\, k^2 - 2\, k\, r + r^2} + 3\, k - r}{2\, k\, (\alpha - 1)}.$$

We can see that since $\alpha > 1$ and $u < 0$ then (4.26) is $f < 0$. If $\alpha < 1$, then $u > 0$ which gives (4.26) $f > 0$. Let us now simplify the second root to help to calculate the boundary of the function f_3 so that we can determine the stability. First consider $r = 0$ for u_2

$$u_2\Big|_{r=0} = -\frac{\alpha k + \sqrt{(\alpha k + 3k)^2} + 3k}{2k(\alpha - 1)} = -\frac{2\alpha + 6}{2\alpha - 2} = \frac{-\alpha - 3}{\alpha - 1}.$$

Assume that $\tau = \frac{-\alpha-3}{\alpha-1}$. Since $\alpha > 1$ and $f < 0$, then the acceptable inequality is given by

$$\tau < u < u_1.$$

That means

$$\tau < W\left(-1, -\frac{t\, \mathrm{e}^{-t}}{k}\right) < u_1.$$

Multiplying them by the inverse of W function and using the property (2.28) gives

$$\tau\, e^{\tau} < -\frac{t\, \mathrm{e}^{-t}}{k} < u_1\, e^{u_1},$$

or

$$0 > \frac{1}{\tau}\, e^{-\tau} > \frac{k}{-t\, e^{-t}} > \frac{1}{u_1}\, e^{-u_1}.$$

Solve for k

$$\frac{-t\, e^{-t-\tau}}{\tau} < k < \frac{-t\, e^{-t-u_1}}{u_1}.$$

As a result, the region corresponding to inequality det $> -\operatorname{tr} -1$ is equivalent to

$$\begin{cases} k < \frac{1}{\alpha+3} e^{\frac{\alpha+3}{\alpha-1}} r e^{\frac{-r}{\alpha-1}} & \& \quad \alpha > 1, \\ k > \frac{1}{\alpha+3} e^{\frac{\alpha+3}{\alpha-1}} r e^{\frac{-r}{\alpha-1}} & \& \quad \alpha < 1. \end{cases} \tag{4.27}$$

Thus, (4.27) means that:

$$k < \frac{1}{\alpha+3} e^{\frac{\alpha+3}{\alpha-1}} r e^{\frac{-r}{\alpha-1}} \quad \& \quad \alpha > 1 \Longrightarrow k < f_3(\alpha, r) < f_3(\alpha, 0),$$

$$k > \frac{1}{\alpha+3} e^{\frac{\alpha+3}{\alpha-1}} r e^{\frac{-r}{\alpha-1}} \quad \& \quad \alpha < 1 \Longrightarrow k > f_3(\alpha, r) > f_3(\alpha, 0).$$

where f_3 is obtained by implicitly solving the following equation for k

$$-\frac{r}{(\alpha-1)k} \cdot e^{(-\frac{r}{\alpha-1})} = -\frac{\alpha k + \sqrt{\alpha^2 k^2 + 6\alpha k^2 + 2\alpha k r + 9k^2 - 2kr + r^2} + 3k - r}{2k(\alpha-1)} \cdot e^{-\frac{\alpha k + \sqrt{\alpha^2 k^2 + 6\alpha k^2 + 2\alpha k r + 9k^2 - 2kr + r^2} + 3k - r}{2k(\alpha-1)}}$$

and we showed that it is bounded from above by $\beta = \frac{1}{\alpha+3} e^{\frac{\alpha+3}{\alpha-1}} r e^{\frac{-r}{\alpha-1}}$ where $\alpha > 1$.

Therefore, for $\alpha > 1$ the stable region takes the range between the yellow curve and red curve, $f_1(\alpha) < k < f_3(\alpha)$. The repeller region takes the range between the green curve and yellow curve, $f_2(\alpha) < k < f_1(\alpha)$. Also, the saddle region takes the range either above the red curve, $f_3(\alpha) < k < \infty$, or between zero and the yellow curve, $0 < k < f_2(\alpha)$. These are shown in Figure (4.11) below. □

Note that it can be similarly proven for $(r, k)-$plane. Now we want to prove the stability for the two co-dimension of $(\alpha, r)-$plane.

Theorem 4.4.5. *Suppose $r > 0$, $\alpha > 0$, $k > 0$ and $x \geq 1$ then the following statements are true for system (4.6) for (α, r)-plane :*

(i) The stable region is delimited between $f_3(\alpha) < r < f_1(\alpha)$.

(ii) The repeller region is delimited between $f_1(\alpha) < r < f_2(\alpha)$.

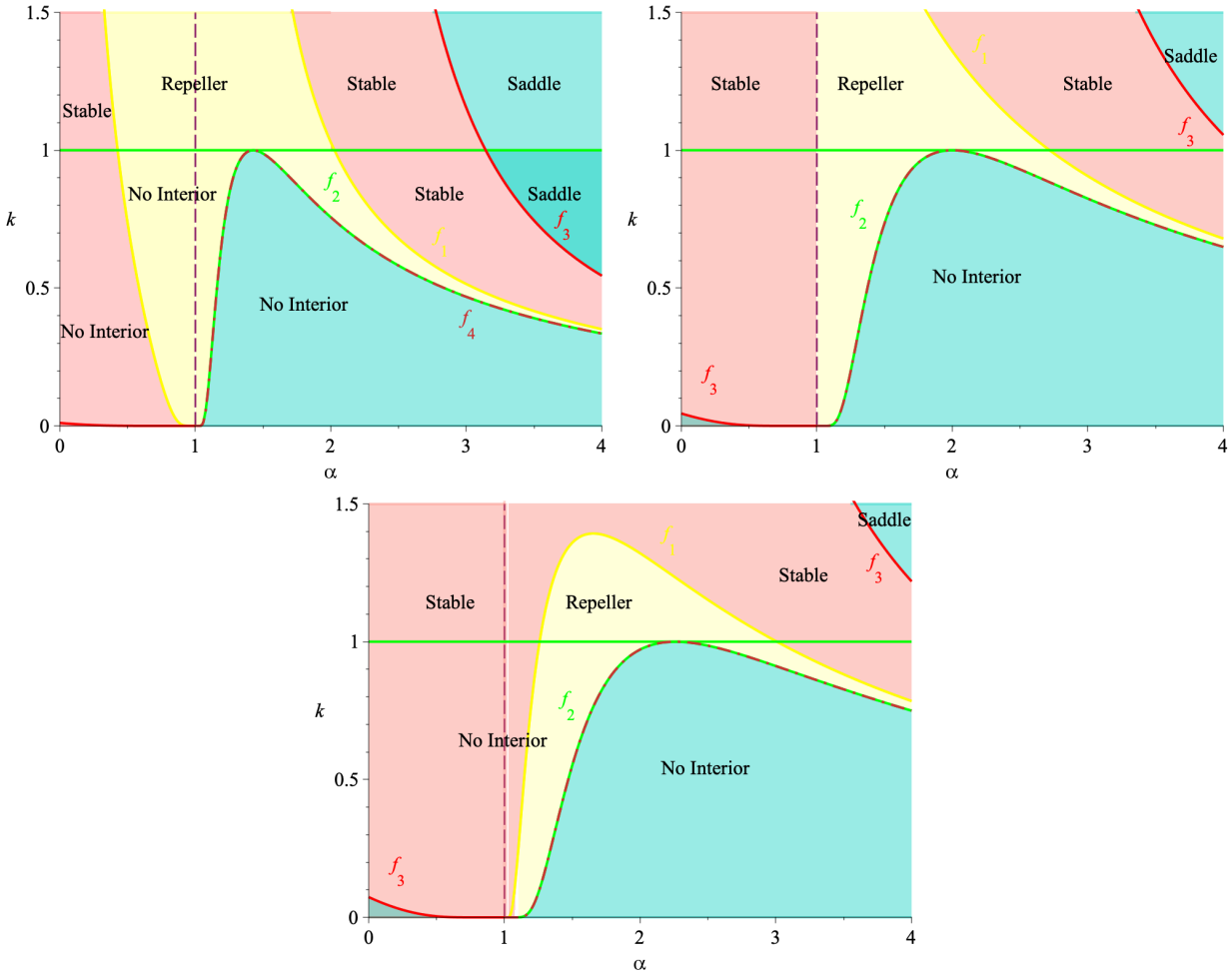

Figure 4.11: Stability regions of co-dimension two for the $(\alpha, k)-$plane where the parameter $r = 0.42625$ (top left), $r = 1$ (top right) and $r = 1.2588$ (bottom).

(iii) The saddle region is either delimited between $0 < r < f_3(\alpha)$ *or* $f_2(\alpha) < r < \infty$.

Proof. We can follow the same technique as in the proof of (α, k)-plane. The identities $\det = 1$ and $\det = \mathrm{tr} - 1$ are equivalent to $r = f_1 = -(\alpha - 1)W\left(-\frac{\alpha\, k\, \mathrm{e}^{-\frac{\alpha}{\alpha-1}}}{\alpha-1}\right)$ (yellow curve), $r = f_2 = 1$ or $(-\alpha+1)W\left(-\frac{k}{e}\right)$ (green curve), respectively. However, for $\det = -\mathrm{tr} - 1$, we can only find a lower bound $\beta \leq r = f_3 = -W\left(-\frac{\mathrm{e}^{-\frac{\alpha+3}{\alpha^2-2\alpha+1}}\, k\,(\alpha+3)}{\alpha-1}\right)(\alpha - 1)$, where β is the lower bound of the red curve when $\alpha > 1$.

(i) Similar to the previous theorem, we have

$$\alpha\, e^{W\left(-1,-\frac{r\, e^{-\frac{r}{\alpha-1}}}{k\,(\alpha-1)}\right)+\frac{r}{\alpha-1}} - \frac{r}{k} < 0 \Longrightarrow e^{\mathrm{W}\left(-1,-\frac{r\, e^{-\frac{r}{\alpha-1}}}{k\,(\alpha-1)}\right)} < \frac{r\, e^{-\frac{r}{\alpha-1}}}{\alpha\, k},$$

then

$$\frac{-\frac{r\,e^{-\frac{r}{\alpha-1}}}{k\,(\alpha-1)}}{W\left(-1,-\frac{r\,e^{-\frac{r}{\alpha-1}}}{k\,(\alpha-1)}\right)}<\frac{r}{k\,\alpha}e^{-\frac{r}{\alpha-1}}\Longrightarrow-\frac{\alpha}{(\alpha-1)}>W\left(-1,-\frac{r\,e^{-\frac{r}{\alpha-1}}}{k(\alpha-1)}\right),$$

take the inverse of W function for both sides and use $W^{-1}(x)=xe^{x}$, it then follows that

$$-\frac{\alpha\,e^{-\frac{\alpha}{\alpha-1}}}{\alpha-1}<-\frac{r\,e^{-\frac{r}{\alpha-1}}}{k(\alpha-1)},$$

then

$$-\frac{\alpha\,k\,\mathrm{e}^{-\frac{\alpha}{\alpha-1}}}{\alpha-1}<W^{-1}\left(-1,-\frac{r}{\alpha-1}\right),$$

solve it for r, we have

$$r<(1-\alpha)W\left(-1,-\frac{\alpha\,k\,\mathrm{e}^{-\frac{\alpha}{\alpha-1}}}{\alpha-1}\right),$$

as a result the stable region corresponding to inequality $\det<1$ is given as

$$\begin{cases} r<(1-\alpha)W\left(-1,-\frac{\alpha\,k\,\mathrm{e}^{-\frac{\alpha}{\alpha-1}}}{\alpha-1}\right) & \& \quad \alpha>1, \\ r>(1-\alpha)W\left(-1,-\frac{\alpha\,k\,\mathrm{e}^{-\frac{\alpha}{\alpha-1}}}{\alpha-1}\right) & \& \quad \alpha<1. \end{cases}$$

For $\det<\mathrm{tr}-1$, we have

$$\frac{r}{k}\,e^{\frac{(-\alpha+1)W\left(-1,-\frac{r\,e^{-\frac{r}{\alpha-1}}}{k\,(\alpha-1)}\right)-r}{\alpha-1}}+\frac{k\,(\alpha-1)}{k}\,e^{\frac{(\alpha-1)W\left(-1,-\frac{r\,e^{-\frac{r}{\alpha-1}}}{k\,(\alpha-1)}\right)+r}{\alpha-1}}+\frac{(-\alpha+1)\,k}{k}-\frac{r}{k}>0,$$

then

$$\frac{r}{k}\frac{W\left(-1,-\frac{r\,\mathrm{e}^{-\frac{r}{\alpha-1}}}{k\,(\alpha-1)}\right)}{\left(-\frac{r\,\mathrm{e}^{-\frac{r}{\alpha-1}}}{k\,(\alpha-1)}\right)\,e^{\frac{r}{\alpha-1}}}+\frac{(\alpha-1)\left(-\frac{r\,\mathrm{e}^{-\frac{r}{\alpha-1}}}{k\,(\alpha-1)}\right)}{W\left(-1,-\frac{r\,\mathrm{e}^{-\frac{r}{\alpha-1}}}{k\,(\alpha-1)}\right)}\,e^{\frac{r}{\alpha-1}}+(-\alpha+1)-\frac{r}{k}>0,$$

simplifying them gives

$$\frac{1}{\alpha-1}\left(-\mathrm{W}\left(-1,-\frac{r\,\mathrm{e}^{-\frac{r}{\alpha-1}}}{k\,(\alpha-1)}\right)(\alpha-1)+\frac{\left(-\frac{r}{k}\right)}{\mathrm{W}\left(-1,-\frac{r\,\mathrm{e}^{-\frac{r}{\alpha-1}}}{k\,(\alpha-1)}\right)}+(-\alpha+1)-\frac{r}{k}\right)>0,$$

or

$$-W\left(-1,-\frac{r\,\mathrm{e}^{-\frac{r}{\alpha-1}}}{k\,(\alpha-1)}\right)+\frac{\left(-\frac{r}{k\,(\alpha-1)}\right)}{W\left(-1,-\frac{r\,\mathrm{e}^{-\frac{r}{\alpha-1}}}{k\,(\alpha-1)}\right)}-1-\frac{r}{k\,(\alpha-1)}>0. \tag{4.28}$$

Assume $u=W\left(-1,-\frac{r\,e^{-\frac{r}{\alpha-1}}}{k\,(\alpha-1)}\right)$. From the definition of W, we obtain $k=-\frac{r}{u\,(\alpha-1)}\,e^{-\frac{r}{\alpha-1}-u}$. Substituting k and u in (4.28), it follows that

$$-u+\frac{\left(-\frac{r\,u\,(\alpha-1)}{-r\,(\alpha-1)}\,e^{\frac{r}{\alpha-1}+u}\right)}{u}-1-\frac{r\,u\,(\alpha-1)}{-r\,(\alpha-1)}\,e^{\frac{r}{\alpha-1}+u}>0.$$

It is clear that $u=-1$ and $e^{\frac{r}{\alpha-1}+u}=1$ are two solutions of the left hand side of the above inequality. We can start the computation when $u=-1$:

$$W\left(-1,-\frac{r\,\mathrm{e}^{-\frac{r}{\alpha-1}}}{k\,(\alpha-1)}\right)<-1$$

From the domain of W_{-1} function, we have

$$-\frac{1}{e}\leq-\frac{r\,\mathrm{e}^{-\frac{r}{\alpha-1}}}{k\,(\alpha-1)}<0,$$

or

$$-\frac{k}{e}\leq W^{-1}\left(-1,-\frac{r}{\alpha-1}\right). \tag{4.29}$$

Applying the Lambert W function W to both sides gives

$$W\left(-1,-\frac{k}{e}\right)\geq\left(-\frac{r}{\alpha-1}\right)\Longrightarrow r\geq(1-\alpha)W\left(-1,-\frac{k}{e}\right). \tag{4.30}$$

For the other solution when we have $e^{\frac{r}{\alpha-1}+u}=1$, by some calculations we acquire

$$W\left(-1,-\frac{r\,\mathrm{e}^{-\frac{r}{\alpha-1}}}{k\,(\alpha-1)}\right)>-\frac{r}{\alpha-1}, \tag{4.31}$$

or

$$-\frac{r\mathrm{e}^{-\frac{r}{\alpha-1}}}{k(\alpha-1)}>-\frac{r}{\alpha-1}e^{-\frac{r}{\alpha-1}}, \tag{4.32}$$

simplifying them and solving it for r gives $k>1$. As a result the region corresponding to inequality $\det>\mathrm{tr}-1$ is given by

$$\begin{cases} r\geq(1-\alpha)W\left(-1,-\frac{k}{e}\right) & \& \quad \alpha>1,k>1 \\ r\leq(1-\alpha)W\left(-1,-\frac{k}{e}\right) & \& \quad \alpha<1,k<1. \end{cases}$$

The region corresponding to inequality $\det>-\mathrm{tr}-1$ is equivalent to

$$\begin{cases} r<-(\alpha-1)W\left(-\frac{k(\alpha+3)}{\alpha-1}e^{-\frac{\alpha+3}{\alpha-1}}\right) & \& \quad \alpha>1, \\ r>-(\alpha-1)W\left(-\frac{k(\alpha+3)}{\alpha-1}e^{-\frac{\alpha+3}{\alpha-1}}\right) & \& \quad \alpha<1. \end{cases}$$

This result is coming from solving (4.27) for r as follow.

$$k<\frac{1}{\alpha+3}\,e^{\frac{\alpha+3}{\alpha-1}}re^{\frac{-r}{\alpha-1}}\Longrightarrow k(\alpha+3)e^{-\frac{\alpha+3}{\alpha-1}}<re^{\frac{-r}{\alpha-1}},$$

for $\alpha>1$

$$\Longrightarrow k\frac{(\alpha+3)}{\alpha-1}e^{-\frac{\alpha+3}{\alpha-1}}<\frac{r}{\alpha-1}e^{\frac{-r}{\alpha-1}}\Longrightarrow-\frac{k(\alpha+3)}{\alpha-1}e^{-\frac{\alpha+3}{\alpha-1}}>-\frac{r}{\alpha-1}e^{\frac{-r}{\alpha-1}},$$

$$\Longrightarrow-\frac{k(\alpha+3)}{\alpha-1}e^{-\frac{\alpha+3}{\alpha-1}}>W^{-1}\left(-1,\frac{-r}{\alpha-1}\right).$$

It then follows that

$$W\left(-1,-\frac{k(\alpha+3)}{\alpha-1}e^{-\frac{\alpha+3}{\alpha-1}}\right)<W\left(W^{-1}\left(-1,\frac{-r}{\alpha-1}\right)\right),$$

$$W\left(-\frac{k(\alpha+3)}{\alpha-1}e^{-\frac{\alpha+3}{\alpha-1}}\right) < \frac{-r}{\alpha-1} \Longrightarrow -W\left(-\frac{k(\alpha+3)}{\alpha-1}e^{-\frac{\alpha+3}{\alpha-1}}\right) > \frac{r}{\alpha-1},$$

$$r < -(\alpha-1)W\left(-\frac{k(\alpha+3)}{\alpha-1}e^{-\frac{\alpha+3}{\alpha-1}}\right).$$

Therefore, for (α, r)- plane, the stable regions are in the range between $f_3(\alpha) < r < f_1(\alpha)$. The repeller region is the region delimited between $f_1(\alpha) < r < f_2(\alpha)$ or empty space. The saddle region is either above $r > f_2(\alpha)$ or $0 < r < f_3(\alpha)$. Figure (4.12) summarizes the results of this theorem.

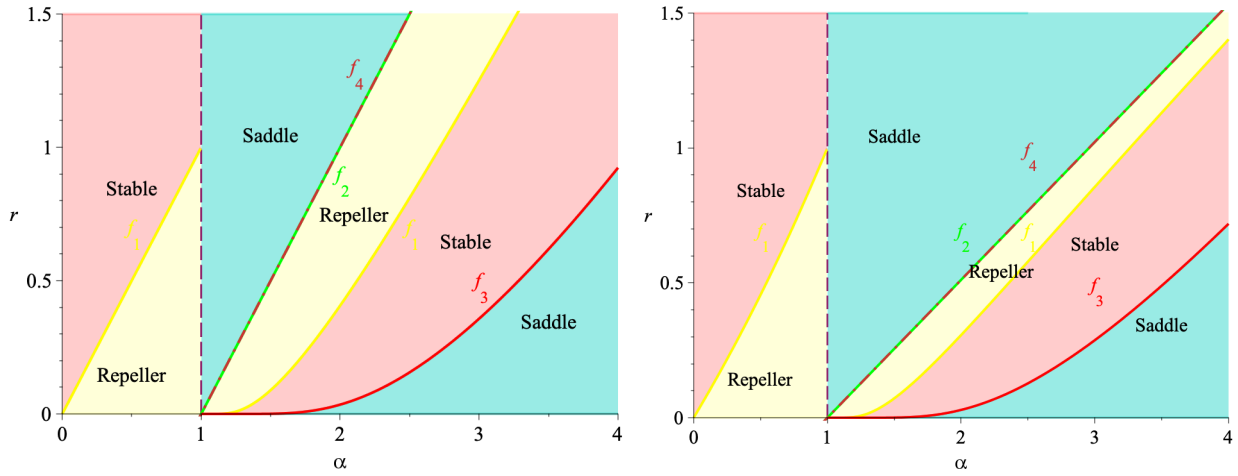

Figure 4.12: Stability regions of the two co-dimension (α, r) plane where the parameter $k = 1$ (left) and $k = 1.6668$ (right).

□

4.5 Bifurcation Analysis

In this section, we investigate the dynamics of two types of bifurcation that the model experiences: Neimark–Sacker bifurcation and Period-doubling bifurcation.

4.5.1 Neimark–Sacker Bifurcation

In this section, we study the stability of Neimark-Sacker bifurcation for the interior steady states of system (4.6). Neimark–Sacker bifurcations generate dynamically closed invariant cycles. As a result, isolated periodic orbits can be observed along with trajectories that cover the invariant cycle densely. We seek conditions for system (4.6) to have a non-hyperbolic steady state with a pair of complex conjugate eigenvalues of modulus 1. This interesting result occurs at the positive steady state. Jacobian matrix has two complex conjugate eigenvalues with modulus 1 in the case of $\det(J^*) = 1$ and $|\operatorname{tr}(J^*)| < 2$. The bifurcation parameter r (the reproductive parameter for the parasite population) is the curve

$$r = -\alpha \ln(x) + \ln(x) + \alpha,$$

and $|\operatorname{tr}(J^*)| < 2$ is

$$|1 + \alpha - r + \ln(x^*) - \alpha \ln(x^*) + \frac{1}{x^*}| < 2.$$

Suppose for the positive parameters that

$$\eta = \left\{ (\alpha, r, k) \middle| \; r = -\alpha \ln(x) + \ln(x) + \alpha, \; \left| 1 + \alpha - r + \ln(x^*) - \alpha \ln(x^*) + \frac{1}{x^*} \right| < 2 \right\}.$$

Following the standard method, we transform the system to the origin in order to reduce the linear part of the two-dimensional map (4.1) to a normal form using the change of variables for $r \neq 0$:

$$x = x^* + \bar{x}, \; y = y^* + \bar{y}, \; r = r^* + \bar{r}.$$

System (4.6) can then be rearranged by the following two dimensional map

$$f(\bar{x}, \bar{y}) = (x^* + \bar{x})^{1+\alpha} e^{(r^*+\bar{r})\left(1 - \frac{x^*+\bar{x}}{k}\right)} \frac{1}{1 + y^* + \bar{y}} - x^*,$$
$$g(\bar{x}, \bar{y}) = (x^* + \bar{x}) \left(1 - \frac{1}{1 + y^* + \bar{y}} \right) - y^*.$$

Applying the Taylor series of f and g gives

$$
\begin{aligned}
f(\bar{x},\bar{y}) &= \frac{(1+\alpha)\,k-(r^*+\bar{r})\,(y^*+1)}{k}\,\bar{x}-\bar{y}-\frac{1}{y^*+1}\,\bar{y}^2-\frac{(1+\alpha)\,k-(r^*+\bar{r})\,(y^*+1)}{k\,(y^*+1)}\,\bar{x}\,\bar{y}\\
&+\frac{\left(\alpha^2+\alpha\right)\,k^2-2\,(r^*+\bar{r})\,(1+\alpha)\,(y^*+1)\,k+(r^*+\bar{r})^2\,(y^*+1)^2}{2\,k^2(y^*+1)}\,\bar{x}^2\\
&+\Bigg[\frac{\left(-(r^*+\bar{r})^3\,(y^*+1)^3+3\,(1+\alpha)\,(y^*+1)^2\,(r^*+\bar{r})^2\,k\right)}{6\,(y^*+1)^2\,k^3}\\
&+\frac{\left(-3\,(r^*+\bar{r})\,(y^*+1)\,\alpha\,(1+\alpha)\,k^2+\left(\alpha^3-\alpha\right)\,k^3\right)\,x\,b^3}{6\,(y^*+1)^2\,k^3}\Bigg]\bar{x}^3\\
&-\frac{\left(\alpha^2+\alpha\right)\,k^2-2\,(r^*+\bar{r})\,(1+\alpha)\,(y^*+1)\,k+(r^*+\bar{r})^2\,(y^*+1)^2}{2\,k^2\,(y^*+1)^2}\,\bar{y}\,\bar{x}^2\\
&+\frac{(1+\alpha)\,k-(r^*+\bar{r})\,(y^*+1)}{k\,(y^*+1)^2}\,\bar{x}\,\bar{y}^2-\frac{1}{(y^*+1)^2}\,\bar{y}^3+\mathcal{O}(4),\\
g(\bar{x},\bar{y}) &= \frac{y^*}{y^*+1}\,\bar{x}+\frac{1}{y^*+1}\,\bar{y}+\frac{1}{(y^*+1)^2}\,\bar{x}\,\bar{y}+\frac{(-y^*-1)}{(y^*+1)^3}\,\bar{y}^2-\frac{1}{(y^*+1)^3}\,\bar{x}\,\bar{y}^2\\
&+\frac{1}{(y^*+1)^3}\,\bar{y}^3+\mathcal{O}(4).
\end{aligned}
\tag{4.33}
$$

Therefore, the Jacobian matrix of (4.33) is given by

$$
J=\begin{pmatrix}
\frac{-(r^*+\bar{r})\,y^*+(1+\alpha)\,k-(r^*+\bar{r})}{k} & -1\\
\frac{y^*}{y^*+1} & \frac{1}{y^*+1}
\end{pmatrix},
\tag{4.34}
$$

from which we have

$$
\begin{aligned}
\mathrm{tr}(J) &= \frac{-(r^*+\bar{r})\,y^*+(1+\alpha)\,k-(r^*+\bar{r})}{k}+\frac{1}{y^*+1},\\
\det(J) &= \frac{(y^*+\alpha+1)\,k-(r^*+\bar{r})\,(y^*+1)}{k\,(y^*+1)},
\end{aligned}
$$

and the eigenvalues are complex numbers with $\lambda_1(\bar{r})=\bar{\lambda_2}(\bar{r})$, and $|\lambda_1|=|\lambda_2|=1$. Then from the characteristic equation of the Jacobian matrix we have

$$
\lambda_{1,2}=\frac{\mathrm{tr}(J)\pm\sqrt{\mathrm{tr}(J)^2-4\det(J)}}{2}:=\gamma\pm\sqrt{-1}\beta,
$$

where γ is the real part of the eigenvalues, and β is the imaginary part of the eigenvalues.

To find the eigenvectors, first we can define Jacobin matrix (4.34) by $J = \begin{pmatrix} a & b \\ c & d \end{pmatrix}$. We now easily obtain the span of eigenvectors matrix called P using the definition $(J - \lambda\, I)\mathsf{x} = 0$, or

$$\begin{pmatrix} a-\lambda & b \\ c & d-\lambda \end{pmatrix} \begin{pmatrix} \mathsf{x}_1 \\ \mathsf{x}_2 \end{pmatrix} = \begin{pmatrix} 0 \\ 0 \end{pmatrix}.$$

Assume that $\mathsf{x}_1 = b = -1$ and $\mathsf{x}_2 = \lambda - a$ where $\lambda = \gamma + \beta\, i$ and $a = \frac{-(r^*+\bar{r})y^* + (1+\alpha)k - (r^*+\bar{r})}{k}$, we will then have

$$\begin{pmatrix} \mathsf{x}_1 \\ \mathsf{x}_2 \end{pmatrix} = \begin{pmatrix} b \\ \lambda - a \end{pmatrix} = \begin{pmatrix} -1 \\ (\gamma + \beta\, i) - a \end{pmatrix} = \begin{pmatrix} -1 + 0\, i \\ (\gamma + \beta\, i) - a \end{pmatrix}.$$

As a result, we can use the followig change of variables based on the eigenvector matrix for the linear part:

$$\begin{pmatrix} \bar{x} \\ \bar{y} \end{pmatrix} = \begin{pmatrix} 0 & -1 \\ \beta & \gamma - \frac{\alpha\, k - (r^*+\bar{r})\, y^* - (r^*+\bar{r})}{k} - 1 \end{pmatrix} \begin{pmatrix} u \\ v \end{pmatrix},$$

Now we can have the following two-dimensional map

$$\begin{pmatrix} u \\ v \end{pmatrix} \mapsto \begin{pmatrix} \gamma & -\beta \\ \beta & \gamma \end{pmatrix} \begin{pmatrix} u \\ v \end{pmatrix} + \begin{pmatrix} \tilde{f}(u, v, \bar{r}) \\ \tilde{g}(u, v, \bar{r}) \end{pmatrix}. \tag{4.35}$$

To find the linear matrix $\begin{pmatrix} \gamma & -\beta \\ \beta & \gamma \end{pmatrix}$ we can use the matrix P where

$$P = \begin{pmatrix} 0 & -1 \\ \beta & \gamma - \xi - 1 \end{pmatrix},$$

for $\xi = \frac{-ry^*+\alpha k-r}{k}$. Then the inverse matrix P^{-1} is given by

$$p^{-1} = \begin{pmatrix} \frac{\gamma-1-\xi}{\beta} & \frac{1}{\beta} \\ -1 & 0 \end{pmatrix}.$$

We can now simplify the multiplication to obtain $P^{-1}\,J\,P$ by

$$p^{-1}JP = \begin{pmatrix} \gamma & -\beta \\ \beta & \gamma \end{pmatrix}.$$

and the same process can be applied to obtain the non-linear part of (4.35) by

$$\begin{aligned}
\tilde{f}(u,v,\bar{r}) = &-\frac{\beta((-\gamma+1+\xi)y^*+\xi-\gamma+2)}{(y^*+1)^2}u^2 + \left[-\frac{(-\gamma+1+\xi)(\xi-\gamma)}{(y^*+1)^2\beta}\right. \\
&\left. - \frac{\left(\gamma^2+(-2\xi+\alpha-1)\gamma+\xi^2+(-\alpha+1)\xi+\frac{\alpha^2}{2}-\frac{\alpha}{2}\right)(-\gamma+1+\xi)}{\beta(y^*+1)}\right]v^2 \\
&+ \left[\frac{2\xi-2\gamma+1}{(y^*+1)^2} + \frac{(\gamma-1-\xi)(-1+\alpha+2\gamma-2\xi)}{y^*+1}\right]uv \\
&+ \frac{\beta^2((-\gamma+1+\xi)y^*+\xi-\gamma+2)}{(y^*+1)^3}u^3 + \left[\frac{(\gamma-1-\xi)^2(\gamma-\xi)}{(y^*+1)^3\beta}\right. \\
&\left. + \frac{(\gamma-1-\xi)\left(-\frac{\alpha\left(\alpha^2-1\right)}{6(y^*+1)^2} - \frac{(1+\alpha)\alpha(\gamma-1-\xi)}{2(y^*+1)^2} - \frac{(1+\alpha)(\gamma-1-\xi)^2}{(y^*+1)^2} - \frac{(\gamma-1-\xi)^3}{(y^*+1)^2}\right)}{\beta}\right]v^3 \\
&+ \left[\frac{(\gamma-1-\xi)(-1+3\gamma-3\xi)}{(y^*+1)^3}\right. \\
&\left. - \frac{(\gamma-1-\xi)\left(\alpha^2+4\alpha\gamma-4\alpha\xi+6\gamma^2-12\gamma\xi+6\xi^2-3\alpha-8\gamma+8\xi+2\right)}{2(y^*+1)^2}\right]uv^2 \\
&+ \left[-\frac{(\gamma-1-\xi)\beta(-2+\alpha+3\gamma-3\xi)}{(y^*+1)^2} + \frac{\beta(-2+3\gamma-3\xi)}{(y^*+1)^3}\right]u^2v
\end{aligned}$$

$$\begin{aligned}
\tilde{g}(u,v,\bar{r}) = &-\frac{\beta^2}{y^*+1}\,u^2 + \frac{-\alpha^2+(2\,\xi-2\,\gamma+1)\,\alpha-2\,(-\gamma+1+\xi)\,(\xi-\gamma)}{2\,y^*+2}\,v^2 \\
&+ \frac{\beta\,(2\,\xi-\alpha-2\,\gamma+1)}{y^*+1}\,uv + \frac{\beta^3}{(y^*+1)^2}\,u^3 + \frac{1}{6\,(y^*+1)^2}\left[\alpha^3+(-3\,\xi+3\,\gamma-3)\,\alpha^2\right. \\
&\left. + \left(6\,\gamma^2+(-12\,\xi-9)\,\gamma+6\,\xi^2+9\,\xi+2\right)\,\alpha - 6\,(\xi-\gamma)\,(-\gamma+1+\xi)^2\right]v^3
\end{aligned}$$

$$+\frac{1}{(y^*+1)^2}\left[3\,\beta\left(\frac{\alpha^2}{6}+\left(-\frac{1}{2}-\frac{2\,\xi}{3}+\frac{2\,\gamma}{3}\right)\alpha+\left(\xi-\gamma+\frac{1}{3}\right)(-\gamma+1+\xi)\right)\right]uv^2$$
$$+\frac{\beta^2\,(-2+\alpha+3\,\gamma-3\,\xi)}{(y^*+1)^2}\,u^2v+\mathcal{O}(4).$$

Our analysis for this bifurcation is typically based on the complex variables given as follows

$$w:=u+\mathrm{i}v,\quad \bar{w}:=u-\mathrm{i}v.$$

Using equation (4.35), it then follows for w that (see Lemma 2.4.4):

$$w\mapsto(\gamma+\mathrm{i}\beta)w+\left(\tilde{f}_1+\mathrm{i}\tilde{f}_2\right)=\lambda(\bar{r})w+\mathcal{G}(w,\bar{w},\mu).$$

Simplifying $\mathcal{G}$ gives

$$\begin{aligned}\mathcal{G}(w,\bar{w},\bar{r})&=\tilde{f}_1\left(\frac{w+\bar{w}}{2},\frac{w-\bar{w}}{2\mathrm{i}},\bar{r}\right)+\mathrm{i}\tilde{f}_2\left(\frac{w+\bar{w}}{2},\frac{w-\bar{w}}{2\mathrm{i}},\bar{r}\right)\\&=\sum_{k+l\geq 2}\frac{1}{k!\,l!}\,g_{kl}(\bar{r})\,w^l\,\bar{w}^k+O\left(|w|^4\right),\end{aligned}$$

where a few terms that will be needed in the sequel are given as follows

$$\begin{aligned}\mathcal{G}_{20}=\frac{1}{8(y^*+1)^2k^2i^2\beta}\Big[&\Big(-2(i\beta-\gamma+\xi+1)\Big(\gamma^2+(2i\beta+\alpha-2\xi-1)\gamma+\xi^2\\&+(-2i\beta-\alpha+1)\xi+i^2\beta^2+i(\alpha-1)\beta+\frac{\alpha^2}{2}-\frac{\alpha}{2}\Big)y^*+(2i\beta+2\alpha-6\xi-6)\gamma^2\\&+2\gamma^3+\left(6\xi^2+(-4i\beta-4\alpha+12)\xi-2i^2\beta^2-8i\beta+\alpha^2-3\alpha+4\right)\gamma-2\xi^3\\&+(2i\beta+2\alpha-6)\xi^2+\left(2i^2\beta^2-\alpha^2+8i\beta+3\alpha-4\right)\xi-2i^3\beta^3-2i^2(1+\alpha)\beta^2\\&-i\left(\alpha^2+\alpha-4\right)\beta-\alpha^2+\alpha\Big)k^2+2r(y^*+1)^2(i\beta-\gamma+\xi+1)(i\beta+\alpha+\gamma-\xi)k\\&-r^2(y^*+1)^3(i\beta-\gamma+\xi+1)\Big],\end{aligned}$$

$$\mathcal{G}_{11}=\frac{1}{4(y^*+1)^2k^2i^2\beta}\left[\left(-2\left(-\gamma^2+(2\xi-\alpha+1)\gamma-\xi^2+(\alpha-1)\xi+i^2\beta^2-\frac{\alpha^2}{2}+\frac{\alpha}{2}\right)\right.$$

$$
\begin{aligned}
&(i\beta-\gamma+\xi+1)y^*-2\gamma^3+(2i\beta-2\alpha+6\xi+6)\gamma^2+\big(-6\xi^2+(-4i\beta+4\alpha-12)\xi\\
&+2i^2\beta^2+2i(\alpha-1)\beta-\alpha^2+3\alpha-4\big)\gamma+2\xi^3+(2i\beta-2\alpha+6)\xi^2\\
&+\big(-2i^2\beta^2-2i(\alpha-1)\beta+\alpha^2-3\alpha+4\big)\xi-2i^3\beta^3-4i^2\beta^2+i\alpha(\alpha-1)\beta+\alpha^2-\alpha\big)\,k^2\Big)\\
&+2r(y^*+1)^2(\xi-\alpha-\gamma)(i\beta-\gamma+\xi+1)k+r^2(y^*+1)^3(i\beta-\gamma+\xi+1)\Big],
\end{aligned}
$$

$$
\begin{aligned}
\mathcal{G}_{02}=-\frac{1}{4(y^*+1)^2k^2i^2\beta}\Bigg[&(i\beta-\gamma-\xi+1)\Big(\Big(\Big(i^2\beta^2+2\Big(\xi-\frac{\alpha}{2}-\gamma_{\frac{1}{2}}\Big)i\beta+\gamma^2\\
&+(-2\xi+\alpha-1)\gamma+\xi^2+(-\alpha+1)\xi+\frac{\alpha^2}{2}-\frac{\alpha}{2}\Big)y^*+i^2\beta^2+2\Big(\xi-\frac{\alpha}{2}-\gamma+1\Big)i\beta\\
&+(-2+\alpha-2\xi)\gamma+\xi^2+(2-\alpha)\xi+\frac{\alpha^2}{2}-\frac{\alpha}{2}\Big)k^2+(y^*+1)^2(i\beta-\alpha-\gamma+\xi)k\\
&+\frac{r^2(y^*+1)^3}{2}\Big)\Bigg]
\end{aligned}
$$

$$
\begin{aligned}
\mathcal{G}_{20}=\frac{1}{16(y^*+1)^3k^3i^3\beta}\Bigg[&\Big(6(i\beta-\gamma+\xi+1)(-\gamma^3+(i\beta-\alpha+3\xi+2)\gamma^2\\
&+(-3\xi^2+2i\beta+2\alpha-4)\xi-\frac{\alpha^2}{2}+\Big(\frac{3}{2}-\frac{2i\beta}{3}\alpha+i^2\beta^2+\frac{4i\beta}{3}-1\Big)\gamma+\xi^3\\
&+(-i\beta-\alpha+2)\xi^2+\Big(\frac{\alpha^2}{2}+\Big(-\frac{3}{2}+\frac{2i\beta}{3}\Big)\alpha-i^2\beta^2-\frac{4i\beta}{3}+1\Big)\xi-\frac{\alpha^3}{6}\\
&+\Big(-\frac{i\beta}{6}+\frac{1}{2}\alpha^2+\Big(\frac{1}{3}i^2\beta^2+\frac{1}{2}i\beta-\frac{1}{3}\Big)\alpha-\frac{i\beta}{3}+i^3\beta^3-\frac{2i^2\beta^2}{3}y^*+6\gamma\\
&+(36\xi^2+(-18\alpha+72)\xi+3\alpha^2+(-2i\beta-15)\alpha-12i^2\beta^2-8i\beta+30)\gamma^2\\
&+(-24\xi^3+(18\alpha-72)\xi^2+(-6\alpha^2+(4i\beta+30)\alpha+24i^2\beta^2+16i\beta-60)\xi\\
&+\alpha^3+(-2i\beta-6)\alpha^2+(-6i^2\beta^2+2i\beta+11)\alpha+24i^2\beta^2+12i\beta-12)\gamma+6\xi^4\\
&+(-6\alpha+24)\xi^3+(3\alpha^2+(-2i\beta-15)\alpha-12i^2\beta^2-8i\beta+30)\xi^2\\
&+(-\alpha^3+(2i\beta+6)\alpha^2+(6i^2\beta^2-2i\beta-11)\alpha-24i^2\beta^2-12i\beta+12)\xi\\
&+(-i\beta-1)\alpha^3+(-i^2\beta^2+2i\beta+3)\alpha^2+(2i^3\beta^3+5i^2\beta^2+i\beta-2)\alpha+6i^4\beta^4\\
&+8i^3\beta^3-10i^2\beta^2-4i\beta)k^3-2r(-3\gamma^2+(-2i\beta-3\alpha+6\xi+3)\gamma-3\xi^2\\
&+(2i\beta+3\alpha-3)\xi-\frac{3\alpha^2}{2}+\Big(-i\beta+\frac{3}{2}\Big)\alpha+i^2\beta^2+i\beta)(i\beta-\gamma+\xi+1)
\end{aligned}
$$

$$(y^*+1)^2k^2 - r^2(y^*+1)^3(i\beta-\gamma+\xi+1)(i\beta+3\alpha+3\gamma-3\xi)k$$
$$+ r^3(y^*+1)^4(i\beta-\gamma+\xi+1)\Big)\Big].$$

The final result to determine the stability of the Neimark-Sacker bifurcation can be computed via (see equation (2.26)):

$$a(0) = \mathrm{Re}\left(\frac{\mathrm{e}^{-\mathrm{i}\theta_0}\mathcal{G}_{21}}{2}\right) - \mathrm{Re}\left(\frac{\left(1-2\mathrm{e}^{\mathrm{i}\theta_0}\right)\mathrm{e}^{-2\mathrm{i}\theta_0}}{2\left(1-\mathrm{e}^{\mathrm{i}\theta_0}\right)}\mathcal{G}_{20}\mathcal{G}_{11}\right) - \frac{1}{2}\left|\mathcal{G}_{11}\right|^2 - \frac{1}{4}\left|\mathcal{G}_{02}\right|^2, \tag{4.36}$$

where θ is the angle of the eigenvalues. As a result, the sign of the coefficient $a(0)$ can be used to determine its stability. The non-linear solution is a stable closed invariant set if $a(0) < 0$ or is unstable if $a(0) > 0$. When a Neimark-Sacker bifurcation exists, the numerical simulation results can be found as shown in Table 4.1. From which it can be seen that for what values of the three parameters the Neimark-Sacker bifurcation can be negative (unstable) or positive (stable).

Table 4.1: The numerical values for the positive steady state and for the coefficient $a(0)$ corresponding to parameters (α, k).

α	k	x^*	y^*	r^*	θ_0	$a(0)$
0.8000	1.0000	1.0000	0	0.8000	0	$-\infty$
	2.3465	1.9999	0.9999	0.9386	0.7227	0.0078
	3.8239	2.9999	1.9999	1.0197	0.8410	-0.0652
	5.3862	4.0000	3.0000	1.0772	0.8956	-3.1945
	7.0117	5.0000	4.0000	1.1218	0.9272	-26.1241
0.9000	1.0000	1.0000	0	0.9000	0	$-\infty$
	2.1540	2.0000	1.0000	0.9693	0.7227	0.0083
	3.3662	2.9999	1.9999	1.0098	0.8410	-0.0538
	4.6161	3.9999	2.9999	1.0386	0.8956	-2.5385
	5.8941	5.0000	4.0000	1.0609	0.9272	-18.7607
1.1000	1.0000	5.9863	5.9862	0.1837	1.0471	-3.0042×10^{-5}
	1.8739	5.9853	5.9852	0.3444	1.0471	-1.0478×10^{-3}
	2.7003	5.9844	5.9843	0.4963	1.0471	-8.2822×10^{-3}
	0.9613	5.9863	5.9862	0.1766	1.0471	-2.3748×10^{-5}
	4.2684	5.9827	5.9826	0.7848	1.0471	-1.1531×10^{-1}
1.2000	1.0000	3.9738	3.9638	0.0030	1.0457	-1.0236×10^{-5}
	1.7689	3.9267	3.9167	0.0054	1.0457	-2.7322×10^{-4}
	2.4506	3.8844	3.8744	0.0075	1.0457	-1.7841×10^{-3}
	3.0758	3.8452	3.8352	0.0095	1.0456	-6.7077×10^{-3}
	3.6588	3.8083	3.7983	0.0115	1.0456	-1.8639×10^{-2}
1.3000	1.0000	71.7309	70.7309	0.0181	1.0391	-4.0875×10^{-4}
	1.6800	68.5166	67.5166	0.0318	1.0387	-8.9800×10^{-3}
	2.2394	65.7408	64.7408	0.0442	1.0383	-5.0213×10^{-2}
	2.7203	63.2394	62.2394	0.0559	1.0380	-0.1651
	3.1429	60.9363	59.9363	0.0670	1.0376	-0.4069

We can also see the results for different values of parameters $k \in [0.1, 3]$ in Figure 4.13.

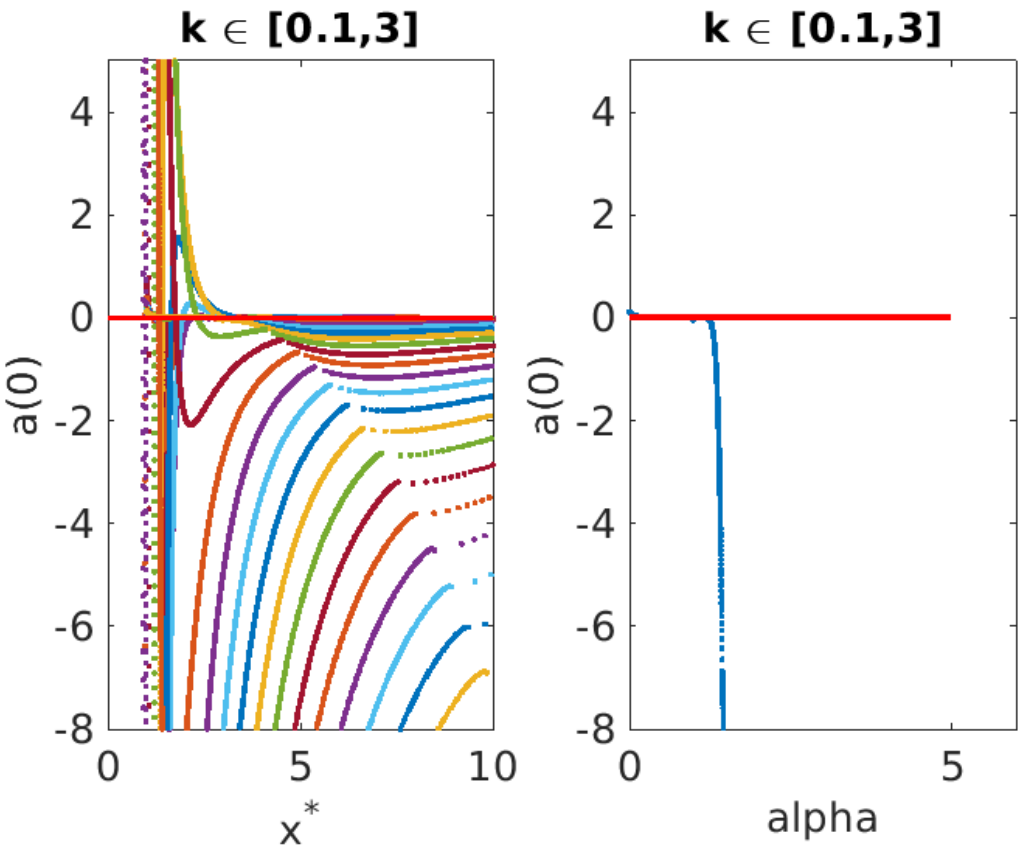

Figure 4.13: Neimark-Sacker bifurcation for different k values. It is unstable when $a(0) > 0$ and stable when $a(0) < 0$.

4.5.2 Period-Doubling Bifurcations

Below we plan to study the period doubling bifurcation of the positive steady-state S_4 of system (4.6). We can calculate the Jacobin matrix for the positive steady-state (x^*, y^*) where $k = \frac{x^* r}{r - \ln(x^*) + \alpha \ln(x^*)}$ as follows

$$J^* = \begin{pmatrix} 1 + \alpha - \frac{x^* r}{k} & -1 \\ 1 - \frac{1}{x^*} & \frac{1}{x^*} \end{pmatrix} = \begin{pmatrix} 1 + \alpha - r + \ln(x^*) - \alpha \ln(x^*) & -1 \\ 1 - \frac{1}{x^*} & \frac{1}{x^*} \end{pmatrix}.$$

For the given parameter function $r_{red} = f_3(x) := \frac{-(\alpha-1)(x+1)\ln(x)+(\alpha+3)x+\alpha+1}{x+1}$, it has one eigenvalue $\lambda_1 = -1$ and the other one is inside the unit circle given by $\lambda_2 = \frac{(y^*)^2-2}{(y^*)^2+3y^*+2}$ where $x^* = y^* + 1$.

Similar to before, we plan to use the change of variable $x = x^* + \bar{x},\ y = y^* + \bar{y},\ r = r^* + \bar{r}$ to transform the steady-state to the origin. With this change of variable, system (4.6) can be written by:

$$\begin{aligned} f(\bar{x},\bar{y}) &= (x^*+\bar{x})^{1+\alpha} e^{(r^*+\bar{r})\left(1-\frac{x^*+\bar{x}}{k}\right)} \frac{1}{1+y^*+\bar{y}} - x^*, \\ g(\bar{x},\bar{y}) &= (x^*+\bar{x})\left(1-\frac{1}{1+y^*+\bar{y}}\right) - y^*. \end{aligned} \tag{4.37}$$

Applying the Taylor series to map (4.37) gives

$$\begin{aligned} f(\bar{x},\bar{y}) = \frac{1}{6\,k^3\,(y^*+2)^3\,(y^*+1)^2}\Bigg[& -12k^2(y^*+1)^3(y^*+2)^2\left(\frac{1}{2}y^*\bar{r}+k+\bar{r}\right)\bar{x} \\ & -6\,(y^*+2)^3\,(y^*+1)^2\,\bar{y} + 12\,k^2(y^*+1)^2(y^*+2)^2\left(\frac{1}{2}y^*\bar{r}+k+\bar{r}\right)\bar{x}\bar{y} \\ & -3\,k\,(y^*+1)\,(y^*+2)\left((-y^*)^4\bar{r}^2+\left(-4\bar{r}\,k-6\,\bar{r}^2\right)\,(y^*)^3\right. \\ & +\left((\alpha-3)k^2-16\bar{r}k-13\bar{r}^2\right)(y^*)^2+\left((4\alpha-4)k^2-20\bar{r}k-12\,\bar{r}^2\right)\,y^* \\ & \left.+4\alpha\,k^2-8\,\bar{r}\,k-4\bar{r}^2\right)\bar{x}^2+6\,(y^*+1)\,(y^*+2)^3\,\bar{y}^2 \\ & -12k^2(y^*+1)(y^*+2)^2\left(\frac{1}{2}y^*\bar{r}+k+\bar{r}\right)\bar{x}\bar{y}^2\Bigg] + \mathcal{O}(3), \\ g(\bar{x},\bar{y}) = \frac{y^*}{(1+y^*)}\bar{x} + \frac{1}{(1+y^*)}\,\bar{y} + \frac{\bar{x}\,\bar{y}}{(1+y^*)^2} - \frac{(-y^*-1)\,\bar{y}^2}{(1+y^*)^3} & + \mathcal{O}(3). \end{aligned} \tag{4.38}$$

The eigenvector matrix when $\bar{r} = 0$ is

$$P = \begin{pmatrix} -\frac{y^*+2}{y^*} & -\frac{y^*+1}{y^*+2} \\ 1 & 1 \end{pmatrix}.$$

From which it then follows that

$$\begin{pmatrix} x \\ y \end{pmatrix} = \begin{pmatrix} -\frac{y^*+2}{y^*} & -\frac{y^*+1}{y^*+2} \\ 1 & 1 \end{pmatrix} \begin{pmatrix} u \\ v \end{pmatrix}.$$

Then map (4.38) can be transformed to the following two dimensional map

$$\begin{pmatrix} u \\ v \end{pmatrix} \mapsto \begin{pmatrix} -1 & 0 \\ 0 & \lambda_2 \end{pmatrix} \begin{pmatrix} u \\ v \end{pmatrix} + \begin{pmatrix} \mathcal{H}(u,v,\bar{r}) \\ \mathcal{P}(u,v,\bar{r}) \end{pmatrix},$$

where

$$\begin{aligned} \mathcal{H}(u,v,\bar{r}) &= \mathcal{H}_{200}u^2 + \mathcal{H}_{110}u\bar{r} + \mathcal{H}_{101}uv + \mathcal{H}_{011}v\bar{r} + \mathcal{H}_{020}\bar{r}^2 + \mathcal{H}_{002}v^2 + \mathcal{H}_{300}u^3 + \cdots, \\ \mathcal{P}(u,v,\bar{r}) &= \mathcal{P}_{200}u^2 + \mathcal{P}_{110}u\bar{r} + \mathcal{P}_{101}uv + \mathcal{P}_{011}v\bar{r} + \mathcal{P}_{020}\bar{r}^2 + \mathcal{P}_{002}v^2 + \cdots, \end{aligned} \tag{4.39}$$

are the nonlinear parts. To analyze the stability we need to use the center manifold theory defined by the following function:

$$v = h^c(u,\bar{r}) = au^2 + bu^3 + \mathcal{O}\left(|u,\bar{r}|^3\right).$$

Substituting v into equation (4.39) gives

$$\begin{aligned} \mathcal{H}(u,v,\bar{r}) &= \mathcal{H}_{002}u^4a^2 + \mathcal{H}_{011}u^2a\bar{r} + \mathcal{H}_{101}u^3a + \mathcal{H}_{300}u^3 + \mathcal{H}_{020}\bar{r} + \mathcal{H}_{110}u\bar{r} + \mathcal{H}_{200}u^2 + \cdots, \\ \mathcal{P}(u,v,\bar{r}) &= \mathcal{P}_{002}u^4a^2 + \mathcal{P}_{011}u^2a\bar{r} + \mathcal{P}_{101}u^3a + \mathcal{P}_{020}\bar{r}^2 + \mathcal{P}_{110}u\bar{r} + \mathcal{P}_{002}v^2 + \cdots. \end{aligned}$$

where a few terms of interest are given as follows:

$$\begin{aligned} \mathcal{P}_{200} &= -\frac{(y^*+2)\left((\alpha-1)(y^*)^2 + (4\alpha+4)y^* + 4\alpha + 8\right)}{6(y^*)^3 + 14(y^*)^2 + 8y^*}, \\ \mathcal{H}_{200} &= \frac{(\alpha-1)(y^*)^3 + (6\alpha+2)(y^*)^2 + (12\alpha+4)y^* + 8\alpha}{6(y^*)^3 + 14(y^*)^2 + 8y^*}, \\ \mathcal{H}_{110} &= -\frac{(y^*+1)(y^*+2)^2}{3ky^* + 4k}, \\ \mathcal{H}_{101} &= \frac{(\alpha-1)(y^*)^3 + (5\alpha+3)(y^*)^2 + (8\alpha+15)y^* + 4\alpha + 12}{3(y^*)^3 + 13(y^*)^2 + 18y^* + 8}, \end{aligned}$$

$$\mathcal{H}_{300} = \frac{(5\alpha+3)(y^*)^4 + (40\alpha+12)(y^*)^3 + (120\alpha+72)(y^*)^2 + (160\alpha+128)y^* + 80\alpha + 64}{6(y^*)^2(3y^*+4)(y^*+1)^2}.$$

By some computation we acquire the center manifold in the following:

$$v = h^c(u,\bar{r}) = -\frac{\mathcal{P}_{200}u^2}{\lambda_2 - 1} + \mathcal{O}\left(|u,\bar{r}|^3\right).$$

Now the reduced center manifold map takes the following form:

$$\begin{aligned}\Omega(u,\bar{r}) = &- u + \mathcal{H}_{200}u^2 + \mathcal{H}_{110}u\bar{r} + \left(\mathcal{H}_{210} - \frac{\mathcal{H}_{011}\mathcal{P}_{200}}{\lambda_2 - 1}\right)\bar{r}u^2 \\ &+ \left(\mathcal{H}_{300} - \frac{\mathcal{H}_{101}\mathcal{P}_{200}}{\lambda_2 - 1}\right)u^3 + \mathcal{O}\left(|(u,\bar{r})|^4\right).\end{aligned}$$

Using the conditions of period doubling bifurcation in (2.18), we have

$$\begin{aligned}\Omega(\Omega(u,\bar{r}),\bar{r}) =& u - 2\,\mathcal{H}_{110}\,u\,\bar{r} - 2\left(\mathcal{H}_{300} - \frac{\mathcal{H}_{101}\,\mathcal{P}_{200}}{\lambda_2 - 1} + \mathcal{H}_{200}^2\right)u^3 \\ &- \left(\mathcal{H}_{200}\mathcal{H}_{110}\right)u^2\bar{r} + \left(\mathcal{H}_{110}\right)^2 u\bar{r}^2 + \mathcal{O}(4).\end{aligned}$$

Then, the period doubling bifurcation is analyzed by the following equation

$$\mathcal{X} \equiv 4\,\mathcal{H}_{110}\left(\mathcal{H}_{300} - \frac{\mathcal{H}_{101}\,\mathcal{P}_{200}}{\lambda_2 - 1} + \mathcal{H}_{200}^2\right) \neq 0,$$

where

$$\begin{aligned}&-2\,\mathcal{H}_{300} + \frac{2\,\mathcal{H}_{101}\,\mathcal{P}_{200}}{1-\lambda_2} - 2\,\mathcal{H}_{200}^2 = \\ &\frac{1}{6(\lambda_2-1)y^{*2}(3y^{*2}+7y^*+4)^2} - 3(\alpha-1)^2(\lambda_2+1)y^{*6} + ((-36\lambda_2-18)\alpha^2 + (-6\lambda_2+18)\alpha \\ &-6\lambda_2+48)y^{*5} + ((-180\lambda_2-12)\alpha^2 + (-304\lambda_2+46)\alpha - 84\lambda_2 + 150)y^{*4} + ((-480\lambda_2+144)\alpha^2 \\ &+(-1280\lambda_2+368)\alpha - 576\lambda_2+144)y^{*3} + ((-720\lambda_2+432)\alpha^2 + (-2304\lambda_2+1176)\alpha - 1392\lambda_2+384)y^{*2}\end{aligned}$$

$$((-576\lambda_2+480)\alpha^2+(-1952\lambda_2+1472)\alpha-1408\lambda_2+832)y^*-192(\lambda_2-1)\Big(\alpha+\frac{4}{3}\Big)(\alpha+2)). \tag{4.40}$$

Therefore, the result in Table 4.2 shows that the period doubling bifurcation $\mathcal{X}$ is stable.

Table 4.2: The numerical exact values for $(r^*, \lambda_2, \mathcal{H})$ for the given values of the parameter r^*.

α	k	r^*	λ_2	x	$\mathcal{P}_{200}$	$\mathcal{H}_{300}$	$\mathcal{H}_{110}$	$\mathcal{H}_{101}$	$\mathcal{X}$
	2.0884	3.2719	0.1666	2.0000	-1.9500	3.5892	-1.2312	1.0333	2.5533
	3.1997	3.5197	-0.1666	3.0000	-0.8266	0.8222	-1.5001	0.7033	0.8509
0.8000	4.3261	3.6772	-0.3500	4.0000	-0.4967	0.3706	-1.7780	0.5269	0.5080
	5.4642	3.7885	-0.4666	5.0000	-0.3450	0.2200	-2.0588	0.4166	0.3747
	6.6118	3.8726	-0.5476	6.0000	-0.2591	0.1509	-2.3403	0.3411	0.3061
	2.0428	3.3026	0.1666	2.0000	-2.0464	3.8303	-1.2587	1.0761	2.8731
	3.0969	3.5098	-0.1666	3.0000	-0.8800	0.8814	-1.5499	0.7433	0.9603
0.9000	4.1584	3.6386	-0.3500	4.0000	-0.5368	0.3984	-1.8498	0.5653	0.5746
	5.2256	3.7276	-0.4666	5.0000	-0.3787	0.2368	-2.1528	0.4541	0.4247
	6.2974	3.7934	-0.5476	6.0000	-0.2892	0.1626	-2.4571	0.3779	0.3476
	2.0000	3.3333	0.1666	2.0000	-2.1428	4.0714	-1.2857	1.1190	3.2142
	3.0000	3.5000	-0.1666	3.0000	-0.9333	0.9407	-1.6000	0.7833	1.0785
1.0000	4.0000	3.6000	-0.3500	4.0000	-0.5769	0.4262	-1.9230	0.6038	0.6471
	4.9999	3.6666	-0.4666	5.0000	-0.4125	0.2537	-2.2500	0.4916	0.4795
	5.9999	3.7142	-0.5476	6.0000	-0.3192	0.1743	-2.5789	0.4147	0.3934
	1.9596	3.3640	0.1666	2.0000	-2.2392	4.3125	-1.3122	1.1619	3.5772
	2.9084	3.4901	-0.1666	3.0000	-0.9866	1.0000	-1.6503	0.8233	1.2056
1.1000	3.8501	3.5613	-0.3500	4.0000	-0.6169	0.4541	-1.9979	0.6423	0.7259
	4.7863	3.6057	-0.4666	5.0000	-0.4462	0.2706	-2.3504	0.5291	0.5394
	5.7181	3.6351	-0.5476	6.0000	-0.3493	0.1860	-2.7060	0.4516	0.4437
	1.9215	3.3947	0.1666	2.0000	-2.3357	4.5535	-1.3382	1.2047	3.9623
	2.8218	3.4802	-0.1666	3.0000	-1.0400	1.0595	-1.7010	0.8633	1.3421
1.2000	3.7081	3.5227	-0.3500	4.0000	-0.6570	0.4819	-2.0744	0.6807	0.8112
	4.5837	3.5447	-0.4666	5.0000	-0.4800	0.2875	-2.4543	0.5666	0.6048
	5.4507	3.5559	-0.5476	6.0000	-0.3794	0.1977	-2.8388	0.4884	0.4990
	1.8855	3.4253	0.1666	2.0000	-2.4321	4.7946	-1.3637	1.2476	4.3700
	2.7398	3.4704	-0.1666	3.0000	-1.0933	1.1185	-1.7519	0.9033	1.4883
1.3000	3.5734	3.4841	-0.3500	4.0000	-0.6971	0.5097	-2.1526	0.7192	0.9035
	4.3913	3.4838	-0.4666	5.0000	-0.5137	0.3043	-2..5618	0.6041	0.6761
	5.1965	3.4767	-0.5476	6.0000	-0.4095	0.2094	-2.9776	0.5253	0.5597

We can also see the results in Figure 4.14.

Below we also provided an .mp4 file that shows the bifurcation of Allee effect when period doubling bifurcations exist and they are stable for the parameter values $\alpha = 0.1$ and $k = 1$.

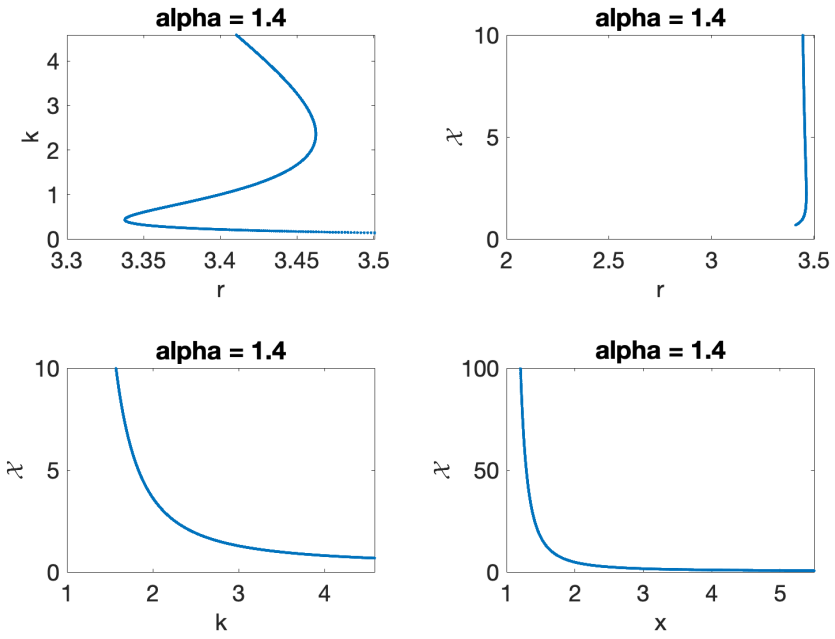

Figure 4.14: Results for period doubling bifurcation when $\alpha = 1.4$ which is stable.

Figure (4.15) shows a summary of the stability regions and dynamics of the population model according to multiple theorems including (4.3.1) and (4.4.4). We found that there are a maximum of five steady states in $\mathcal{Q}_1$.

(i) Origin steady state $(0, 0)$ is always an attractor.

(ii) Two boundary steady state points on the $x-$axis: $(x_1^*, 0)$ and $(x_2^*, 0)$.

(iii) Two interior steady state points: $(z_1^*, z_1^* - 1)$ and $(z_2^*, z_2^* - 1)$.

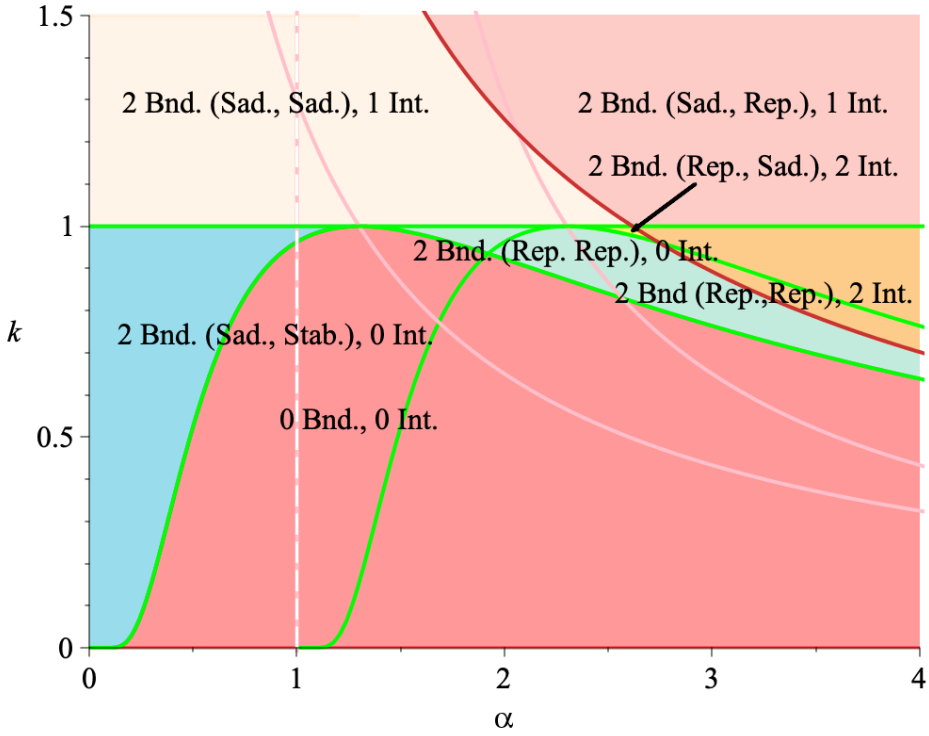

Figure 4.15: Stability regions of the boundary steady-state points $(x_1^*, 0)$ and $(x_2^*, 0)$ where $r = 1.3$ with the regions of the interior steady states $(z_1^*, z_1^* - 1)$ and $(z_2^*, z_2^* - 1)$.

Bibliography

[1] Moghadas, Seyed M and Jaberi-Douraki, Majid *Mathematical Modelling: A Graduate Textbook*, John Wiley & Sons, (2018).

[2] Caughley, Graeme *Plant-herbivore systems*, Theoretical ecology, Blackwell, (1981).

[3] May, RM *Stability and Complexity in Model Ecosystems*, Princeton, NJ, (2001).

[4] Thanos, Costas A *Aristotle and Theophrastus on plant-animal interactions*, Plant-animal interactions in Mediterranean-type ecosystems, Springer, (1994), 3–11.

[5] Lotka, Alfred James *Elements of physical biology*, Williams & Wilkins, (1925).

[6] Volterra, Vito *Variations and fluctuations of the number of individuals in animal species living together*, Oxford University Press, 3(1), (1928), 2–51.

[7] Feng, Zhilan and DeAngelis, Donald *Mathematical Models of Plant-herbivore Interactions*, CRC Press, (2017).

[8] Caughley, G *Wildlife management and the dynamics of ungulate populations*, Applied Biology, Academic Press: New York, (1976), 183–246.

[9] Gutierrez, AP and Williams, DW and Kido, H *A model of grape growth and development: the mathematical structure and biological considerations 1*, Crop science, 25(5), (1985), 721–728.

[10] Edelstein-Keshet, Leah *Mathematical theory for plant—herbivore systems*, Journal of Mathematical Biology, Springer, (1986), 25–58.

[11] Colato, Alexandre and Mizrahi, Salomon S *Effects of random migration in population dynamics*, Physical Review E, APS, 64(1), (2001), 1–14.

[12] Allen, Linda JS and Hannigan, Mary K and Strauss, Monty J *Mathematical analysis of a model for a plant-herbivore system*, Bulletin of mathematical biology, Elsevier, 55(4), (1993), 847–864.

[13] Powell, James A and Logan, Jesse A and Bentz, Barbara J *Local projections for a global model of mountain pine beetle attacks*, Journal of Theoretical Biology, Elsevier, 179(3), (1996), 243–260.

[14] Geiszler, DR and Gallucci, VF and Gara, RI *Modeling the dynamics of mountain pine beetle aggregation in a lodgepole pine stand*, Oecologia, Springer, (1980), 244–253.

[15] Powell, James and Kennedy, Bruce and White, Peter and Bentz, Barbara and Logan, Jesse and Roberts, David *Mathematical elements of attack risk analysis for mountain pine beetles*, Journal of Theoretical Biology, Elsevier, 204(4), (2000), 601–620.

[16] Powell, James A and Logan, Jesse A *Insect seasonality: circle map analysis of temperature-driven life cycles* Theoretical population biology, Elsevier, 67(3), (2005), 161–179.

[17] Summers, Danny and Cranford, Justin G and Healey, Brian P *Chaos in periodically forced discrete-time ecosystem models*, Chaos, Solitons & Fractals, Elsevier, 11(14), (2000), 2331–2342.

[18] Li, Ya and Feng, Zhilan and Swihart, Robert and Bryant, John and Huntly, Nancy *Modeling the impact of plant toxicity on plant–herbivore dynamics* Journal of Dynamics and Differential equations, Springer, 18(4), (2006), 1021–1042.

[19] Sui, Guangyu and Fan, Meng and Loladze, Irakli and Kuang, Yang *The dynamics of a stoichiometric plant-herbivore model and its discrete analog*, Mathematical Biosciences & Engineering, American Institute of Mathematical Sciences, 4(1), (2007), 29-46.

[20] Kang, Yun and Armbruster, Dieter and Kuang, Yang *Dynamics of a plant–herbivore model*, Journal of Biological Dynamics, Taylor & Francis, 2 (2), (2008), 89–101.

[21] Jing, Zhujun and Yang, Jianping *Bifurcation and chaos in discrete-time predator–prey system*, Chaos, Solitons & Fractals, Elsevier, 27(1), (2006), 259–277.

[22] Liu, Xiaoli and Xiao, Dongmei *Complex dynamic behaviors of a discrete-time predator–prey system*, Chaos, Solitons & Fractals, Elsevier, 32(1), 2007, 80–94.

[23] Agiza, HN and Elabbasy, EM and El-Metwally, H and Elsadany, AA *Chaotic dynamics of a discrete prey–predator model with Holling type II*, Nonlinear Analysis: Real World Applications, Elsevier, 10(1), (2009), 116–129.

[24] Liu, Rongsong and Gourley, Stephen A and DeAngelis, Donald L and Bryant, John P *Modeling the dynamics of woody plant–herbivore interactions with age-dependent toxicity* Journal of mathematical biology, Springer, 65(3), (2012).

[25] Kartal, S *Dynamics of a plant–herbivore model with differential–difference equations* Cogent Mathematics, Taylor & Francis, 3(1), (2016).

[26] Din, Qamar and Shabbir, M Sajjad and Khan, M Asif and Ahmad, Khalil *Bifurcation analysis and chaos control for a plant–herbivore model with weak predator functional response* Journal of biological dynamics, Taylor & Francis, 13(1), (2019), 481–501.

[27] Liebhold, Andrew M and Halverson, Joel A and Elmes, Gregory A *Gypsy moth invasion in North America: a quantitative analysis*, Journal of Biogeography, JSTOR (1992), 513-520.

[28] Elkinton, JS and Liebhold, AM *Population dynamics of gypsy moth in North America*, Annual review of entomology, Annual Reviews 4139 El Camino Way, (1990), 35(1), 571-597.

[29] Beddington, JR and Free, CA and Lawton, JH *Dynamic complexity in predator-prey models framed in difference equations*, Nature, Nature Publishing Group, 255(5503), (1975), 5.

[30] Asheghi, Rasoul *Bifurcations and dynamics of a discrete predator–prey system*, Journal of biological dynamics, Taylor & Francis, 8(1), (2014), 161–1868–60.

[31] Nicholson, Alexander John *Supplement: the balance of animal populations* The Journal of Animal Ecology, JSTOR, (1933), 131-178.

[32] Nicholson, Alexander J and Bailey, Victor A *The Balance of Animal Populations.—Part I.* Proc. Zoolog. Soc. Lond. 3 (1935), 105(3), (1935), 551-598.

[33] Kapçak, Sinan and Ufuktepe, Ünal and Elaydi, Saber, *Stability and invariant manifolds of a generalized Beddington host-parasitoid model* Journal of biological dynamics, Taylor & Francis, (2013), 7(1), 233–253.

[34] Edelstein-Keshet, Leah *Mathematical models in biology* SIAM, 2005.

[35] Kulenovic, Mustafa RS and Ladas, Gerasimos *Dynamics of second order rational difference equations: with open problems and conjectures*, Chapman and Hall/CRC, (2001).

[36] Elaydi, Saber N *Discrete chaos: with applications in science and engineering*, Chapman and Hall/CRC, (2007).

[37] Cabré, Xavier and Fontich, Ernest and De, Rafael and de la Llave, Rafael *Allee effects in ecology and conservation*, Oxford University Press, (1995).

[38] Carr, J *Applied mathematical sciences*, Applications of Centre Manifold Theory, Springer-Verlag New York, (1981), (35).

[39] Kelley, A *The stable, center-stable, center, center-unstable, and unstable manifolds*, New York: Benjamin, (1967).

[40] Marsden, JE and McCracken, M *The Hopf Bifurcation and Its Applications*, New York etc, Springer, (1976).

[41] Vanderbauwhede, André *Centre manifolds, normal forms and elementary bifurcations*, Dynamics reported, Springer, (1989), 89–169.

[42] Wiggins, Stephen *Introduction to applied nonlinear dynamical systems and chaos*, Springer Science & Business Media, (2), (2003), 2331–2342.

[43] Freedman, Herbert I and Moson, Peter *Persistence definitions and their connections*, Proceedings of the american mathematical society, 109(4), (1990), 1025–1033.

[44] Massatt, Paul *Limiting behavior for strongly damped nonlinear wave equations*, Journal of Differential Equations, Elsevier, 48(3), (1983), 334–349.

[45] Guzowska, Malgorzata and Luís, Rafael and Elaydi, Saber *Bifurcation and invariant manifolds of the logistic competition model*, Journal of Difference Equations and Applications, Taylor & Francis, 17(12), (2011), 1851–1872.

[46] Corless, Robert M and Gonnet, Gaston H and Hare, David EG and Jeffrey, David J and Knuth, Donald E *On the LambertW function*, Advances in Computational mathematics, Springer, 5(1), (1996), 329–359.

[47] Karydas, Nicholas and Schinas, John *The center manifold theorem for a discrete system*, Applicable Analysis, Taylor & Francis (1992), 44(3-4), 267–284.

[48] Glendinning, Paul*Stability, instability and chaos: an introduction to the theory of nonlinear differential equations*, Cambridge university press, (1994).

[49] Kuznetsov, Yuri A *Elements of applied bifurcation theory*, Springer Science & Business Media, (112), (2013).

[50] Allee, Warder Clyde *The social life of animals*, WW Norton & Co, (1938).

[51] Allee, Warder Clyde and Park, Orlando and Emerson, Alfred Edwards and Park, Thomas and Schmidt, Karl Patterson and others *Principles of animal ecology*, Saunders Company Philadelphia, Pennsylvania, USA, (1949).

[52] Allee, WC *Animal Aggregations, a Study in General Sociology*, Press, Chicago, (1931).

[53] Courchamp, Franck and Berec, Ludek and Gascoigne, Joanna *Allee effects in ecology and conservation*, Oxford University Press, (2008).

[54] Stephens, Philip A and Sutherland, William J and Freckleton, Robert P *What is the Allee effect?*, Oikos, (1999), 185-190.

[55] Elaydi, Saber N and Sacker, Robert J *Population models with Allee effect: A new model*, Journal of Biological Dynamics, 4(4), (2010), 397-408.

[56] Wendi, Wang, *Difference and Differential Equations*, American Mathematical Soc, (42), (2004), 357–361.

[57] Jing, Zhujun and Yang, Jianping, *The orgins and evolution of predator-prey theory*, Ecology, Wiley Online Library, 5 (73), (1992), 1530–1535.

[58] Fan, Meng and Agarwal, Sheba *Periodic solutions of nonautonomous discrete predator-prey system of Lotka-Volterra type*, Applicable Analysis, Taylor & Francis, 4 (81), (2002), 801–812.

[59] Moghadas, SM and Corbett, BD *Limit cycles in a generalized Gause-type predator–prey model*, Chaos, Solitons & Fractals, Elsevier, 5 (37), (2008), 1343–1355.

[60] Thieme, Horst R, Sheba *Persistence under relaxed point-dissipativity (with application to an endemic model)*, SIAM Journal on Mathematical Analysis, SIAM, 2 (24), (1993), 407–435.

[61] Hirsch, Morris W and Smith, Hal L and Zhao, Xiao-Qiang *Chain transitivity, attractivity, and strong repellors for semidynamical systems*, Journal of Dynamics and Differential Equations, Springer, 1 (13), (2001), 107–131.

[62] Smith, Hal L and Thieme, Horst R *Dynamical systems and population persistence*, American Mathematical Soc, (118), (2011).

[63] Meyer, Carl D *Matrix analysis and applied linear algebra*, Siam, 71, (2000).

[64] Luque, Gloria M and Vayssade, Chloé and Facon, Benoît and Guillemaud, Thomas and Courchamp, Franck and Fauvergue, Xavier *The genetic Allee effect: a unified framework for the genetics and demography of small populations*, Ecosphere, Wiley Online Library, 7(7), 2016, 1-13.

[65] Kang, Yun and Sasmal, Sourav Kumar and Bhowmick, Amiya Ranjan and Chattopadhyay *A host–parasitoid system with predation-driven component Allee effects in host population*, Journal of biological dynamics, 9, (2015), 213–232.

[66] Sullivan, Nicholas *The Blue Revolution: Hunting, Harvesting, and Farming Seafood in the Information Age*, Island Press, (2022).

[67] Liu, Hua and Li, Zizhen and Gao, Meng and Dai, Huawei and Liu, Zhiguang *Dynamics of a host–parasitoid model with Allee effect for the host and parasitoid aggregation*, Ecological Complexity, 6(3), (2009), 337–345.

[68] Wu, Daiyong and Zhao, Hongyong *Global qualitative analysis of a discrete host-parasitoid model with refuge and strong Allee effects*, Mathematical Methods in the Applied Sciences, Wiley Online Library, 41(5), (2018), 2039–2062.

[69] Luis, Rafael and Elaydi, Saber and Oliveira, Henrique *Stability of a Ricker-type competition model and the competitive exclusion principle*, Journal of Biological Dynamics, Taylor & Francis, 5(6), (2011), 636–660.

[70] Elaydi, Saber N and Sacker, Robert J *Population models with Allee effect: A new model*, Journal of Biological Dynamics, Taylor & Francis, 4(4), (2010), 397–408.

[71] Livadiotis, G and Elaydi, Saber *General Allee effect in two-species population biology*, Journal of Biological Dynamics, Taylor & Francis, 6(2), (2012), 959–973.